# INVESTIGATING THE PATHOGENESIS OF HIV-ASSOCIATED SENSORY NEUROPATHY IN THE SIV-MACAQUE MODEL

by
Lisa M. Mangus, DVM, Dipl. ACVP

A dissertation submitted to Johns Hopkins University in conformity with the requirements for the degree of Doctor of Philosophy

Baltimore, Maryland

March, 2016

**Abstract**

Sensory neuropathy (SN) continues to be a frequent and challenging neurologic complication of HIV infection despite widespread use of modern combination antiretroviral therapy (cART). Symptoms of HIV-associated sensory neuropathy (HIV-SN) are often painful and only partially mitigated by conventional analgesics. Because clinical studies of HIV-SN are limited by the inability to sample key components of the sensory pathway, our group has developed a simian immunodeficiency virus (SIV)/macaque model to investigate the underlying neuropathologic mechanisms of this condition and elucidate new therapeutic strategies. Here, I build upon previous work in the macaque model by conducting in depth analyses of multiple components of the sensory pathway, namely the epidermal nerve fibers (ENF), spinal cord, and dorsal root ganglia (DRG). I show that quantitative techniques for assessing ENF loss, a method commonly used to diagnose SN in HIV patients, can be adapted for use in Asian macaques. Furthermore, by employing these techniques in both rhesus and pigtailed macaques, I have uncovered significant differences in SIV-induced ENF loss between species, highlighting the importance of host factors in determining disease outcomes. Focusing on pigtailed macaques, I investigated the effects of SIV infection on the spinal cord, which transmits and modulates sensory signals. I found significant glial activation and upregulation of proinflammatory mediators in the spinal cords of untreated SIV-infected macaques, as well as animals receiving cART. I also demonstrated significant correlation between SIV-induced alterations in the spinal cord and the degree of ENF loss in untreated animals. Finally, I sought to gain a comprehensive understanding of the molecular alterations occurring at the level of the DRG during acute SIV, a time point

that precedes significant ENF decline. Using a combination of RNA and protein analyses, I found evidence of significant immune activation, as well altered expression of enzymes related to glutamate metabolism and the oxidative stress response, all of which could contribute to early sensory nerve damage. Taken together, this dissertation supports the premise that HIV-SN involves neuronal dysfunction at multiple levels of the sensory pathway and provides novel insights into mechanisms at play during early phases of disease, a time when neuroprotective strategies could be of great clinical benefit.

Thesis advisor: Joseph L. Mankowski, DVM, PhD, Dipl. ACVP
Professor, Dept. of Molecular and Comparative Pathobiology

Second reader: Frank Bosmans, PharmD, PhD
Assistant Professor, Dept. of Physiology

Committee: Ahmet Höke, MD, PhD (Chair)
Michael Caterina, MD, PhD
Frank Bosmans, PharmD, PhD

**Acknowledgements**

They say it takes a village to raise a child. I would argue that it also takes a village to raise a graduate student, and it certainly helps when that village is full of highly skilled individuals who are extraordinarily generous with their time and knowledge. Throughout my training at Johns Hopkins, I have benefited immensely from the guidance and assistance of many such individuals, both professionally and personally.

First, I would like to thank my thesis advisor, Dr. Joseph Mankowski, who has been a truly exceptional teacher and mentor. Despite his demanding schedule, Joe always manages to make himself accessible to his graduate students – ever ready with the support and insight needed to tackle the next hurtle, be it a simple technical challenge in the lab, or something as daunting as the veterinary pathology board exam. His enthusiastic, optimistic attitude sets an example for all of us who are just crazy enough to pursue careers as veterinarian-scientists. It also helps that we share an allegiance to certain western Pennsylvanian sports franchise, whose name shall not be mentioned here.

Another major advantage of joining the Mankowski lab has been the constant support of our incredibly dedicated lab manager, Suzanne Queen, and amazing technicians Jamie Dorsey (who has gone on to attend graduate school, herself) and Rachel Weinberg. These women have shared the unenviable job of getting this non lab-savvy graduate student up to speed at the benchtop, and have done so with endless patience and good humor. I also owe considerable gratitude to my PhD predecessors in the Mankowski lab, Drs. Kelly Metcalf-Pate, Katie Kelly, and Sarah Beck. Their hard work and accomplishments, both in the lab and beyond, are sources of inspiration and I am very fortunate to have had the opportunity to learn from them first hand. It also helps

that these are all extraordinarily warm, funny people, and that we have shared many memorable experiences outside of the lab, including competing in the Baltimore marathon relay race. Go RetroviRunners!

I am also grateful for the collaborative working and learning environment provided by the Retrovirus laboratory as a whole. The faculty members, Drs. Janice Clememts, Chris Zink, Lucio Gama, David Graham, Ken Witwer, Zhahao Liao, and Kelly Metcalf-Pate, have all imparted helpful insight and guidance throughout my graduate training. Monkey studies are another pursuit that requires a village, and I give credit to our large team of excellent technicians, especially Brandon Bullock, Erin Shirk, Ming Li, and Elizabeth Engle for making this important research happen, as well as the clinical veterinary team for making sure that our monkeys receive the best possible care before and during our studies. And many thanks to my fellow graduate students and post docs in the Retrovirus lab for all of their help, advice, commiseration, and laughs along the way.

I would like to acknowledge my thesis committee members - Ahmet Hoke, Michael Caterina, and Frank Bosmans - for taking the time out of their busy schedules to share their experience and insight, and provide valuable feedback on my projects. Frank was also gracious enough to act as the official 'second reader' of this dissertation. Many thanks also to the wonderful CMM program administrators – Colleen Graham and Leslie Lichter – for cheering me on, keeping me on track, and always having a bowl of free candy in their office. Grad students really appreciate free candy.

In addition pursuing a PhD, my time at Hopkins was also spent completing the veterinary pathology postdoctoral training program in the Department of Molecular and

Comparative Pathobiology. I owe much of my success in that arena to the efforts of our world-class veterinary pathology faculty, which includes Joe, as well as Drs. Chris Zink, Kathy Gabrielson, Corey Brayton, and David Huso. I was also would not have made it through the program without the support and friendship of the pathology trainees – my predecessors Katie Kelly, Gillian Shaw, Sarah Beck, and Simon Long who patiently showed me the ropes and taught me to speak 'Pathologese,' my Buckeye compatriot and co-resident Jennell Romero, and our current fellows, Latasha Crawford, Dilllon Muth, Nathan Pate, Jeremy Foote, Beth Ihms, and Lauren Peiffer. Completing a dual training program is a long, often arduous, undertaking and I'm extremely fortunate to have had such good company along the way.

I am also grateful to my family. I can't say that my parents have completely understood my decision to go to school for such a long time, but they have always been entirely supportive – calmly listening when I call in search of sympathetic ear, and never asking why I didn't just get a real job. Thanks also to my little sister, Kelsey, for being my first European travel partner and for taking care of business back in Wheeling when I couldn't be there. Finally, I'd like to thank my husband, Juergen, who, luckily for me, already had his PhD when we met and came well-versed in the ups and downs of academic research. His unconditional encouragement, love, and general hilarity have kept me going over the past five years. It also helps he has a cute accent and shares my affection for cats.

## Table of Contents


Title Page ..... i

Abstract ..... ii

Acknowledgements ..... iv

Table of Contents ..... vii

List of Tables ..... viii

List of Figures ..... ix

List of Abbreviations ..... xi

I. Introduction ..... 1

II. Tracking epidermal nerve fiber changes in Asian macaques: tools and techniques for quantitative assessment ..... 17

III. Neuroinflammation and virus replication in the spinal cord of SIV-infected macaques ..... 38

IV. Immune Activation in the PNS during Acute SIV Infection ..... 63

V. Summary and Future Directions ..... 93

References ..... 99

Curriculum Vitae ..... 123

## List of Tables

Chapter IV

Table 1. Primary antibodies used for Western blotting and immunohistochemistry assays ..... 83

Table 2. Secondary antibodies used for Western blotting ..... 83

## List of Figures

Chapter II

Figure 2-1. Illustration of the stereologic technique for measuring ENF length in a footpad skin biopsy ..... 32

Figure 2-2. Two ENF quantification methods yield strongly correlative results. ..... 33

Figure 2-3. Species differences in ENF loss during SIV infection ..... 34

Figure 2-4. Differences in baseline ENF length based on country of origin. ..... 36

Figure 2-5. Measuring change from baseline allows longitudinal assessment of ENF loss ..... 37

Chapter III

Figure 3-1. Morphologic changes in the lumbar spinal cord of untreated SIV-infected macaques ..... 57

Figure 3-2. Glial activation in the lumbar spinal cord of untreated SIV-infected macaques ..... 59

Figure 3-3. SIV induces expression of TNFα and CCL2 in the lumbar spinal cord of untreated SIV-infected macaques. ..... 60

Figure 3-4. Among untreated SIV-infected macaques, declining ENF density is associated with increasing viral load and neuroinflammation in the lumbar spinal cord ..... 61

Figure 3-5. SIV-infected macaques on long-term cART showed ..... 62
evidence of significant astrocyte activation in the lumbar spinal
cord despite non-detectable SIV viral load

Chapter IV

Figure 4-1. Genes related to immune signaling and activation are ..... 84
upregulated in the DRG during acute SIV infection
Figure 4-2. Cellular immune activation in the DRG during acute ..... 86
SIV infection
Figure 4-3. Expression of genes related to glutamate metabolism ..... 87
and oxidative stress in the DRG during acute SIV infection.
Figure 4-4. Quantification of DRG protein expression by Western blot ..... 88
Figure 4-5. βIII tubulin expression in the DRG during acute SIV ..... 90
infection.
Figure 4-6. DRG immunohistochemistry..... 91

Chapter V

Figure 5-1. Glutamine synthetase gene expression in the DRG ..... 98
correlates with markers of immune activation and oxidative stress

## List of Abbreviations

| | |
|---|---|
| AIDS | Acquired immunodeficiency syndrome |
| ATN | Antiretroviral toxic neuropathy |
| cART | Combination antiretroviral therapy |
| CNS | Central nervous system |
| CV | Conduction velocity |
| dpi | Days post infection |
| DRG | Dorsal root ganglia |
| DSP | Distal sensory polyneuropathy |
| ENF | Epidermal nerve fiber(s) |
| gp120 | Glycoprotein 120 |
| GFAP | Glial fibrillary acid protein |
| HIV | Human immunodeficiency virus |
| HIV-PN | HIV-associated peripheral neuropathy |
| HIV-SN | HIV-associated sensory neuropathy |
| IHC | Immunohistochemistry |
| MCP1 | Monocyte chemoattractant protein - 1 |
| SIV | Simian immunodeficiency virus |
| PGP9.5 | Protein gene product 9.5 |
| PNS | Peripheral nervous system |
| qRT-PCR | Quantitative reverse transcription polymerase chain reaction |
| TG | Trigeminal ganglia |
| TNFα | Tumor necrosis factor alpha |

# I. Introduction

Portions of this chapter have been previously published as:

**Mangus LM**, Dorsey JL, Laast VA, Ringkamp M, Ebenezer GJ, Hauer P, Mankowski JL. Unraveling the pathogenesis of HIV peripheral neuropathy: insights from an SIV/macaque model. 2014. ILAR Journal. 54(3): 296-303.

**HIV Sensory Neuropathy Background**

Human immunodeficiency virus-associated sensory neuropathy (HIV-SN) is currently the most frequent neurologic complication of HIV infection. It affects approximately 30-50% of individuals living with HIV, including those receiving effective combination antiretroviral therapy (cART) [1,2]. The most common clinical manifestation of HIV-SN is distal sensory polyneuropathy (DSP), a progressive and often painful syndrome characterized by bilateral numbness, tingling and burning sensations most pronounced in the feet and lower legs [3,4]. In severe cases, sensory abnormalities may extend above the knees or involve the hands [5]. While HIV-SN is not a life-threatening condition, the debilitating pain and parasthesias associated with the disease can significantly impair patients' quality of life. HIV patients with chronic neuropathic pain have a greater likelihood of unemployment, dependence in activities of daily life, and depressive symptoms [6]. Treating HIV-SN is challenging in that conventional analgesic medications such as opioids and anti-inflammatory drugs are often poorly effective in alleviating painful symptoms and carry many troublesome off-target side effects [7,8]. With the number of HIV-infected individuals approaching 37 million worldwide (WHO), there is an urgent need for the development not only of more effective symptomatic treatments for HIV-SN, but also of agents aimed at preventing or reversing the underlying sensory nerve damage.

A major reason for the lack of suitable treatments lies in our limited insight into the pathologic mechanisms that lead to HIV-SN. While the clinical features are consistent with a length-dependent 'dying back' of sensory nerve fibers [9], it is uncertain whether HIV induces damage primarily to the neuron cell body at the level of the dorsal root

ganglia (DRG) or if the inciting pathologic change is primarily damage to the peripheral nerve fiber, either of which could ultimately result in a distal axonopathy. Furthermore, while we know that HIV is unable to infect neurons productively, it is unclear whether the neuronal injury arising in HIV-SN is due to persistent release of neurotoxic products by activated macrophages and satellite glial cells (tumor necrosis factor-alpha, IL-1β, chemokines), expression of neurotoxic viral proteins such as glycoprotein (gp)41, gp120, or Tat, by infected peri-neuronal cells, or an additive combination of these processes [7,10-13]. In addition to PNS alterations, HIV-associated neuroinflammation in the spinal cord may also contribute to the generation of pain in HIV-SN through the process of central sensitization [14-17].

Adding to this complexity, it is now clear that several of the 'd-class' nucleoside reverse transcriptase inhibitors (dNRTIs) including zacitabine, stavudine, and didanosine are potently neurotoxic and that use of these agents to treat HIV can lead to antiretroviral toxic neuropathy (ATN), a syndrome clinically indistinguishable from primary HIV-SN [18-20]. Exposure to protease inhibitors has also been proposed as a risk factor for the development of peripheral neuropathy, although this remains a topic of debate [21,22]. Dose reduction or discontinuation of known neurotoxic antiretroviral drugs is often the first step in clinical management of neuropathic signs in HIV patients, and for many patients results in symptomatic improvement [5,23]. However, the frequency of DSP remains unacceptably high despite declining use of dNRTIs, attesting to the ongoing importance of primary HIV-mediated PN, as well as contributions of other proposed risk factors such as advancing age, impaired immune status, metabolic abnormalities, and genetic predisposition [2,24-27].

Studying the pathogenesis of HIV-SN in human patients is limited not only by the inability to sample key components of the somatosensory pathway, including the dorsal root ganglia and spinal cord, but also the frequency of confounding factors such as cART treatment, incomplete adherence, and common comorbidities. Thus, the use of relevant animal models of HIV-SN will be critical to dissect the underlying pathogenesis of this disorder and direct the development of new therapeutic strategies.

**A Simian Immunodeficiency Virus-Infected Macaque Model of HIV Peripheral Neuropathy**

Simian immunodefiency virus (SIV) infected macaques have been widely used to study host and viral aspects of HIV infection in humans. The appropriateness of such models is underpinned by the close resemblance of macaque immune responses during SIV infection to those of HIV-infected individuals, as well as extensive homology shared by SIV and HIV, including the binding of SIV envelope glycoprotein gp120 to the host receptors CD4 and CCR5 for viral entry [28]. Because SIV models vary widely with respect to progression to fulminant AIDS and development of neurologic disease, a refined pigtailed macaque model was developed to study SIV-induced CNS disease efficiently. This model, which entails simultaneous intravenous inoculation of pigtailed macaques with both the neurovirulent molecular SIV clone SIV/17E-Fr and the immunosuppresive virus strain SIV/DeltaB670 results in an accelerated and highly reproducible progression to AIDS by 84 days post-inoculation with approximately 60-70% of SIV-infected macaques also developing encephalitis within this time frame [29,30]. The encephalitis observed in these animals shares many morphologic similarities with HIV-associated

encephalitis including characteristic multifocal perivascular infiltrates of macrophages and formation of multinucleated giant cells bearing replicating virus [31,32]. Further, this model has been useful to study numerous translationally relevant aspects of SIV-associated CNS disease such as the effectiveness of neuroprotective agents, relevance of biomarkers in the CSF, characterization of neuroprotective MHC class I alleles, persistence of neuroinflammation with suppressive cART, and identification of CNS latency reservoirs [33-38].

Recapitulating the neuropathologic features of HIV-SN in rodent models has proven challenging. Because these species are not susceptible to infection by HIV or a closely analogous lentivirus, *in vitro* rodent studies of HIV-SN have required creation of transgenic mice expressing HIV gp120 in perineuronal cell populations or direct inoculation of viral proteins into the peripheral nerves [17,39,40]. To determine whether the SIV/pigtailed macaque model could serve as a reliable model for HIV-SN, key components of the sensory pathway, including samples of skin from the distal leg, sural and sciatic nerves, and somatosensory ganglia including trigeminal and dorsal root ganglia, were collected from SIV-inoculated pigtailed macaques and examined at the morphologic and molecular level.

**Lesions in the Somatosensory Ganglia of Simian Immunodeficiency Virus-Infected Macaques**

Studies examining the morphologic changes in both the trigeminal ganglia and dorsal root ganglia of SIV-infected pigtailed macaques revealed lesions that closely resemble those described in patients with HIV-SN [3,9]. Somatosensory ganglia from SIV-

infected macaques contained multifocal perineuronal inflammatory cells including macrophages and lymphocytes. In animals with moderate to severe ganglionitis, there was evidence of neuronophagia, characterized by macrophages within the neuronal compartment of degenerate neurons, as well as nodules of Nageotte, with neuron cell bodies replaced by compact aggregates of satellite glial cells and macrophages. In the pigtailed macaque model, neuronal loss in the trigeminal and dorsal root ganglia was evaluated using the area fraction fractionator technique, a method to estimate neuron density. In both locations, significant neuronal loss was identified in SIV-infected macaques at 12 weeks p.i. compared with uninfected control animals [41,42]. In the trigeminal ganglia, decline in neuronal density was inversely proportional with the extent of macrophage infiltration as measured by CD68 immunostaining [41]. A similar pattern of neuropathologic changes and macrophage infiltration into the DRG also has been reported in a SIV-infected, CD8 T cell-depleted rhesus macaque model (*Macaca mulatta*) [43].

**Changes in Levels of Viral Replication and Inflammatory Markers Over the Course of Simian Immunodeficiency Virus Infection**

To determine the temporal dynamics of SIV replication and associated neuroinflammatory changes in the PNS during disease progression, we examined somatosensory ganglia from SIV-infected macaques euthanized during acute, asymptomatic, and terminal stages of infection. In the trigeminal ganglia, SIV RNA was detected by *in situ* hybridization in 2 of 6 animals euthanized at 7 and 10 days p.i., but none (0 of 6) of the animals examined at 21 days p.i. In contrast, at 56 days p.i., viral

replication was only detected in one of 6 infected animals [41]. This pattern, in which low levels of SIV replication occurs during acute infection in the somatosensory ganglia, followed by suppression by 21 days and subsequent recrudescence at 56 days, parallels the trend reported for SIV replication in the CNS of SIV-infected macaques [44]. In the dorsal root ganglia, SIV replication was measured by qRT-PCR using SIV gag region primers and probe, and was found to be relatively constant among animals euthanized at 6 through 12 weeks p.i., demonstrating that SIV replication in the DRG is continuous throughout the late asymptomatic and terminal stages of infection. At the terminal disease time point, approximately 12 weeks p.i., both the TG and DRG of SIV-infected macaques contained abundant SIV-infected cells as demonstrated by immunostaining for the transmembrane glycoprotein gp41 [41,42]. Similar to the pattern of HIV replication in human ganglia [45], SIV-infected cells were observed among infiltrating mononuclear cells as well as the perineuronal compartment. To identify infected cell types, ganglia were double immunostained for gp41 and the macrophage marker Iba-1. Laser confocal microscopy revealed clear co-localization of SIV gp41 within Iba-1 positive macrophages, confirming that macrophages were the predominant infected cell type [41,42].

To characterize the severity and composition of inflammatory changes in the somatosensory ganglia during SIV infection, we performed immunohistochemistry and quantitative image analysis on sections of TG and DRG from animals euthanized at multiple time points post-SIV inoculation. Immunostaining revealed a resident population of CD68-positive macrophages distributed diffusely throughout the perineuronal compartment in both uninfected controls and SIV-infected macaques. In SIV-infected animals, this resident population of perineuronal endogenous macrophages

stained more intensely than controls and was accompanied by additional, randomly distributed infiltrating CD68 positive cells. Although this immunostaining pattern likely represents concurrent activation of resident macrophages and infiltration by circulating macrophages, there are currently no available immunologic markers that can readily distinguish between these two populations. Compared to uninfected control animals, total CD68 immunostaining was found to be significantly elevated in the DRG of SIV-infected macaques by 6 weeks p.i., and remained elevated at 8 and 12 weeks p.i. [42], CD68 immunostaining was also significantly higher in the trigeminal ganglia of SIV-infected macaques at terminal stages compared to control animals (Laast et al. 2007). Contrasting with the increase in macrophages, there was modest decline in the number of cytotoxic T cells (TIA-1+, CD3+) in the trigeminal ganglia of SIV-infected animals versus uninfected controls [41].

Several recent studies have a proposed a integral role for glial cell activation in the induction and maintenance of neuropathic pain, including painful HIV-SN [14,46-48]. To determine whether satellite glial cells were immune activated during SIV-infection, DRG sections were immunostained for glial fibrillary acid protein (GFAP) followed by digital image analysis to measure GFAP expression. GFAP expression was significantly increased in SIV-infected macaques at 6 weeks p.i. and remained upregulated at 8 weeks p.i. However, in animals euthanized at 12 weeks p.i., median GFAP staining had declined to the control animal level [42]. These compelling results suggest that satellite glial cell activation plays a key role in the pathogenesis of SIV-induced damage to the DRG. Further studies in the SIV-infected macaque model may elucidate the functional

significance of SGC activation during disease progression, including its association with neuronal viability and sensitivity.

**Simian Immunodeficiency Virus-Induced Functional Alterations in Peripheral Nerves**

In contrast to changes observed in the somatosensory ganglia, we found little morphologic evidence of neuritis or damage to myelinated fibers by examining plastic-embedded, toluidine blue-stained sections of sural and peroneal nerves [42]. A similar paucity of lesions in sural nerve biopsies has been reported in HIV neuropathy [5,49]. Possible explanations for this observation include the extensive length of peripheral nerves and multifocal distribution of inflammatory changes, as well the primary involvement of small, unmeylinated fibers. Given the lack of widespread inflammatory lesions in the peripheral nerve, the focus of our investigation of peripheral nerves was concentrated on alterations in neurophysiology and correlations between these changes and SIV-induced pathology in the DRG.

Because current clinical methods of measuring peripheral nerve conduction velocity (CV) are relatively insensitive to changes in small unmeylinated fibers, such electrophysiologic studies are often of limited diagnostic value in patients with HIV-SN [5,49]. To circumvent this limitation, we employed an *ex vivo* teased fiber technique to measure CV in single, unmeylinated fibers in the sural nerves from control and SIV-infected macaques. Electophysiology experiments demonstrated a significant decrease in mean C-fiber conduction velocity in SIV-infected macaques by 12 weeks p.i., during late stages of the disease. Additionally, there was strong inverse correlation between mean C-

fiber CV of SIV-infected animals and the degree of CD68 expression in the DRG indicating that the extent of macrophage infiltration in the DRG corresponded closely with functional changes in C-fiber conduction properties [42].

**Epidermal Nerve Fiber Density Declines with Simian Immunodeficiency Virus Infection**

Skin biopsies have proven to be an invaluable tool in the clinical diagnosis of small fiber neuropathies and have largely replaced more invasive sural nerve biopsies for the assessment of conditions such as diabetic neuropathy and HIV-SN [50-52]. After fixation and sectioning, skin sections are immunostained with the pan-neuronal marker PGP9.5 to allow visualization and quantification of epidermal nerves fibers (ENF)[53]. In HIV-infected patients, decreased ENF density in skin of the distal leg has ben shown to correlate with lower CD4 counts, higher viral loads, and the presence of neuropathic pain [54]. To examine whether a parallel decline in ENF density occurs in SIV-infected macaques, cutaneous biopsies from footpads were collected at necropsy, immunostained for PGP9.5, and analyzed by quantitative image analysis. Compared with uninfected control animals, SIV-infected animals exhibited a progressive decline in ENF density throughout disease resulting in a significant decrease by 8 weeks p.i. and a marked reduction at 12 weeks p.i. [42]. Interestingly, rhesus macaques inoculated with the same combination of viruses do not develop a decline in ENF density, suggesting that additional host factors are involved in PNS damage.

**Simian Immunodeficiency Virus -induced Impairment of Neurovascular Regeneration**

In addition to simulating closely HIV-induced damage to the peripheral nervous system, the SIV-infected macaque model has also been used to study the impact of infection on the capacity of peripheral nerves to regenerate following injury. Similar to techniques previously described in man [55], we utilized an excisional intracutaneous axotomy model in macaques to study both the normal features of nerve regeneration in this species and the affect of SIV infection on this process. Briefly, cutaneous axotomies were performed at two-week intervals following SIV inoculation using 3mm circular skin punches to transect the epidermis and dermis. On the 70$^{th}$ day after the initial axotomy, all 3mm punch incision sites were harvested using a 5mm skin punch, producing skin samples containing excision sites from 14, 28, 42, 56, and 70 days post-axotomy. Samples were then immunostained for the pan-neuronal marker PGP9.5 and the length of regenerating epidermal nerve fiber sprouts within the axotomy site was compared to the length of normal epidermal nerve fibers located outside of the initial axotomy zone. In both SIV-infected and uninfected macaques, epidermal reinnervation was rapid and complete by 56 days post-axotomy, which is in contrast to the slower, incomplete reinnervation observed in humans following this technique [55]. However, in SIV-infected animals epidermal nerve fiber regeneration was delayed at every time point post-axotomy compared to uninfected controls [56].

Because Schwann cells play a crucial role in guiding axonal regrowth following injury [57-60], we also assessed the degree of Schwann cell migration into denervated epidermis by immunostaining for Schwann cell marker p75 nerve growth factor receptor.

In both control and SIV-infected animals, Schwann cell density was highest at the earliest time points post-axotomy and declined at a similar rate in both groups. At every time point post-axotomy, SIV-infected animals consistently had lower mean Schwann cell density measurements than uninfected controls [56].

Another key contributor to axonal regeneration following injury is the regrowth of blood vessels, which travel in close morphologic approximation with nerves forming a well-organized network of neurovascular bundles. Further studies investigating neurovascular repair in the pigtailed macaque model revealed that while SIV-infection does not affect blood vessel regrowth at cutaneous biopsy sites, expression of vascular endothelial growth factor (VEGF) around regenerating neurovascular units, measured by immunostaining, is lower in SIV-infected animals compared to controls. Additionally, a strong positive correlation was demonstrated between VEGF expression and the extent of ENF regeneration [61]. Downregulation of VEGF expression may alter the perivascular extracellular matrix such that is less conducive to nerve regrowth. Taken together, these results indicate that SIV-infection leads to deficient epidermal nerve fiber regeneration and that this impairment is mediated, at least in part, by altered Schwann cell migration and decreased VEGF expression along neurovascular tracts. In addition, these studies illustrate that the macaque model can accelerate study of human nerve regrowth biology.

**Summary and Project Goals**

As reviewed in Chapter I, SIV-infected pigtailed macaques develop key pathologic features of HIV-SN, making this model invaluable for understanding the complex molecular mechanisms of this condition and elucidating new therapeutic targets.

By sampling and examining key components of the peripheral nervous system at multiple time points throughout SIV infection, we have found that the virus infects and immune-activates perineuronal cells of the somatosensory ganglia during early stages of infection, setting the scene for insidious neuronal damage that becomes evident later in the disease as decreased neuronal density in somatosensory ganglia, altered C-fiber conduction properties, and decreased epidermal nerve fiber density. SIV-infection also impairs the regenerative capacity of small epidermal nerve fibers, a factor that will be imperative to address when designing therapeutic strategies for HIV-SN.

Another notable outcome of these studies in the pigtailed macaque model is the development and refinement of various techniques to assess peripheral nervous system integrity. These tools are applicable to studies of HIV-SN and will be instrumental for studies involving non-human primate models of other clinically relevant small fiber neuropathies including those associated with diabetes mellitus and cancer chemotherapy. Chapter II provides detailed descriptions of the methodology and quantitative image analysis techniques that our group uses to measure epidermal nerve fiber loss in SIV-infected macaques and outlines important experimental considerations for ENF studies in primates. Specifically, I address macaque species differences in the development of significant ENF decline during SIV infection, discrepancy in baseline ENF values in pigtailed macaques from different countries of origin, and the feasibility of longitudinal ENF assessment in macaque models.

In addition sensitization at the level of the peripheral nerves, it is widely recognized that functional alterations within the spinal cord, where sensory neurons synapse to relay information to the brain, are a critical component in the pathogenesis of

neuropathic pain. This is attested to by the effectiveness of some centrally-acting medications, such as tri-cyclic anti-depressants and pregabalin, in managing other forms of sensory neuropathy [62]. Studies addressing the role of spinal cord changes in the setting of HIV-SN are few, but a recent series of reports has demonstrated increased glial activation, enhanced pro-inflammatory signaling, and elevated concentrations of HIV envelope glycoprotein gp120 in the spinal cords of autopsy patients with histories of HIV-associated pain when compared to "pain negative" HIV patients [14-16]. Consequently, I set out to determine whether such potentially pain-enhancing alterations also occur in the spinal cord of SIV-infected macaques and whether these changes persist in the setting of virally suppressive cART. In Chapter III, I show that in untreated SIV-infected animals, there was a strong correlation between amount of SIV RNA in the spinal cord and expression of the macrophage marker CD68, as well as key pro-inflammatory mediators TNF $\alpha$ and CCL*2*. In contrast, cART-treated animals showed markedly increased spinal expression of the astrocyte activation marker GFAP and enhanced CCL2 expression, suggesting that spinal glial activation and pro-inflammatory signaling persist despite viral suppression and may contribute to neuropathic pain in HIV patients on effective cART.

Another largely unexplored aspect of HIV-SN is the presence of sensory abnormalities during acute/early HIV infection. Examination of early pathologic changes in the PNS of HIV patients is limited due to the inability to obtain samples of nervous tissue prior to autopsy, a point when most patients have died during advanced stages of disease. However, a recent clinical study by Wang et al [63] showed that among a cohort of cART-naïve men evaluated during primary HIV infection (defined as less than one year

since transmission), 35% of patients met diagnostic criteria for SN and 22% had symptomatic PN. Our group has also reported significant changes in the PNS of macaques euthanized at early time points during SIV infection. These findings include significantly increased CD68 expression in the DRG at 10 d.p.i. and significantly decreased ENF density by 14 d.p.i. Furthermore, significant ENF loss was found to persist despite suppressive cART treatment starting at 12 d.p.i. [64]. Taken together, these findings in human patients and macaques imply that damage to the PNS occurs early during the course of HIV/SIV disease and likely 'sets the stage' for development neuropathic symptoms as the disease progresses or as potentially neurotoxic cART is initiated. In Chapter IV, I attempt to elucidate possible mechanisms underlying this early sensory nerve damage by investigating changes in RNA and protein expression within the dorsal root ganglia at 7 d.p.i., a time point during acute infection that proceeds detectable increase in DRG CD68 expression and significant ENF loss. I demonstrate that, during acute SIV infection, there is significant upregulation in the DRG of genes involved in immune activation and signaling, including interferon-stimulated genes, which are critical to the early antiviral response. I also found alterations in the expression of genes and proteins related to glutamate metabolism and the oxidative stress response, which may be related to altered cellular metabolism in the DRG in the setting of systemic and local immune activation. Furthermore, metabolic stress at the level of the sensory nerve cell bodies could contribute to early die-back of distal nerve fibers and render nerve cells more vulnerable to cART toxicity.

HIV-SN is a complex disorder that involves altered nerve function at multiple points along the somatosensory pathway, both in the periphery and in the central nervous

system. It follows that effective, analgesic treatments for HIV patients with established neuropathic symptoms will likely need to be multimodal and target molecular processes related to central sensitization, as well as inhibiting aberrant nociceptive signaling at the level of the peripheral nerves. Moving forward, a comprehensive understanding of pathologic changes occurring during the early stages of HIV will allow for the development of strategies aimed at mitigating additional damage accrued through the use of antiretroviral treatments as well as chronic inflammation and residual low-level viral replication.

# II. Tracking epidermal nerve fiber changes in Asian macaques: tools and techniques for quantitative assessment

**Abstract**

Quantitative assessment of ENF has become a widely used clinical tool for the diagnosis of small fiber neuropathies such as diabetic neuropathy and HIV-SN. As part of our group's efforts to model and investigate the pathogenesis of HIV-SN using SIV-infected Asian macaques, we have successfully adapted the skin biopsy and immunostaining techniques currently employed in human patients, and developed two unbiased image analysis techniques for quantifying ENF in macaque footpad skin. This chapter provides detailed descriptions of these tools and techniques for ENF assessment in macaques and outlines important experimental considerations that have become apparent over several years of work. Although initially developed for studies of HIV-SN in the SIV-infected macaque model, these methods could be easily translated to a range of studies involving peripheral nerve degeneration and neurotoxicity in non-human primates, as well preclinical investigations of agents aimed at neuroprotection and regeneration.

## Introduction

Transmission of afferent sensory information from the periphery to the CNS is accomplished by a variety of sensory nerve types, ranging from the large caliber, thickly-myelinated fibers that convey the senses of innocuous touch and limb position, to the small-diameter thinly-myelinated Aδ fibers and unmyelinated C-fibers that transmit the sensations of temperature and pain [65]. Small fiber neuropathies (SFN) are defined as conditions that selectively or predominantly affect the Aδ or C-fibers [66]. The clinical manifestations of SFN typically involve a spectrum of positive and negative sensory abnormalities such as neuropathic pain, paresthesias, hyperalgesia, and numbness [52,66,67]. The etiologies associated with SFN are numerous and include common metabolic disorders, such as diabetes mellitus [68] and hyperlipidemia [69], infectious diseases such as HIV[70] and herpesviral infections [71], as well as rare hereditary [72] and autoimmune conditions [73]. Relevant to the topic of toxicologic pathology, several pharmaceutical compounds, including chemotherapeutic agents [74] and antiretroviral drugs [20,21,64], have frequently been associated with peripheral neurotoxicity leading to SFN. For some patients, these detrimental side effects can be dose-limiting and negatively impact their quality of life [75]. Thus, it is imperative to assess the peripheral neurotoxicity of new drugs during preclinical testing [76].

The diagnosis and study of SFN has historically been challenging [52]. Standard nerve conduction studies are not sensitive enough to detect abnormalities in small diameter nerve fibers [77]. Similarly, morphologic examination of peripheral nerve tissue, such as the sural or sciatic nerves, may not reflect early changes to small fibers that may begin in distal regions [78]. In recent years, visualization and assessment of ENF in skin

biopsies has become a standard clinical tool for the diagnosis of SFN caused by a wide variety of conditions [50,79]. Unlike quantitative sensory testing, which relies on patient responses and is subject to bias [80], ENF analysis is objective and can be applied to animal models [81]. Skin biopsy is also a relatively quick, noninvasive technique that is applicable to longitudinal sampling (compared to sural or sciatic nerve biopsies)[82]. In several conditions, including HIV infection, loss of ENF density has been shown to correlate strongly with severity of neuropathic symptoms [83,84].

In this report, we describe the development and implementation of skin biopsy as a tool to study sensory nerve alterations in SIV-infected macaques. Previous studies by our group have shown that SIV-infected pigtailed macaques (*Macaca nemestrina*) develop morphologic and functional lesions of the peripheral nervous system that closely parallel those seen in HIV patients with neuropathy [42]. These include inflammation, glial activation, and viral replication in the lumbar spinal cord [85] and dorsal root ganglia, as well as decreased conduction velocity in isolated C-fibers from the sural nerve [42] Because skin biopsy and ENF quantification is currently the gold standard to diagnose and monitor SFN in HIV patients and can be performed longitudinally, we also sought to adapt this technique for use in macaques. In addition to pigtailed macaques, we have also evaluated ENF of uninfected and SIV-infected rhesus macaques (*Macaca mullata*), allowing for comparison of normative and experimental data between macaque species. Through these studies, we have learned valuable lessons regarding skin sample collection and processing, quantitative image analysis of ENF, and selection of study animals. These lessons are highly applicable to any study evaluating the peripheral nervous system

of non-human primates, including preclinical testing of potentially neurotoxic compounds or novel drugs aimed at the treatment of SFN.

## Materials and Methods

### *Animals*

Juvenile pigtailed macaques (*Macaca nemestrina*) and adult rhesus macaques (*Macaca mulatta*) were inoculated intravenously with a combination of the neurovirulent clone SIV/17E-Fr and the immunosuppressive viral swarm SIV/DeltaB670 as previously described [86]. Age-matched, sham-inoculated animals served as procedural controls. At study endpoints, animals were euthanized and whole-body saline perfused prior to the collection of tissues. For the pigtailed macaques, which demonstrate an accelerated, predictable SIV disease progression [30], specific end points were predetermined according to stage of disease [acute disease at 7 and 10 dpi, asymptomatic at 35, 42, and 56 dpi, terminal at 84 dpi]. Because the course of disease progression is more variable in rhesus macaques, these animals were euthanized when two or more AIDS-defining criteria were met (mean length of infection 213 days)[87]. All macaques were housed in facilities accredited by the Association for the Assessment and Accreditation of Laboratory Animal Care International (AAALAS), and all procedures were performed according to principles set forth by the Johns Hopkins University Institutional Animal Care and Use Committee (IACUC) and the National Research Council's Guide for the Care and Use of Laboratory Animals.

*Skin biopsy collection and fixation*

Although skin biopsies for ENF analysis in human patients are typically obtained from an area of the distal leg above the lateral malleolus [66], the high density of hair follicles and adnexa present in haired macaque skin necessitated the collection of skin samples from non-haired or 'glabrous' skin. Thus, we obtained skin samples from the metatarsal footpad (between the third and fourth digits) using a 3mm punch biopsy tool at necropsy. For studies assessing change in ENF from pre-infection baseline, biopsies were also collected prior to inoculation (sham or SIV), and necropsy samples were obtained from the opposite foot. Skin sections were fixed for 12 to 24 hours in Zamboni's fixative (2% paraformaldehyde and picric acid) at 4°C, then rinsed with 0.08 mol/L Sorensen's phosphate buffer. Fixed sections were transferred to a cryprotective buffer (20% glycerol in 0.08 mol/L Sorensen's phosphate buffer) and stored at 4°C until processing (typically within one week).

*Immunohistochemistry*

Cryoprotected skin samples were cut perpendicular to the epidermis at a thickness of 50µm using a freezing-sliding microtome. Each biopsy yielded approximately 60, 50µm-thick sections, from which 4 representative sections were chosen for immunostaining. Individual sections were transferred to 96 well plates and immunostained for the pan-axonal marker PGP9.5 (rabbit polyclonal, ABD Serotec, 1:10,000) using a free floating section method as previously described [88]. Briefly, sections were first bleached with 0.25% potassium permanganate followed by oxalic acid to reduce melanin pigmentation. The sections were blocked with a solution of 1.0% Triton X-100 (Sigma) with 0.5%

powdered milk and 5% normal goat serum in TBS (pH 7.4), then incubated with the primary antibody overnight on an orbital shaker at room temperature. The following day, sections were incubated with a biotinylated secondary antibody (goat anti-rabbit, 1:100, Vector), and treated with 1% hydrogen peroxide in 30% methanol/PBS to quench endogenous peroxidase activity. Sections were then incubated in avidin/biotin complex solution (ABC, Vector Labs, Burlingame, CA) and developed using the Vector SG peroxidase substrate kit, which produces dark blue-gray chromogenic staining. Finally, the sections were mounted on alum/gelatin subbed slides, lightly counterstained with eosin, and coverslipped with Permount (Fisher).

*Quantitative epidermal nerve fiber assessment*

Measurement of ENF density in human skin biopsies is typically achieved by manually counting all PGP9.5-stained epidermal nerve fibers that cross the dermal-epidermal junction and dividing this number by the linear length of the skin section in millimeters [88]. Although this method is highly sensitive and reproducible in human skin samples [89], the remarkably rich sensory innervation of the macaque footpad makes manual counting of individual fibers cumbersome and error-prone. Thus, we developed two quantitative image analysis techniques, one based on ENF density and another on ENF length, to facilitate ENF assessment in our macaque skin samples.

*Measurement of epidermal nerve fiber density*

The method used to determine ENF density in macaque footpad samples was adapted from the confocal 'optical sectioning' technique described by Kennedy and colleagues [90].

Using a brightfield microscope equipped with a Z-axis motor (Carl Zeiss, Oberkochen, Germany), Z-stack images were obtained from 15 adjacent, non-overlapping, 400X fields for each immunostained skin section. Serial Z-stack images for each field were collected at 0.5µm intervals and then collapsed into a single image. Positive PGP9.5 immunoreactivity was measured as percent region of interest (%ROI) using iVision software (BioVision Technologies, Exton, PA). To control for variations in skin section thickness, results were normalized to the thickness of each sample (the z distance of the stack).

*Measurement of epidermal nerve fiber length*

An advantage of quantifying length, rather than density of linear structures in tissue sections is the ability to employ non-biased, stereologic image analysis techniques. These methods are based on counting random intersections of the object of interest, such as an axon or blood vessel, with a geometric probe that is superimposed over the image of the tissue [91]. Additionally, stereologic algorithms provide an estimate of the total length of objects in a specimen by systematically sampling a subset of the total sections, which saves time compared to analyzing an entire specimen. To measure length of epidermal nerve fibers in macaque footpad samples, we used the Stereo Investigator space ball probe (MBF Biosciences, Version 9), similar to the method described by Ebenezer and colleagues [92] and [61]. Three, 50µm thick, PGP9.5 immunostained skin sections were evaluated per animal. For each section, a region of interest (ROI) in the epidermis, extending from the dermal-epidermal junction to the stratum corneum, was traced under a Nikon 4x/0.2 Plan Apo objective on a Nikon Eclipse E600 light microscope (see Fig 1A

for illustration). Magnification was then switched to a Nikon 60x/1.4 oil Plan Apo objective, and total ENF length was estimated by counting intersections of nerve fibers with a hemispheric probe that had a 30µm radius and 2µm guard zones (to account for tissue irregularity at the edges of the sections). Only nerve fibers that were clearly within the epidermis were counted (Fig 1B). All stereology measurements were obtained using Stereo Investigator DAT files and results were expressed as the estimated total length of PGP9.5-stained epidermal nerve fibers.

*Statistics*

All statistical analyses were performed using GraphPad Prism software (version 5.0d) and nonparametric methods. The Mann-Whitney U test was used for two-group comparisons and the Spearman correlation coefficient was used to analyze relationships between continuous variables. Statistical inferences were considered significant when $p < 0.05$.

**Results**

*Two ENF quantification methods yield strongly correlative results*

In our SIV/macaque studies, we have found that epidermal nerve fibers can be effectively visualized in footpad biopsies by immunostaining thick cryosections with the pan-neuronal marker PGP9.5. Using these immunostained sections, two different image analysis techniques, one assessing nerve fiber density and the other measuring fiber length, were developed and found to be effective means of objectively quantifying ENF. Furthermore, when both quantification methods were applied to the same skin samples,

we found strong, direct correlation between the results (Fig 2), showing that either technique could serve as a valid tool in other macaque ENF studies.

*Species differences in ENF loss during SIV infection*

The species of macaque used in our group's SIV work is based on the desired phenotypic outcome for each study. Since most of our studies have aimed to model the neurologic consequences of HIV infection, the vast majority of our study animals are pigtailed macaques, which more quickly and consistently develop SIV-associated CNS and PNS disease [30]. Smaller numbers of rhesus macaques have been used in studies involving HIV-associated cardiac dysfunction, as this species survives longer following SIV infection and more readily develops functional cardiac abnormalities [93]. We have collected normative ENF data on uninfected control groups of both pigtailed and rhesus macaques. While the median ENF density among control rhesus was lower than that of pigtailed macaques, this difference did not reach statistical significance ($p = 0.081$, data not shown). However, in the context of SIV infection, only infected pigtailed macaques exhibited a significant decline in ENF density compared to control animals ($p = 0.0033$, Fig 3A). There was no significant difference in ENF density between rhesus macaques euthanized at terminal time points and control animals ($p = 0.26$, Fig 3B). This finding demonstrates the potential for considerable variation in host responses between closely related primate species, and underscores the need for careful species selection in studies evaluating the peripheral nervous system.

*Macaques of US and Indonesian origin have different baseline ENF length*

In addition to considering potential difference in ENF response between species, we also examined whether pigtailed macaques from different originating countries had comparable ENF status prior to entering SIV studies. Interestingly, we found that pigtailed macaques imported from Indonesia had significantly lower baseline ENF length than macaques born in the United States ($p = 0.0048$, Fig 4). Whether this observation results from genetic or environmental differences between Indonesian and US pigtailed macaque populations is currently unclear. However, this finding suggests that uniformity of animal origin may be a critical factor when designing studies evaluating ENF status of primates.

*Measuring change from baseline allows longitudinal assessment of ENF loss*

Skin biopsies are a relatively non-invasive and repeatable tool for assessing the status of peripheral sensory nerves in humans and animal models, and therefore can be used for longitudinal assessment of individual subjects. In our more recent macaque studies, we collected pre-infection footpad biopsies and quantified baseline ENF lengths that were then compared to values obtained from necropsy skin samples. Among pigtailed macaques, we found that SIV-infected animals euthanized during terminal disease (84 dpi) had a median decrease in ENF length of nearly $5x10^4$ μm from their baseline value and that this change was significantly different from that observed among uninfected controls that were also euthanized at 84 days post mock infection ($p = 0.0024$, Fig 5). We believe that this longitudinal manner of ENF assessment produces more reliable data than cross-sectional sampling and measurement, and plan to utilize this method in future

studies of SIV neuropathy. In addition, longitudinal studies can be used to monitor epidermal nerve fiber regeneration in studies of regenerative agents [56] .

**Discussion**

When studying any animal model of human disease or toxicity, a major goal should be to employ experimental outcome measures similar to those currently used in clinical settings. Over the past decade, assessment of sensory nerve fibers in skin biopsies has proven to be a sensitive indicator of early damage to distal unmeylinated nerve fibers, and has supplanted older methods, such as sural nerve morphometry and electrodiagnostic studies, in the clinical diagnosis of HIV-associated sensory neuropathy. In line with this advancement, our group has worked to develop and implement techniques to measure progressive ENF loss in SIV-infected macaques. The techniques described herein for the procurement and immunostaining of footpad skin biopsies and unbiased quantitative analysis of ENF have proven to be key assets in our investigations of the pathogenesis of SIV-SN [42,85,94] and could easily translate to other types of studies evaluating peripheral neurodegeneration and neurotoxicity in non-human primates.

Our work with both pigtailed and rhesus macaques has revealed important experimental variables that need to be considered when planning ENF studies in primates. Firstly, we found that although there was no significant difference in footpad ENF density between normal, uninfected macaques of the two species, only pigtailed macaques exhibited significant ENF loss during the course of SIV infection. ENF density in SIV-infected rhesus macaques with terminal disease was not significantly different from controls. In contrast, Lakritz and colleagues [95] recently reported significant ENF

decline in SIV-infected rhesus macaques that were also CD8-lymphocyte depleted. This major discrepancy in experimental outcomes between closely-related macaque species emphasizes the importance of host response in animal studies of peripheral neuropathy. Rodent studies have also revealed marked differences in the susceptibility of various mouse strains to peripheral neuropathy [39]. For example, in a study investigating the sensitivity of different inbred mouse strains to paclitaxel-induced neuropathy, Smith and colleagues [96] showed that DBA/2J mice exhibited especially robust mechanical hypersensitivity after exposure to paclitaxel, while the C57BL/6J mice were relatively resistant to this change. The influence of genetic background has also been shown to be a critical variable in mouse models of diabetic neuropathy [97].

Secondly, when evaluating pigtailed macaques originating from different countries, we found that animals from Indonesia had significantly lower baseline ENF length than animals born in the United States. Whether this observation is related to genetic or environmental factors is not clear. Significant differences in ENF density have also been reported in people of distinct geographic origins [98]. A recent study investigating ENF density as a marker of neuropathy risk in Thai HIV patients showed that very few subjects in that cohort developed neuropathic signs or symptoms despite use of stavudine, a known neurotoxic antiretroviral drug that is still often used in developing countries [99]. While several factors likely contributed to this finding, the authors note that HIV seronegative Thai subjects have higher ENF density compared to published US control values, and that this higher baseline ENF density may provide Thai subjects with greater "ENF reserve." Together, our findings suggest that both species and geographic origin are important variables to consider when planning studies of peripheral neuropathy in

Asian macaques. While these variables are potential confounding factors in preclinical studies of peripheral neuropathy in primates, they could ultimately be informative in future research aimed at identifying 'neuroprotective' host genes and environmental factors.

Finally, we have shown that by obtaining footpad skin biopsies prior to SIV infection, each animal's ENF measurement at necropsy can then be compared to its own pre-infection ENF measurement. With this longitudinal sampling method, we were able to demonstrate that SIV-infected pigtailed macaques experienced a significantly greater loss of distal ENF length compared to control animals at 84 dpi or post mock-infection. By using 'change-from-baseline' data rather than single, cross-sectional ENF measurements, each macaque serves as it's own control, which helps account for individual variation in baseline ENF values. Longitudinal sampling could be of great benefit for ENF studies with small numbers of animals or when uniformity of animals (age, origin, etc.) is not possible.

Given its extensive distribution and anatomic complexity, systematic sampling and assessment of the PNS can be challenging, especially in large animal models. Skin biopsy and subsequent ENF analysis provide relatively simple methods for obtaining information about the status of peripheral sensory neurons, and can be performed objectively with little specialized training. Moreover, loss of ENF density is a more sensitive indicator of early damage to small unmeylinated nerves than traditional histologic or morphometric nerve analyses. Our group's efforts to evaluate ENF in the context of SIV-associated sensory neuropathy has led to the development of reliable tools and unbiased, quantitative techniques that could be applied to a wide range of peripheral

neuropathy and neurotoxicity studies in primate species. Additionally, the noninvasive, repeatable nature of the skin biopsy technique makes it ideal for studies of interventional strategies aimed at preventing or reversing nerve fiber degeneration.

**Figures**

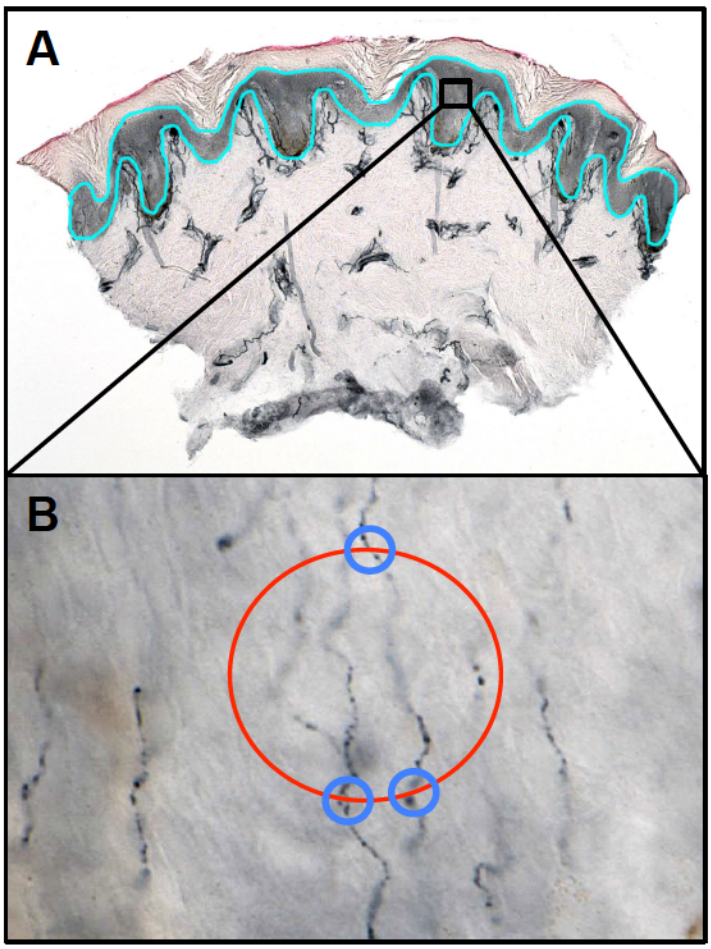


**Figure 2-1.** *Illustration of the stereologic technique for measuring ENF length in a footpad skin biopsy.* As depicted in A, the epidermis is traced (light blue outline) in a PGP9.5-stained skin section under low magnification. This serves as the region of interest (ROI). The Stereo Investigator software then systematically selects a subset of fields within the ROI for measuring ENF (represented by the black rectangle). After switching to high magnification, as shown in B (60X oil objective), the probe is moved through the Z-axis of the tissue by a motorized stage and points of intersection between ENF and a hemispheric probe (represented by red circle) are marked by the user (blue circles). Intersections are only counted when the nerve fiber is in sharp focus at the point of crossing.

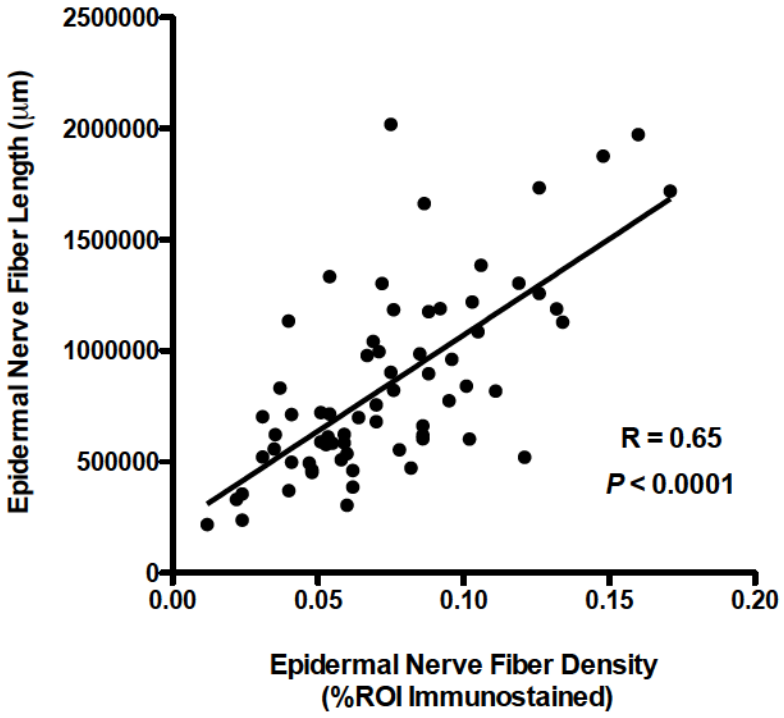


**Figure 2-2.** *Two ENF quantification methods yield strongly correlative results*. Two different image analysis techniques, one measuring nerve fiber density and the other measuring fiber length, were developed. When both quantification methods were applied to the same skin samples there was strong direct correlation between the techniques ($p < 0.0001$, $R = 0.65$, Spearman rank correlation).

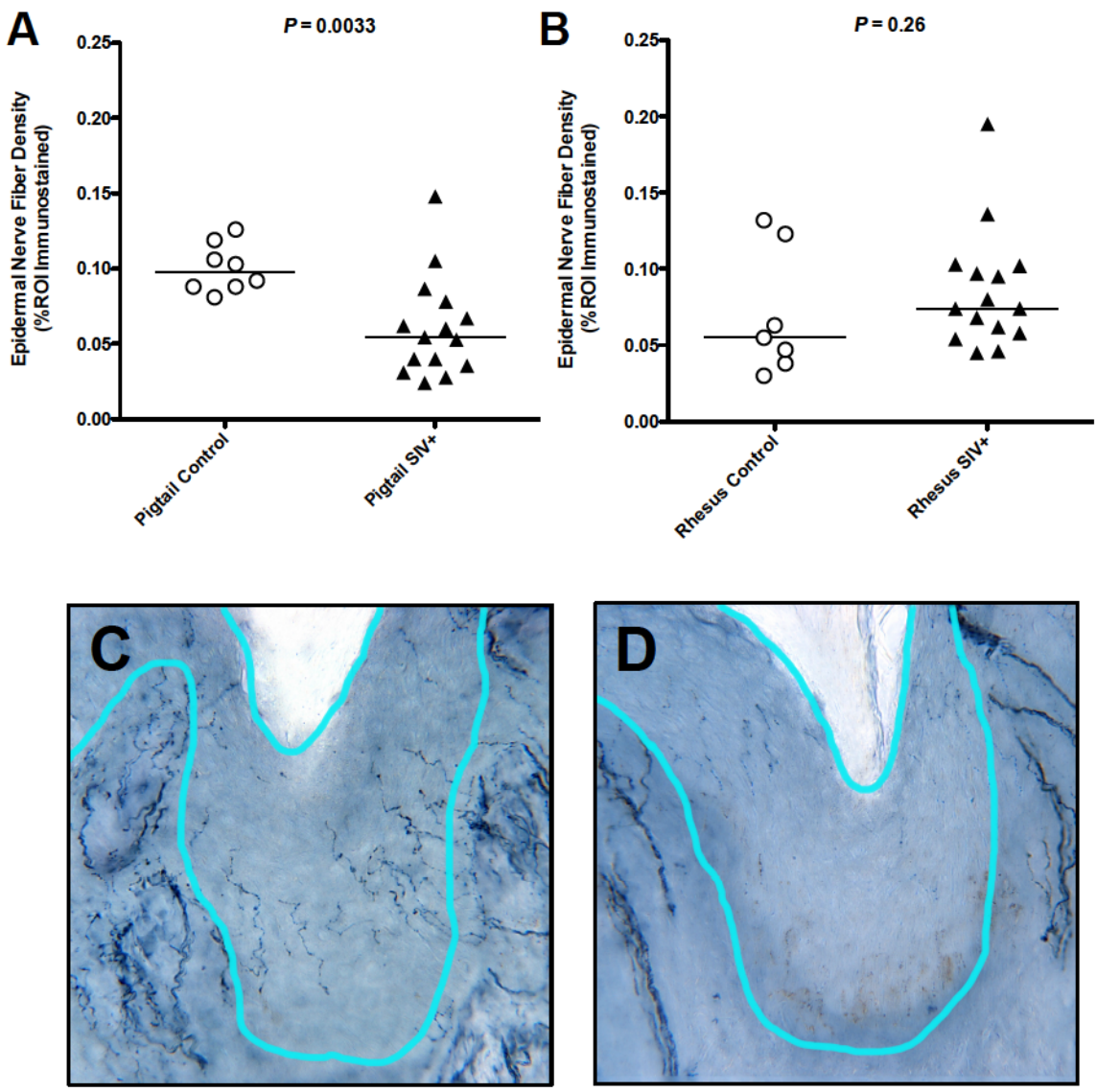
A
P = 0.0033
Epidermal Nerve Fiber Density
(%ROI Immunostained)
0.25
0.20
0.15
0.10
0.05
0.00
Pigtail Control
Pigtail SIV+
B
P = 0.26
Epidermal Nerve Fiber Density
(%ROI Immunostained)
0.25
0.20
0.15
0.10
0.05
0.00
Rhesus Control
Rhesus SIV+
C
D

**Figure 2-3.** *Species differences in ENF loss during SIV infection.* Pigtailed macaques exhibited significant decline in ENF density at 84 days post SIV infection (A; $p = 0.003$), but there was no significant difference in ENF density between rhesus macaques euthanized at terminal SIV time points versus control animals (B; $p = 0.26$, Mann-Whitney U test). Photomicrographs of skin biopsies from control (C) and SIV-infected (D) pigtailed macaques demonstrate a marked decrease in the number of thin, finely-beaded PGP9.5-stained nerve fibers in the epidermis. The light blue line delineates the region of interest (ROI) for assessing epidermal nerve fibers. Bundles of thicker PGP9.5-stained dermal nerve fibers can be seen below the dermoepidermal junction.

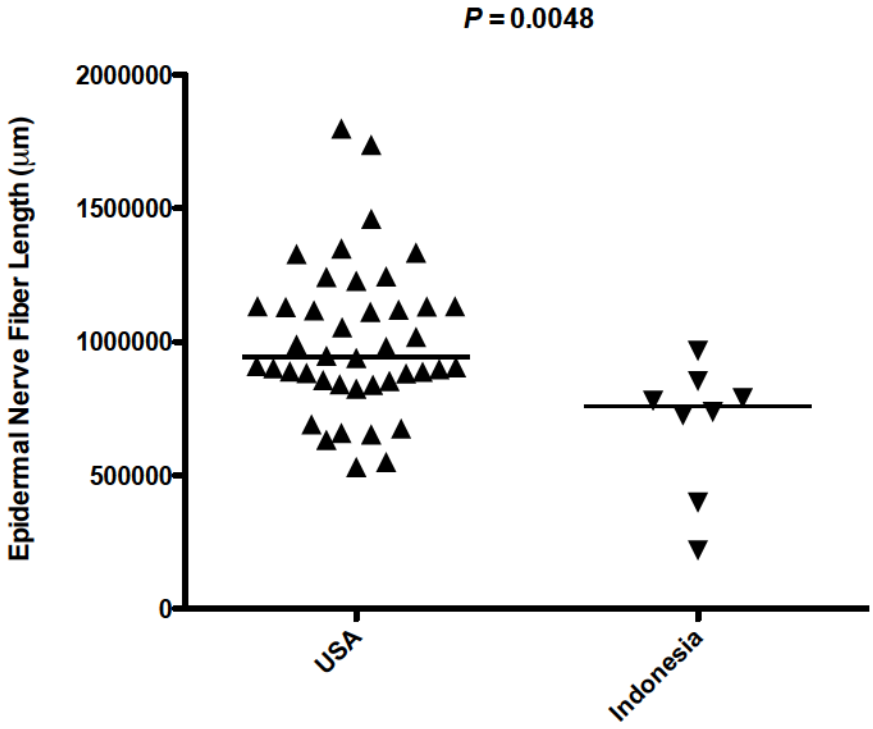


**Figure 2-4**. *Differences in baseline ENF length based on country of origin.* When comparing baseline ENF length of pigtailed macaques originating from different countries, animals from the United states had significantly higher baseline ENF than animals born in Indonesia (p = 00.48, Mann-Whitney U test).

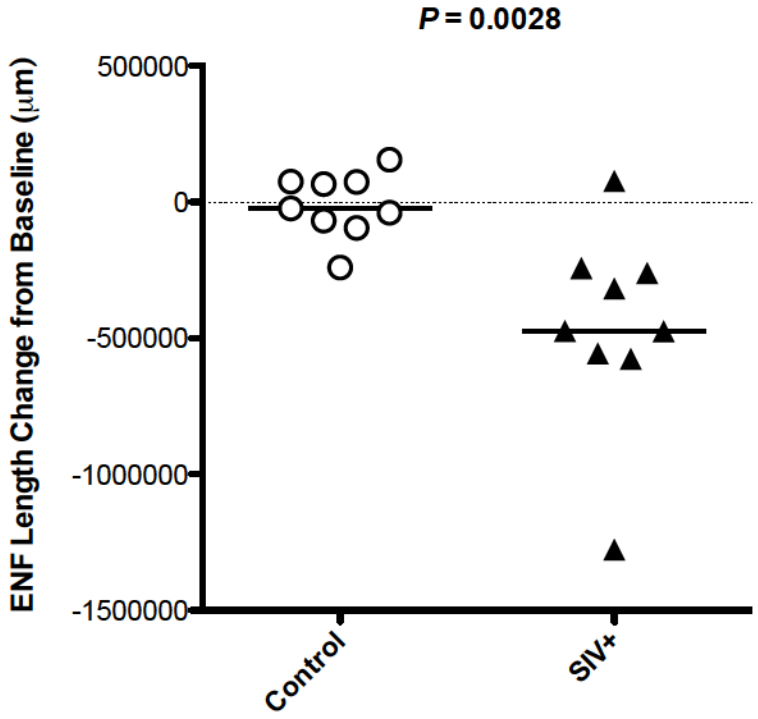


**Figure 2-5**. *Measuring change from baseline allows longitudinal assessment of ENF loss.* Footpad skin biopsies were collected from pigtailed macaques at the time of inoculation (SIV or mock) and at necropsy, 84 dpi. ENF length measurements obtained from each animal's necropsy skin samples were compared to measurement from their pre-infection samples, and results were plotted as "change from baseline." SIV-infected pigtailed macaques had a median decrease of approximately $5x10^4$ μm, which was significantly different from the median change observed in uninfected animals, which was close to zero ($p = 0.0028$, Mann-Whitney U test).

# III. Neuroinflammation and virus replication in the spinal cord of SIV-infected macaques

This chapter has been previously published as:

**Mangus LM**, Dorsey JL, Laast VA, Hauer P, Queen SE, Adams RJ, McArthur JC, Mankowski JL. Neuroinflammmation and virus replication in the spinal cord of SIV-infected macaques. Journal of Neuropathology and Experimental Neurology. 2015. 74(1): 38-47.

**Abstract**

Studies of neurologic disease induced by SIV in Asian macaques have contributed greatly to the current understanding of HIV pathogenesis in the brain and PNS. However, detailed investigations into SIV-induced alterations in the spinal cord, a critical sensorimotor relay point between the brain and PNS, have yet to be reported. In this chapter, lumbar spinal cords from SIV-infected pigtailed macaques were examined to quantify SIV replication and associated neuroinflammation. In untreated SIV-infected animals, there was a strong correlation between amount of SIV RNA in the spinal cord and expression of the macrophage marker CD68, as well as key pro-inflammatory mediators *TNFα* and *CCL2*. We also found a significant correlation between SIV-induced alterations in the spinal cord and the degree of distal epidermal nerve fiber loss among untreated animals. Spinal cord changes also were present in SIV-infected antiretroviral-treated animals including elevated GFAP immunostaining and enhanced *CCL2* expression despite SIV suppression. A fuller understanding of the complex virus and host factor dynamics in the spinal cord during HIV infection will be critical in the development of new treatments for HIV-associated sensory neuropathies and studies aimed at virus eradication from the central nervous system.

## Introduction

Although a multitude of studies thoroughly describe the morphologic and molecular alterations that develop in the brain and peripheral nerves of HIV patients and SIV-infected macaques [30,41-43,100-103], there have been few detailed analyses of the effects of HIV/SIV infection on the spinal cord. The majority of studies that do address HIV-associated spinal cord disease were published during the pre-combination antiretroviral therapy (cART) era, when opportunistic CNS infections, fulminant HIV encephalo-myelitis, and an enigmatic degenerative condition known as vacuolar myelopathy were common findings at autopsy [104-109]. While the frequency of serious complications directly attributable to spinal cord disease has waned since the deployment of modern cART, investigators have recently begun to consider the role of spinal cord alterations in the pathogenesis of what is currently the most common neurologic complication of HIV infection, HIV-SN. HIV-SN is reported to affect up to 60% of individuals living with HIV infection and causes a range of uncomfortable, difficult to manage symptoms including "painful numbness" or burning sensations, hyperalgesia, and allodynia [1,6]. Although the pathogenesis of this condition is incompletely understood, the development of chronic neuropathic pain likely involves sensitization peripherally, at the level of the nerves and ganglia, as well as centrally, within the spinal cord [13]. Notably, three recent studies by Tang and colleagues demonstrated increased glial activation, enhanced pro-inflammatory signaling, and elevated concentrations of HIV gp120 in the spinal cords of autopsy patients with histories of HIV-associated pain when compared to "pain negative" HIV patients [14-16].

In-depth analysis of the HIV/SIV infection in the spinal cord is also highly relevant to ongoing investigations of the CNS as a reservoir for residual viral replication and latent, integrated provirus in patients receiving cART. It is widely recognized that macrophages and microglia, and potentially astrocytes, in the brain serve as reservoirs for viral replication and reactivation, and that neuroimmune activation often persists in the brain despite systemic viral suppression [38,110,111]. Yet, there are currently no reports addressing whether a similar situation exists in the spinal cord. With its positioning behind the blood-CNS-barrier and a full complement of potentially infectable and immunoactive glial cells, residual HIV infection of the spinal cord could significantly contribute to viral persistence in the CNS and impact therapeutic strategies aimed at viral eradication.

In the present study, we performed morphologic and molecular analyses of the spinal cord in SIV-infected pigtailed macaques. This well-established animal model has been shown to closely recapitulate HIV-induced lesions in the brain and peripheral nervous system (PNS) within a consistent time course of 12 weeks [112,113]. In contrast to human studies, use of macaques allows for comprehensive sampling of key CNS and PNS components at progressive time points throughout the course of infection, with and without concurrent cART, and in the absence of potentially confounding comorbid conditions. Because symptomatic HIV-SN occurs predominantly in patients with advanced disease, as well as patients on cART [25,31], we focused on groups of animals euthanized during the terminal stage of SIV infection (84 days post infection) and a group of infected animals that received virally suppressive cART for several months. Individual animal's spinal cord alterations were then compared to PNS changes including loss of

ENF density, a commonly used measure of peripheral nerve injury. We hypothesized that spinal cords of infected animals would show evidence of neuroinflammation such as glial cell activation (microglia and astrocytes), as well as induction of soluble pro-inflammatory mediators that have been associated with pain-facilitating signaling pathways, specifically tumor necrosis factor-α (TNFα) and the chemokine CCL2. Furthermore, we postulated that certain neuroinflammatory parameters would remain elevated in the spinal cords of macaques receiving long-term cART as compared to uninfected control animals, similar to persistent neuroinflammation found in the brain of cART-treated, SIV-infected macaques.

## Materials and Methods

### *Animal Studies*

Twenty male pigtailed macaques were intravenously inoculated with both the neurovirulent clone SIV/17E-Fr and the immunosuppressive swarm SIV/DeltaB670 as previously described [114]. Fifteen animals did not receive antiretroviral treatment (untreated, SIV-infected group) and were euthanized at 12 weeks post infection (p.i.). Five animals were treated with antiretroviral medications beginning at day 12 p.i. and were euthanized at approximately 170 days p.i. (long-term cART group). The four-drug combination therapy consisted of the nucleotide reverse transcriptase inhibitor tenofivir (Gilead), two protease inhibitors, saquinavir (Roche) and atazanivir (Bristol-Myers Squibb), and the integrase inhibitor L-870812 (Merck, [115]). Doses and routes of administration were detailed previously [38]. Five additional uninfected pigtailed macaques served as untreated, virus-negative controls. At necropsy, the animals were saline-

perfused and collected tissues were either immersion fixed in Streck tissue fixative (Streck Labortories, Omaha, NE) followed by paraffin embedding or snap frozen in liquid nitrogen followed by storage at -80C. The animal procedures in this study were in accordance with the principles set forth by the Institutional Animal Care and Use Committee at Johns Hopkins University and the National Research Council's Guide for the Care and Use of Laboratory Animals ($8^{th}$ edition).

*Immunohistochemistry*

Immmunohistochemistry was performed on Streck-fixed paraffin-embedded sections of lumbar spinal cord. Tissues were deparaffinized in Histo-Clear (National Diagnostics, Atlanta, GA) followed by rehydration in a gradient series of alcohol. After antigen retrieval in sodium citrate buffer with 8-minute microwave treatment, sections were washed and then blocked prior to incubation in the appropriate primary antibody dilution (CD68, 1:2000; clone KP1, GFAP, 1:4,000; DAKO, Carpinteria, CA; KK41,1:4000, NIH AIDS Research and Reagent Reference Program), for one hour at room temperature. Sections were then incubated sequentially in biotinylated secondary multilink antibody and horseradish peroxidase-labeled streptavidin (Biogenex, San Ramon, CA). Chromogen detection was performed by incubating the sections in the substrate 3.3'-diaminobenzidine. The sections were then washed, cleared, and coverslipped with Permount mounting medium (Fisher Scientific, Pittsburgh, PA). Image acquisition and quantification of positive CD68 and GFAP immunostaining were performed using a Nikon DS-Ri1 color camera mounted on a Nikon Eclipse 90i microscope and NIS Elements software (version AR710). A composite image of an entire transverse section of

lumbar spinal cord was created by aligning serial images of contiguous 100X fields. Regions of interest (ROI) were traced manually and the percent of total area occupied by positively stained cells was determined for the entire transverse section of spinal cord, as well as the white and gray matter compartments separately.

*Immunofluorescent Staining and Confocal Microscopy*

To demonstrate active SIV infection of microglia/macrophages in the lumbar spinal cord, we performed fluorescent double-labeling for SIV gp41 and the polyclonal macrophage/microglia marker Iba-1 followed by confocal laser microscopy. The staining protocol was similar to that described for immunohistochemistry except that the primary antibodies and concentrations were KK41 (1:100) and Iba-1 (1:100, WAKO Lab Chemicals, Richmond, VA), and secondary antibodies were fluorescent-tagged AF488 Goat anti-mouse AF546 Goat anti-rabbit (both 1:100, Invitrogen). Sections were mounted using Prolong Gold Antifade reagent (Invitrogen, Carlsbad, CA) and sealed with clear nail polish. Colocalization of the resulting green (KK41) and red (Iba-1) fluorescent labeling was visualized using a Nikon C1 confocal laser microscope system mounted on a Nikon Eclipse TE2000-E microscope.

*Quantification of SIV RNA and cytokine mRNA in spinal cord tissue*

Total RNA was isolated from 25 mg of snap frozen tissue from the lumbar spinal cord by first extracting with RNA-Stat 60 (Tel-Test Inc, Friendswood, Tx) and chloroform, followed by purification using the MirVana kit (Invitrogen, Carlsbad, CA). Genomic DNA was removed from the samples using either RQ1 DNase (Promega, Fitchburg, WI)

or Turbo DNAse (Invitrogen) according to the manufacturer's protocols. All tissue samples for RNA isolation were consistently taken from the dorsal half of the spinal cord (dorsal to the central canal) and included both white and gray matter. Purified RNA was analyzed by real-time PCR using specific primers and probes for SIV *gag* [114], *TNFα* and *CCL2* [38]. SIV RNA copy number was determined by comparison to a standard curve. *TNFα* and *CCL2* gene expression was determined using the ddCt (cycle threshold) method [116] with normalization of cellular mRNAs to *18s* ribosomal RNA levels. Gene expression data is reported as fold change relative to that of control animals.

*Measurement of Epidermal Nerve Fiber Density*

Full-thickness skin samples from the plantar footpad were collected from control and infected animals at necropsy using a 3mm punch biopsy tool. Sections were obtained from an identical location in all animals. Skin sections were then fixed and cryoprotected as previously described [42]. Cryoprotected samples were sectioned using a freezing-sliding microtome to a thickness of 50um and immunostained for the panaxonal marker PGP9.5 (1:2000; Chemicon, Temecula, CA) as previously described [88]. Epidermal nerve fiber (ENF) density was measured using a modification of the method described by Kennedy et al [117] and McCarthy et al [88]. Briefly, 15 adjacent, nonoverlapping collapsed Z-stack images were obtained for each immunostained skin section. Serial Z-stack images for each microscopic field were collected at 0.5um intervals using a Zeiss microscope equipped with a z-motor at 400X magnification (Carl Zeiss, Oberkochen, Germany). PGP9.5 immunoreactivity was measured by digital image analysis using iVision software

(Version 4.0.14, BioVision Technologies, Exton, PA). To control for variations in thickness among sections, results were normalized to the thickness of each skin sample.

*Statistics*

All statistical inferences were calculated using nonparametric methods and GraphPad Prism Software (Version 5.0d). Group comparisons were performed using the Mann-Whitney test. Relationships between variables were determined using the Spearman rank correlation. For all analyses, statistical significance was assumed when the P value was less than 0.05.

**Results**

*SIV infection induces morphologic changes in the lumbar spinal cord*

Histopathologic lesions observed in the lumbar spinal cord of untreated, SIV-infected macaques were predominantly mild and consisted of modest perivascular infiltrates of lymphocytes and macrophages, most notable in the gray matter and meninges (mild lesions in n = 6 of 15 animals [40%]). A subset of animals exhibited more severe myelitis with lesions similar to those seen in SIV encephalitis including glial nodules (n = 4), pronounced perivascular cuffing (n = 4, Fig. 1A), and multinucleated giant cells (n = 3, Fig. 1B). Interestingly, all animals in which giant cells were observed in the lumbar spinal cord also had severe encephalitis. Immunostaining for the macrophage marker CD68 and SIV transmembrane glycoprotein 41 (gp41) confirmed that foci of inflammation included variable numbers of activated microglia/macrophages often harboring SIV (Fig. 1C,D). Confocal laser scanning microscopy of double-stained spinal cord sections showed clear co-localization of the macrophage/microglia marker Iba-1 and

SIV gp41, demonstrating active SIV infection of macrophage-lineage cells. Histologic lesions in the lumbar spinal cords of cART treated animals were limited to minimal lymphohistiocytic infiltrates in the meninges. However, in one cART-treated animal there was mild, bilaterally symmetrical vacuolization of the lateral white matter tracts characterized by frequent, dilated myelin sheaths, similar to changes described in mild cases of HIV-associated vacuolar myelopathy [104].

*Viral load is directly associated with increasing CD68, but not GFAP expression in the lumbar spinal cord of untreated, SIV-infected macaques*

SIV and HIV infection elicit immune activation of resident glial cells in the brain and peripheral nervous system, as well as recruitment of infiltrating macrophages [31,108,113,118]. Because the extent of glial cell activation is often not appreciated on routine histopathologic review, we utilized immunohistochemical staining as a measure of macrophage/microglial and astrocytic activation in the spinal cord. In untreated, SIV-infected animals, there was a significant increase in the amount of CD68 immunostaining, reflecting macrophage/microglial activation, in the gray matter of the lumbar spinal cord compared to control animals ($p = 0.045$, Fig. 2A) but not white matter ($p = 0.29$, data not shown). Furthermore, there was a direct correlation between SIV RNA levels and CD68 expression in both the gray matter ($p = 0.027$, $r = 0.59$, Fig. 2C) and white matter ($p = 0.047$, $r = 0.54$, data not shown). In contrast, there was no significant difference in the level of astrocyte activation, as measured by GFAP expression, between control and untreated, SIV-infected animals (gray matter: $p = 0.089$, Fig. 2B; white matter: $p = 1.0$, data not shown) nor was there an apparent relationship between viral load

and astrocyte activation (gray matter: $p = 0.90$, Fig. 2D; white matter: $p = 0.20$, data not shown).

*SIV induces expression of soluble pro-inflammatory mediators,* TNFα *and* CCL2*, in the lumbar spinal cord of untreated, SIV-infected macaques*

The pro-inflammatory cytokine tumor necrosis factor-α (TNFα) and the monocyte-attracting chemokine CCL2 (also known as monocyte chemoattractant protein-1, MCP1), have previously been shown to be elevated in the brain tissue of SIV infected macaques [38,119]. Additionally, enhanced expression of these molecules in the spinal cord has been implicated as a key factor in the genesis of neuropathic pain in a number of rodent models [17,120,121]. Gene expression analysis by qRT-PCR revealed marked induction of these soluble mediators in the lumbar spinal cords of untreated SIV-infected macaques. The degrees of both *TNFα* and *CCL2* expression showed strong direct correlation with SIV RNA levels (*TNFα*: $p = 0.0011$, $r = 0.78$, Fig 3A; *CCL2*: $p < 0.0001$, $r = 0.86$, Fig. 3B), as well as CD68 expression in the lumbar spinal cord (*TNFα*: $p = 0.0064$, $r = 0.67$, Fig. 3C; *CCL2*: $p = 0.0066$, $r = 0.67$, Fig 3D). However, there was no significant association between *TNFα* or *CCL2* expression with GFAP in the cART-naïve animals ($p = 0.42$ and $p = 0.58$, respectively, data not shown).

*In untreated, SIV-infected macaques, loss of epidermal nerve fibers is associated with increasing viral load, CD68,* TNFa*, and* CCL2 *expression in the lumbar spinal cord*

Numerous studies have demonstrated the importance of glial activation and enhanced cytokine and chemokine signaling within the spinal cord during neuropathic pain

syndromes [14,122-124]. To investigate the association between pro-inflammatory alterations in the lumbar spinal cord during SIV infection with pathologic changes in the peripheral nervous system, we compared results of each animal's spinal cord analyses to its degree of epidermal nerve fiber (ENF) loss, which in HIV patients has been shown to correlate with the development of neuropathic symptoms [54]. Striking loss of ENF density has also been previously reported in the accelerated SIV/pigtailed macaque model, with significant decline in epidermal innervation by 8 weeks p.i. [42]. In untreated, SIV-infected macaques, there was a significant inverse correlation between ENF density and spinal cord viral load ($p = 0.030$, $r = -0.58$, Fig. 4A), CD68 immunostaining ($p = 0.014$, $r = -0.62$, Fig. 4B), as well as *TNFα* ($p = 0.016$, $r = -0.61$, Fig. 4C) and *CCL2* gene expression ($p = 0.0091$, $r = -0.65$, Fig. 4D).

*Long-term cART treated macaques show elevated GFAP and* CCL2 *expression in the spinal cord without detectable viral replication*

A previous study using the accelerated SIV/pigtailed macaque model [38] demonstrated that long-term cART effectively suppressed viral replication in the brain, along with normalization of some inflammatory parameters measured, including GFAP and MHC class II expression. However, evidence of persistent inflammation was detected in the brains of treated animals in the form of elevated CD68 immunostaining and expression of *interleukin-6* (IL-6), *TNFα*, and *CCL2*, all of which failed to return to normal levels with treatment. Viral DNA was also detected in the brain tissue of these cART-treated animals, suggestive of latent, integrated provirus. Persistent immune activation has also been observed in the brains of virally-suppressed HIV patients in the absence of

detectable viral replication, and is thought to play a critical role in the progressive neuronal degeneration seen in HIV-associated neurocognitive dysfunction [101,102,125,126]. As in the brain, SIV RNA was below the level of detection (<100 copies per µg RNA) in the lumbar spinal cord of cART-treated animals by qRT-PCR, but there was no significant difference in the levels of spinal cord CD68 immunostaining or *TNFα* expression between cART-treated animals and controls ($p = 0.11$ and $p = 0.79$, respectively, data not shown). Conversely, there was significantly elevated levels of GFAP immunostaining in both the gray and white matter of cART-treated animals ($p = 0.016$ and $p = 0.021$, respectively, Fig. 5A-D), as well as a modest elevation in spinal cord *CCL2* expression ($p = 0.071$, data not shown), indicating that these parameters remain elevated above control values despite long-term suppressive cART.

Similar to the untreated SIV-infected macaques, animals treated with long-term cART had markedly decreased ENF density at the time of necropsy. We did not find a significant correlation between GFAP and epidermal nerve fiber loss among cART-treated animals ($p = 0.92$, $r = 0.20$, data not shown); however, this may be related to the small number of cART treated animals from which paraffin-embedded lumbar spinal cord was available (n=4). Additionally, there was no significant association between spinal cord *CCL2* expression and ENF density among cART-treated animals ($p = 0.083$, $r = 0.90$, data not shown).

**Discussion**

SIV-infected macaques have served as the preeminent animal model for studying HIV pathogenesis for over two decades; however, spinal cord neuropathology has not been

reported in detail in the SIV/macaque model. Together, our findings demonstrate that the spinal cord, like the brain, is an important CNS site of SIV viral replication in untreated animals and that a subset of neuroinflammatory changes persist in the spinal cord despite virally-suppressive cART. In untreated animals euthanized during terminal disease (84 days p.i.), high levels of SIV RNA strongly correlated with increasing expression of the macrophage/microglia activation marker CD68 and robust induction of the innate immune signaling mediators TNFα and CCL2. These findings are similar to those in the brain, and we observed significant correlation between the degree of CD68 expression in the lumbar spinal cord and the basal ganglia of these animals ($p = 0.014$, data not shown). In animals that received long-term cART, levels of CD68 immunostaining and *TNFα* gene expression in the spinal cord were not statistically different from uninfected controls, but astrocyte activation, as measured by GFAP immunostaining, was markedly elevated along with increased *CCL2* gene expression. This is in contrast to findings in the brain of cART-treated animals, as previously reported by Zink and colleagues [38], where GFAP expression was not significant different from control values, but CD68 and *TNFα* expression were elevated.

The lesions present in the PNS of HIV patients with sensory neuropathy and SIV-infected pigtailed macaques have previously been described in detail [42,100,112]. It is well recognized that these patients and macaques show evidence of morphologic and functional abnormalities of the small diameter nerve fibers in the periphery, which detect and transduce noxious stimuli and conduct nociceptive signals to the CNS, as well as inflammatory changes in the dorsal root ganglia, which house the cell bodies of primary afferent sensory neurons. However, it has been proposed that the development of chronic

neuropathic pain in HIV patients also involves pathologic alterations in the spinal cord [13], where primary afferent neurons synapse with second order afferents and interneurons in the dorsal horns, and nociceptive signals are processed and modulated prior to transmission to the brain [127]. Indeed, many studies using rodent models of nociception have clearly established that spinal glial cell activation is a critical and necessary factor in the generation of acute and chronic pain [47,128,129]. Further, soluble inflammatory mediators released by activated glial cells, such as cytokines TNFα, IL-1, IL-6, and chemokines CCL2 and CX3CL1 (fractalkine), have been shown to powerfully modulate synaptic transmission of sensory signals in the spinal cord [122-124,130]. While the physiologic functions of glial activation and enhanced immune signaling may be evolutionarily protective in the setting of acute pain and important in the clearance of injurious agents and damaged neurons, prolonged immune stimulation and dysregulation also may contribute to pathologic pain states.

HIV infection induces chronic, systemic immune activation that often involves the nervous system and is not fully normalized by the use of virally-suppressive cART. Thus it is not surprising that a large proportion of HIV patients are currently living with symptoms of chronic, pathologic pain [23]. To investigate this challenging phenomenon, Tang and colleagues have recently published a series of three reports outlining changes present in the spinal cord dorsal horns of HIV patients with painful symptoms of sensory neuropathy, but absent in HIV-infected individuals without pain [14-16]. Alterations in the glial activation profile that were specific to 'pain-positive' HIV patients included elevated GFAP expression, indicative of astrocyte activation, increased production of cytokines TNFα and IL-1β, and upregulation of proteins involved in MAPK signaling. In

addition, dorsal horns of HIV patients with pain showed evidence of synaptic loss along with increases in markers of neuronal activity and plasticity, consistent with the process of central sensitization. Interestingly, quantification of HIV viral proteins revealed that patients with pain had significantly higher levels of gp120 in the spinal cord dorsal horns compared to 'pain-negative' patients, but relatively lower levels of Tat, suggesting differential viral gene expression and the potential importance of gp120 specifically in the development of painful symptoms. Intrathecal injection of gp120 in the spinal canal of mice resulted in molecular alterations that closely mirrored those seen in the HIV patients with pain [16]. Mice also developed marked spinal macrophage/microglial activation, which was not evident in the HIV patients, along with mechanical hypersensitivity and progressive decline in ENF density in the hind paws.

The reported findings in the spinal cords of HIV patients with pain reflect a combination of the changes present in the spinal cords of both untreated macaques euthanized during terminal disease and in cART-treated animals. This is not surprising since the HIV patients in these studies died with clinical AIDS, but also had received various antiretroviral drugs throughout the course of their disease. It is widely recognized that sensory neuropathy can arise due to neurotoxic effects of certain antiretroviral drugs, resulting in a syndrome known as antiretroviral toxic neuropathy (ATN) that is clinically indistinguishable, and likely often concomitant, with HIV-SN [131]. The predominance of astrocytic reaction in the spinal cords of HIV patients with pain closely resembles that seen in the cART-treated macaques, whereas significant upregulation of pro-inflammatory mediators is more in line with the untreated macaques that had advanced disease. It is possible that astrocyte activation in the spinal cord is associated with toxic

neuronal injury rather than a virus-induced inflammatory response. Another explanation would be that GFAP expression was elevated in untreated animals at earlier time points during the course of disease, but declined during the terminal stage. A distinct pattern has previously been reported in the dorsal root ganglia of SIV-infected pigtailed macaques, where there is an early increase in GFAP expression that is sustained throughout asymptomatic infection but wanes by the 84d.p.i. timepoint [42], possibly reflecting the progression from a state of sustained glial activation to eventual degeneration and loss. Also, although GFAP immunostaining is widely used as a marker of astrocyte activation, GFAP expression does not necessarily correlate with functional changes such as altered expression of surface receptors, ion channels, or production of cytokines and chemokines, which more directly influence pain signaling [122].

Significant correlations between ENF loss and severity of spinal cord inflammation and viral load in the cART-naïve macaques is compelling and, along with Tang and colleague's findings in mice, suggests that chronic stimulation and perhaps injury of the central terminus of sensory nerves can contribute to pathologic changes in the peripheral nerve fibers. In cART-treated animals, which also exhibited significant ENF loss, peripheral nerve damage may be attributable to antiretroviral toxicity rather than virus-induced injury to the sensory pathway. Future studies with uninfected, cART-treated macaques will be instrumental in dissecting this complex pathogenesis.

Study of the spinal cord is also germane to another, critically important topic in contemporary HIV research, viral eradication from the CNS. Several studies have demonstrated the presence of low-level viral RNA, integrated viral DNA, and persistent immune activation in the brains of HIV patients and SIV-infected primates on

suppressive cART, and hypothesized that microglia and infiltrating macrophages serve as reservoirs for residual viral replication and reactivation in the CNS [33,38,101,110,111,132,133]. However, there are currently no published studies addressing whether the spinal cord, a major component of the CNS, is also a potential viral reservoir in patients on modern cART. Our results show that the spinal cord is an active site of viral infection and replication in some cART-naïve animals. Since microglia and infiltrating macrophages are also abundant in the spinal cord, studies investigating CNS viral latency and persistent neuroinflammation should consider evaluating multiple anatomic locations in the spinal cord as well as the brain. Also, rodent models of acute CNS inflammation have revealed major differences in immune responses, microglial activation, and blood-CNS-barrier breakdown when comparing the brain and spinal cord [134-138]. This dichotomy has yet to be investigated in a primate model of chronic CNS inflammation, and could have substantial impact on the pathogenesis of HIV infection and persistence in the CNS. Studies based in the SIV/pigtailed macaque model could investigate the presence of residual low-level viral replication, as well as latent, integrated provirus in macrophages and microglia of the spinal cord.

Although widespread use of cART has drastically reduced morbidity and mortality caused by HIV infection, the continued high frequency of chronic neurologic complications and pursuit of systemic viral eradication are enduring challenges. This investigation into the neuropathology of the spinal cord of SIV-infected macaques demonstrates the importance of considering this key CNS compartment in future studies aimed at elucidating the mechanisms underlying painful HIV-SN and the development of novel treatment strategies for this debilitating condition. Furthermore, careful

examination of the spinal cord is warranted in the continuing effort to understand CNS viral reservoirs and achieve sterilizing cure of HIV infection.

**Figures**

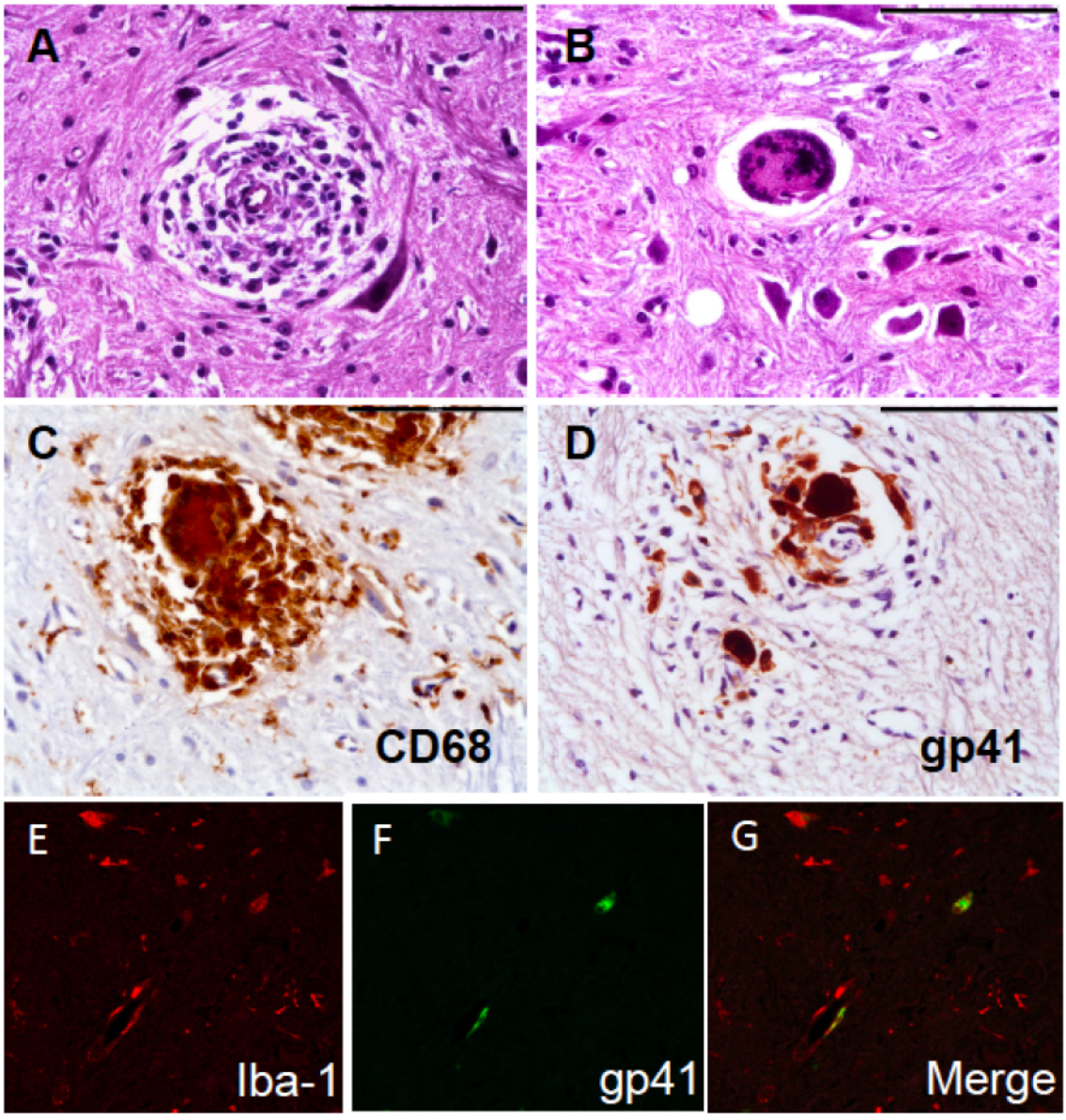

**Figure 3-1.** *Morphologic changes in the lumbar spinal cord of untreated SIV-infected macaques.* While histologic lesions observed in hematoxylin and eosin-stained sections of lumbar spinal cord were typically mild, a subset of SIV-infected animals showed evidence of more severe myelitis, including pronounced perivascular cuffing **(A)** and multi-nucleated giant cells **(B).** Immunostaining for the macrophage marker CD68 and SIV gp41 demonstrated that inflammatory foci included numerous activated macrophages/microglia **(C)**, that were often infected by SIV **(D)**. Confocal laser scanning microscopy was performed in sections of lumbar spinal cord that were double-stained for the macrophage marker Iba-1 (**D**, red) and SIV gp41 (**E**, green). A composite image **(G)** showed clear colocalization of Iba-1 and SIV gp41, confirming that macrophages in the lumbar spinal cord are target cells for SIV infection. Scale bars = (A-D) 100 μm. Original magnification for E-G, 400X.

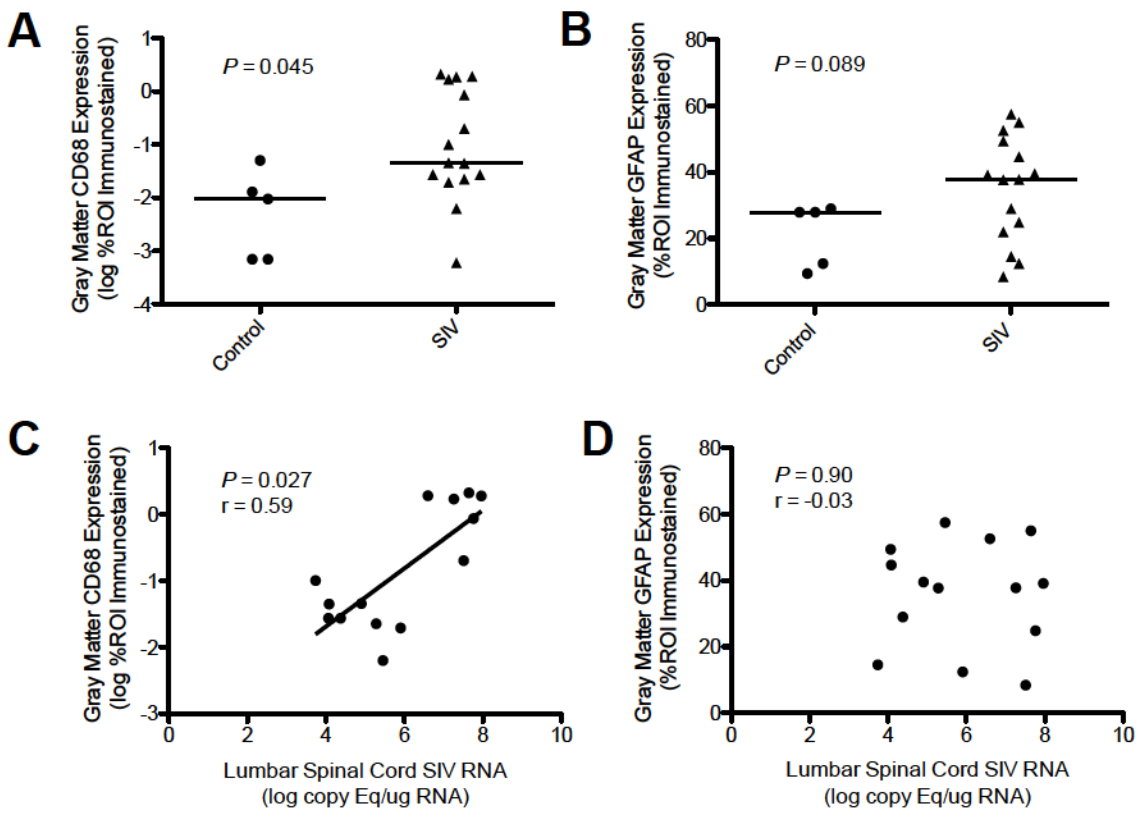


**Figure 3-2.** *Glial activation in the lumbar spinal cord of untreated SIV-infected macaques.* **A:** Reflective of enhanced macrophage/microglia activation, untreated SIV-infected macaques had significantly elevated CD68 immunostaining in the gray matter of the lumbar spinal cord compared to control animals (p = 0.045, Mann-Whitney). **B:** Glial fibrillary acidic protein (GFAP) immunostaining, an indicator of astrocyte activation, was not significantly different between control and untreated SIV-infected macaques (p = 0.089, Mann-Whitney). **C:** Similarly, there was a significant, direct correlation between SIV viral load and CD68 expression in the spinal gray matter of untreated animals (p = 0.027, r = 0.59, Spearman rank correlation), but there was no significant relationship between GFAP expression and viral load **(D)** (p = 0.90, r = -0.03, Spearman rank correlation). Bars in A-B represent median values.

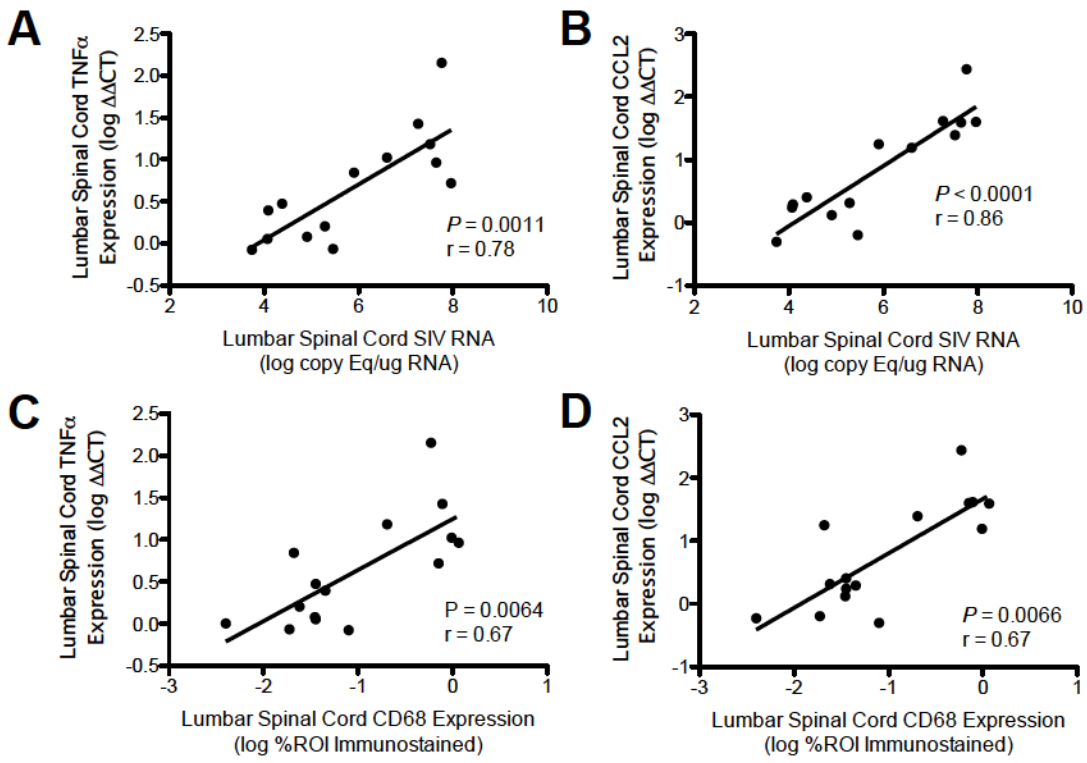


**Figure 3-3.** *SIV induces expression of* TNFα *and* CCL2 *in the lumbar spinal cord of untreated SIV-infected macaques*. **A-B:** Quantitative reverse transcription PCR (qRT-PCR) analysis showed strong, direct correlations between SIV viral load and expression of the soluble pro-inflammatory mediators *TNFα* and *CCL2* (*TNFα*: p = 0.0011, r = 0.78; *CCL2*: p < 0.0001, r = 0.86, Spearman rank correlation). **C-D:** Expression of *TNFα* and *CCL2*, as measured by qRT-PCR, also showed a significant, direct correlation with the degree of CD68 expression in the lumbar spinal cord, indicating that expression of these mediators and macrophage/microglia activation are covariant in this group of animals (*TNFα*: p = 0.0064, r = 0.67; *CCL2*: p = 0.0066, r = 0.67, Spearman rank correlation).

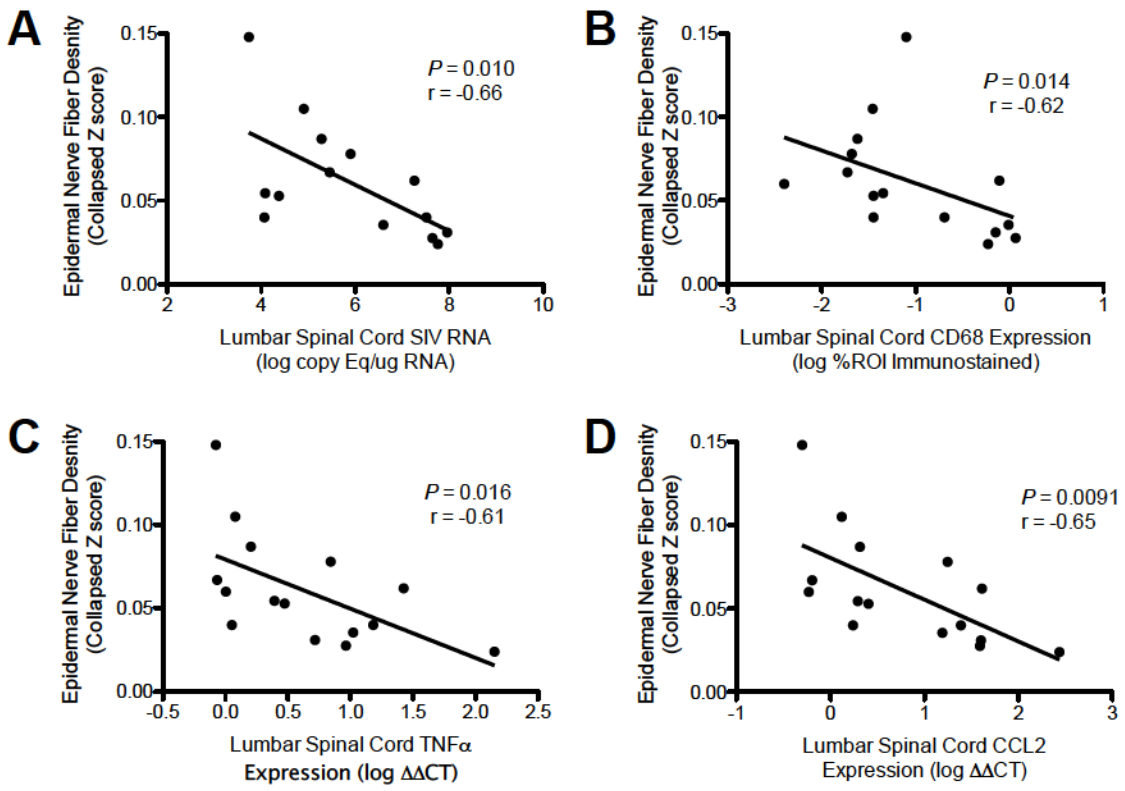


**Figure 3-4.** *Among untreated SIV-infected macaques, declining ENF density is associated with increasing viral load and neuroinflammation in the lumbar spinal cord.* To investigate the relationship between SIV infection and pro-inflammatory alterations in the spinal cord to pathologic changes in the peripheral nerves, we compared results of each animal's spinal cord analysis to its epidermal nerve fiber density in the footpad. In untreated SIV-infected animals, there were significant inverse correlations between ENF density and (A) SIV viral load ($p = 0.030$, $r = -0.58$), (B) CD68 immunostaining ($p = 0.014$, $r = -0.62$), (C) *TNFα* expression ($p = 0.016$, $r = -0.61$), and (D) *CCL2* expression in the lumbar spinal cord ($p = 0.0091$, $r = -0.65$). All statistical inferences based on Spearman rank correlation.

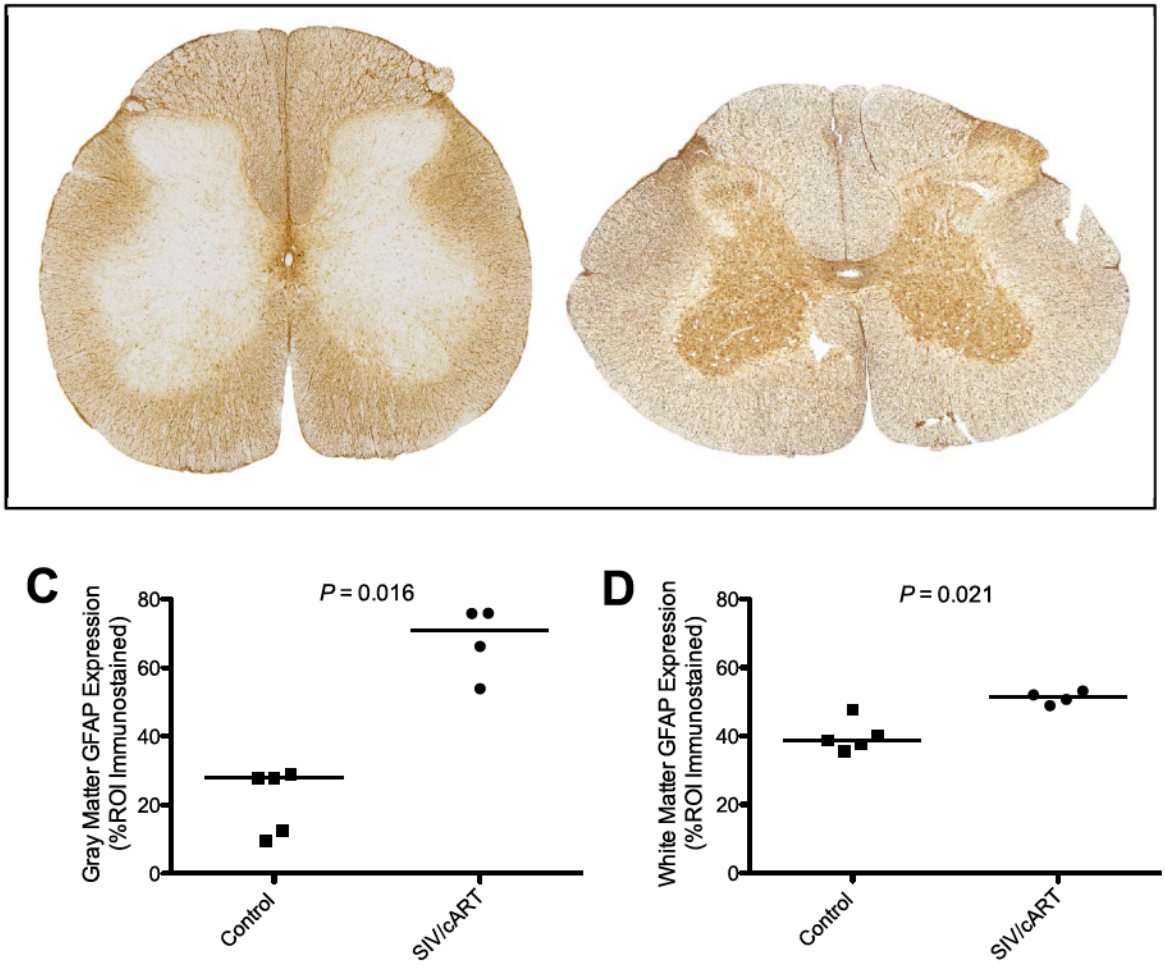


**Figure 3-5.** *SIV-infected macaques on long-term combination antiretroviral treatment (cART) showed evidence of significant astrocyte activation in the lumbar spinal cord despite non-detectable SIV viral load.* **A-B:** Representative images of lumbar spinal cord from a control and SIV-infected, cART-treated macaques immunostained for the astrocyte marker glial fibrillary acidic protein (GFAP; brown staining indicates positive immunoreactivity). **C:** cART-treated animals showed markedly increased GFAP expression in the gray matter compared to controls ($p = 0.016$, Mann-Whitney). **D:** GFAP expression was also significantly higher in the white matter of cART-treated animals, although to a lesser degree ($p = 0.021$, Mann-Whitney).

# IV: Immune activation in the PNS during acute SIV infection

**Abstract**

Efforts to explain the continued high prevalence of human immunodeficiency virus HIV-associated neurologic disorders are increasingly focused on the early stages of infection. It has long been recognized that HIV gains entry into the CNS soon after transmission, and recent studies have shown compelling evidence that significant CNS immune activation, neuronal injury, and cognitive dysfunction arise early during the course of infection in many individuals. Comparatively little is known about the status of the PNS during early stages of disease, despite the fact that HIV-SN remains the most frequent neurologic complication of HIV. In this chapter, we utilized a well-established SIV/macaque model of HIV-SN to examine molecular alterations occurring within the PNS during acute infection. By employing a combination of RNA, protein, and immunohistochemical analyses of the lumbar DRG, we found that acute SIV infection is associated with significant immune activation in the DRG, as well as alterations in the expression of enzymes related to glutamatergic metabolism and the oxidative stress response. Together with our previous finding of significant epidermal nerve fiber loss in macaques euthanized at just 14 days post infection, these results suggest that immune activation and altered cellular metabolism at the level of the DRG precede and likely contribute to early sensory nerve injury, thereby setting the stage for progressive neuronal dysfunction. A comprehensive understanding of the early pathogenic mechanisms in HIV-SN may reveal therapeutic approaches for neuroprotection in HIV patients.

## Introduction

Sensory neuropathy (SN) continues to be a frequent and challenging neurologic complication of HIV infection despite widespread use of modern cART [1,70]. Distal sensory polyneuropathy (DSP) is the most common form of PN seen in HIV patients, and typically presents as numbness, parestethias, and pain of the distal extremities [5,139]. Although DSP is not a life-threatening condition, the painful symptoms can deleteriously affect patients' quality of life and are often only partially mitigated by conventional analgesic medications [6-8,140]. Lack of effective treatment stems from our incomplete understanding of the mechanisms underlying sensory nerve injury in the context of HIV infection. While autopsy studies have demonstrated increased amounts of viral proteins and inflammatory mediators in the DRG and spinal cord of HIV patients with neuropathy [14-16,141,142], such studies have been limited to patients with late-stage disease. Relatively little is known about PNS damage or dysfunction during early stages of HIV infection, a time when interventions aimed at reversing or preventing nerve injury could be prove more successful.

A recent clinical study by Wang and colleagues [63] found that, among a cohort of patients with primary HIV infection (defined as <1 year after transmission), 35% of individuals had signs of PN and 20% were symptomatic for PN. They also demonstrated that the occurrence of PN in this cohort was associated with elevated markers of immune activation in the plasma and cerebrospinal fluid (CSF), suggesting that PN during early HIV infection may be mediated by systemic and nervous system immune responses. Importantly, this group underwent detailed neurologic evaluation prior to the initiation of cART, which itself can cause antiretroviral toxic neuropathy (ATN), a condition that is

clinically indistinguishable from HIV-mediated DSP, and often confounds studies of PN in HIV patients.

Similar to these findings in primary HIV patients, previous studies by our group have demonstrated alterations in the PNS of simian immunodeficiency virus (SIV)-infected pigtailed macaques (*Macaca nemestrina*) euthanized at early time points in the course of disease. In a 2007 study by Laast et al., we showed that SIV RNA was detectable by *in situ hybridization* in the trigeminal ganglia of animals euthanized during acute and asymptomatic stages of infection [41]. Subsequent studies have focused on the lumbar DRG, which contain the cell bodies of sensory neurons that innervate the lower limbs. We found significantly increased amounts of CD68 immunostaining, a marker of macrophage activation, in the DRG of animals at 10 dpi, followed by significant decline in epidermal nerve fiber density (ENFD), a surrogate marker for sensory nerve damage, at 14 dpi. This suggested that inflammation in the DRG during acute infection might contribute to early sensory nerve injury and die-back of distal axons. In addition, significant loss of ENFD persisted in a group of cART-treated macaques despite initiation of therapy at 12 dpi (end of acute phase) and sustained virologic suppression from approximately 50 dpi until necropsy [64], further highlighting the potential importance of early sensory nerve damage in the development of PN.

The observation that CD68 immunostaining is increased in the DRG during acute SIV infection and precedes significant losses of ENFD supports the premise that macrophage-mediated inflammation in the DRG contributes to early sensory nerve injury and degeneration of distal axons. However, while increased CD68 immunostaining is an often-used indicator of macrophage activation, it is a relatively nonspecific marker and

provides no information regarding the molecular processes leading to or resulting from this activation state. In the current study, we sought to gain a more detailed understanding of the immune responses occurring within the DRG during acute SIV infection and to identify potential mechanisms for sensory nerve injury. We performed RNA and protein isolation on lumbar DRG collected from uninfected macaques, as well as SIV-infected animals euthanized at 7 dpi - the acute time point when plasma and CSF viral loads peak following SIV inoculation in our model [113]. RNA was used for Nanostring nCounter gene expression analysis, a technology that allows for the quantification of a large number of mRNA transcripts without reverse transcription or DNA amplification [143,144]. From the Nanostring panel, we focused on genes related to immune signaling and activation, as well as genes involved in glutamate metabolism and oxidative stress, two pathways that have been strongly implicated in the pathogenesis of neuronal injury during HIV-associated neurocognitive disease (HAND) [145-149]. Significant novel findings from the gene expression analysis were further queried at the protein level by Western blot using lumbar DRG homogenates and immuhistochemistry on fixed tissue sections.

## Methods

### *Animals*

Six juvenile male pigtailed macaques were intravenously dual-inoculated with the neurovirulent clone SIV/17E-Fr and the immunosuppressive swarm SIV/DeltaB670 as previously described [114] and euthanized at day 7 post infection (from hereon referred to as 7d SIV-infected animals). Eight uninfected pigtailed macaques served as controls and were euthanized at 12 weeks following sham inoculation. At the time of necropsy,

animals were whole-body saline perfusion to remove blood from tissue vasculature. PNS tissues were dissected and either snap frozen and stored at -80°C until use or fixed in Streck tissue fixative (Streck Labortories, Omaha, NE) and embedded in paraffin. All animal procedures in this study were conducted with the approval of the Johns Hopkins Animal Care and Use Committee and the National Research Council's Guide for the Care and Use of Laboratory Animals (8th edition).

*RNA isolation and gene expression analysis*

Total RNA was isolated from frozen L3 DRG by first extracting with RNA-State 60 (Tel-Test Inc., Friendswood, TX) and chloroform, followed by purification using the RNeasy kit (Qiagen, Valencia, CA) according to the manufacturer's protocol, with the inclusion of on-column genomic DNA removal using the RNase-Free DNAse Set (Qiagen, Hilden, Germany). RNA concentration and purity were measured using a Nanodrop Spectrophotometer (Thermo Fisher Scientific, Waltham, MA).

A total of 100 ng of RNA per sample was used for nCounter Gene Expression Assay (Nanostring Technologies, Seattle, WA), which was performed according to the manufacturer's protocol by the Johns Hopkins Deep Sequencing and Microarray Core Facility. The assay made use of a custom Nanostring Codeset designed to measure 249 transcripts of interest and 11 putative housekeeping transcripts based on rhesus macaque (*Macaca mulata*) and human sequences. For the purpose of this study, analysis was focused on genes involved in immune activation and the early antiviral response (IRF7, STAT1, MX1, CCL8, CXCL10, CXCL11), glutamate metabolism (GLS and GLUL), and

in the oxidative stress response (SOD1 and SOD2). To account for probe-specific background, 100ng of MS2 phage RNA (Roche, Basel, Switzerland) was run in duplicate as a negative control.

Nanostring data were analyzed by first adding a value of 1 to all counts (to exclude any zero values), normalizing to the geometric mean of manufacturer spike-in controls, and normalizing to the geometric mean of the four housekeeping genes that were most stably expressed in the DRG among animal groups (GAPDH, SDHA, HRPT1, and TBP). Data are reported as normalized transcript counts. The lower limit of detection for each probe was set to the mean value for the MS2 phage RNA control +2 standard deviations. Genes that had values falling below the limit of detection were excluded from analyses.

Although TNFα was included in the Nanostring panel, counts for control and 7d SIV-infected animals were low compared to those of other transcripts of interest (< 60 counts). Therefore, results from the Nanostring analysis were further corroborated by a separate qRT-PCR assay. For this, 500ng of RNA was used for complementary DNA synthesis using the High Capacity cDNA Reverse Transcription Kit (Applied Biosystems, Forest City, CA) followed by a 10-cycle pre-amplification reaction using TaqMan PreAmp Master Mix (Applied Biosystems) according to manufacturer instructions. qPCR was then performed using a TaqMan TNFα primer-probe mix (Applied Biosystems, Catalogue # Hs01113624_g1) and the TaqMan Universal PCR Master Mix. Samples were run in triplicate and relative mRNA expression was calculated

using the ΔΔCt method with normalization to 18s ribosomal RNA levels. 18S primer/probe sequences have been previously published [116,150].

*Protein isolation and Western blotting*

Frozen L6 DRG were homogenized in 0.5% NP-40 lysis buffer supplemented with protease and phosphatase inhibitor cocktails (Sigma Aldrich, St. Louis, MO) using a FastPrep bench top homogenizer in 2mL tubes containing lysing matrix M (MP Biomedicals, Santa Ana, CA). Homogenates were then sonicated (3 times for 10 seconds) and centrifuged to remove insoluble material. Protein concentration was estimated using the BioRad Protein Assay Kit (BioRad Laboratories, Hercules, CA) according to manufacturer instructions. Five micrograms of protein were resolved under reducing conditions using 26-well 10% Bis-Tris gels (BioRad) and 1X MOPS buffer. Proteins were transferred to polyvinylidene fluoride (PVDF) membranes, which were subsequently blocked in Tris-buffered saline Tween-20 (TBST) containing 5% nonfat dry milk. Membranes were then incubated with primary and secondary antibodies listed in Tables 1 and 2, washed in TBST, and finally developed with Pierce ECL Western Blotting Substrate (Thermo Fisher) prior to exposure to radiography film. Because glutamine synthetase, β III Tubulin, and β-actin have similar molecular weights, the membranes were first probed for glutamine synthetase, stripped using Restore PLUS Western Blot Stripping Buffer (Thermo Fisher) for 15 minutes at room temperature, then re-probed for βIII tubulin, followed by β-actin. Films were digitally scanned and densitomitry analyses were performed using ImageQuant TL 7.0 software (GE Life Sciences, Sunnyvale, CA). To account for blot-to-blot variation, a standard DRG lysate

was included in each blot for normalization and β-actin expression was utilized as an in-lane loading control.

*Immunohistochemistry*

Indirect, peroxidase-based immunostaining was performed on Streck-fixed sections of L5 DRG from three control and six 7d SIV-infected animals using the Leica Bond-Max automated system (Leica Biosystems, Wetzlar, Germany). The protocol for all antigens included pretreatment with Bond TM Epitope Retrieval 2 and heating for 20 minutes, and positive immunoreactivity was visualized by labeling with 3,3'-diaminobenzidine (DAB) chromogen. Primary antibodies and concentrations are listed in Table 1. Isotype-matched non-immune immunoglobulins were employed as negative controls and showed no significant staining in DRG tissue.

*Statistics*

All statistical analyses were conducted using Prism software (GraphPad, La Jolla, CA, Version 5.0d) and nonparametric methods. The Mann-Whitney U test was used for all two-group comparisons. For Nanostring data, the statistical significance was set at $P < 0.0042$ to account for multiple comparisons (Bonferroni correction). For all other analyses, statistical significance was assumed when the $P$ value was less than 0.05.

## Results

*Quantification of DRG mRNA expression by Nanostring and qPCR analysis*

Immune signaling and activation

During the acute phase of HIV and SIV infection, high levels of plasma viremia are accompanied by an intense systemic cytokine cascade that is thought to contribute to immunopathologic consequences of infection [113,143,151]. However, little is known about immune responses occurring in the PNS during acute HIV/SIV or the role that such responses could plan in early sensory nerve injury. We performed Nanostring analysis of immune-related gene expression in the DRG of 7d SIV-infected macaques, as well as uninfected control animals. We found that at 7 days post infection, there was marked upregulation of genes related to Type I IFN signaling and the early antiviral response in the DRG (IRF7, Mx1, CCL8, CXCL10, and CXCL11) (Fig 1A-F). Because of their previously established importance in the pathophysiology HIV and SIV-associated disease [35,38,119,152,153], we also examined changes in CCL2 (MCP1) and TNFα gene expression in the DRG during acute SIV infection. CCL2 gene expression was elevated in 7d SIV-infected macaques compared to controls; however this difference did not reach statistical significance after correction for multiple comparisons ($p = 0.029$, Fig 1G). TNFα expression, which was measured by a separate qPCR assay, was significantly increased in the DRG at 7 days post SIV infection ($p = 0.0024$, Fig 1F). We also looked at expression of genes related to macrophage (CD68) and satellite glial cell (GFAP) activation. By Nanostring analysis, CD68 gene expression was significantly elevated at 7 days post SIV infection ($p < 0.001$, Fig 2A). GFAP gene expression was also elevated in 7d SIV-infected animals, but this did not reach statistical significance after correction for

multiple comparisons ($p = 0.0047$, Fig 2B). These results indicate that there is significant local cellular immune activation in the DRG at 7 days post SIV-infection, a time point that proceeds detectable DRG macrophage activation by CD68 IHC (10 dpi) and significant loss of ENFD (14 dpi) [64].

Glutamate metabolism and oxidative stress

Previous studies have proposed that altered glutamate homeostasis and increased oxidative stress contribute to neuronal damage in the brain during HIV-associated neurocognitive disease (HAND) [145-148]. Thus, to investigate potential mechanisms of early sensory nerve damage in the SIV model, we evaluated the expression of genes related to glutamate metabolism and the oxidative stress response in the DRG of acutely infected and control animals. Nanostring analysis revealed that, in 7d SIV-infected animals, glutaminase (GLS1) gene expression was significantly downregulated ($p < 0.001$, Fig 3A) compared to uninfected controls, while glutamine synthetase (GLUL) was significantly upregulated ($p < 0.001$, Fig 3B). To assess induction of an oxidative stress response in the DRG, we focused on the expression of two distinct isoforms of superoxide dismutase (SOD), the first enzyme in the reaction to detoxify the superoxide anion. For SOD1, the isoform that localizes to the cytosol, there was no significant difference in gene expression between control and 7d SIV-infected macaques ($p = 0.081$, Fig 3C). In contrast, there was significant upregulation of SOD2 RNA, which encodes the mitochondrial SOD isoform ($p < 0.001$, Fig 3D), also known as manganese super oxide dismutase (MnSOD).

*Quantification of DRG protein expression by Western blot*

To extend findings from the RNA analyses to the protein level, Western blots were performed that measured expression of glutaminase, glutamine synthetase, and SOD2 in DRG homogenates. Densitometry results were normalized to the cellular loading control β-actin. As shown in an image of a representative blot and graphically in Figure 4, there was no significant difference in the amounts of glutaminase ($p = 0.58$, Fig 4B) or glutamine synthetase expression ($p = 0.23$, Fig 4C) in the DRG of 7d SIV-infected animals compared to controls. In contrast, the relative amount of SOD2 expression in the DRG was elevated in 7d SIV-infected animals ($p = 0.0013$, Fig 4D), in accordance with RNA expression data (Fig 3D). Surprisingly, the amount of βIII tubulin expression, which is typically used as a neuron-specific loading control, was significantly and consistently decreased at 7 days post SIV infection ($p < 0.001$, Fig 5A), while this was not evident at the RNA level ($p = 0.14$, Fig 5B).

*Immunohistochemistry*

We performed immunostaining on fixed sections of L5 DRG from control and 7d SIV-infected macaques to identify which cell types in the ganglia express glutaminase, glutamine synthetase, and SOD2 in normal conditions, and to determine whether the amount of expression or cell specificity changes during acute SIV infection. Glutaminase expression in both control and 7d SIV-infected animals was primarily restricted to the neurons, with diffuse, moderate to strong cytoplasmic staining of the neuronal cell bodies (Fig 6A-B). Scattered interstitial cells, likely macrophages, also showed light cytoplasmic reactivity for glutaminase in both control and 7d SIV-infected ganglia. In uninfected

animals, glutamine synthetase expression in the DRG was most apparent in the satellite glial cells, with little to no staining in the neuron cell bodies (Fig 6C). In contrast, all 7d SIV infected ganglia exhibited moderate glutamine synthetase expression in the cytoplasm of neuron cell bodies (Fig 6D). Furthermore, this upregulation in neuronal glutamine synthetase expression was primarily observed in small- to medium-sized neuronal cell bodies, a population which is thought to represent nociceptive neurons [154]. SOD2 immunostaining demonstrated diffuse, light to medium cytoplasmic staining in all cell types in the DRG, with a finely stippled pattern consistent with mitochondrial localization (Fig 6E). In 7d SIV-infected ganglia, increased intensity of SOD2 immunostaining localized primarily to the satellite glial cells and interstitial macrophages (Fig 6F).

**Discussion**

Previous work in the pigtailed macaque model of HIV-SN has demonstrated that immune activation in the DRG correlates with and likely contributes to sensory nerve dysfunction during late stages of SIV infection [42]. More recently, we found that significant DRG macrophage activation and ENFD decline were detectable much earlier than previously realized, at just 14 dpi, and that this loss of ENFD persisted in cART-treated SIV-infected animals despite viral suppression and normalization of CD68 immunostaining in the DRG [64]. The aim the current study was to gain a more comprehensive understanding of molecular alterations in the lumbar DRG during the acute phase of SIV infection and to explore potential mechanisms for early neuronal injury.

By evaluating gene expression in the DRG of animals euthanized during acute SIV infection (7 dpi), we found significant upregulation of several genes involved in the antiviral immune response, namely IRF7, STAT1, MX1, CCL8, CXCL10, CXCL11, and activation of macrophages (CD68), as well as key pro-inflammatory mediators (TNFα and CCL2). Changes were largely uniform among 7d SIV-infected animals and did not significantly correlate with the amount of SIV RNA detected in the DRG (data not shown), suggesting that local immune activation in the DRG is associated with the rapid systemic immune response exhibited by all animals during acute SIV viremia [113] and not a result of local SIV replication. Because of their fenestrated capillaries and location within the intradural space [155-157], the DRG are readily exposed to proinflammatory factors in plasma and CSF such as cytokines, chemokines, and activated leukocytes. Therefore, covariance of systemic and local DRG immune activation would not be an unexpected finding. Moreover, several of the immune-related genes that were most strongly upregulated in the 7d SIV-infected macaques were those induced by interferon signaling, which has been shown to play a major role in the early antiviral immune responses to both SIV and HIV infection [113,143,150,158-160].

An association between systemic immune activation and the occurrence of PN has been observed in patients during the early stages of HIV infection. In a cohort of individuals evaluated at a median of 3.5 months following HIV transmission, Wang and colleagues [63] found that patients with signs of PN had elevated levels of the inflammatory marker neopterin in the plasma and CSF, as well as higher CSF levels of the chemokines MCP-1 and IP-10 (CXCL10), both of which enhance viral replication and local inflammation by recruiting monocytes and lymphocytes. The authors postulated that, due

to the lack of a local blood-nerve-barrier, the DRG might be a site where peripheral neurons are particularly vulnerable to the toxic effects of circulating proinflammatory factors. By evaluating DRG tissues directly, this macaque study complements these findings by demonstrating that immune-reactive cells in the DRG are themselves undergoing activation during acute SIV infection, expressing cytokines and chemokines that promote a proinflammatory environment and likely potentiate neuronal injury.

The neurotoxic effects of numerous cytokines, chemokines, and viral proteins have been extensively characterized in rodent and *in vitro* models of HIV-associated neurologic disease [10,11,161-163]. While it is possible that these factors alone could account for neuronal dysfunction during early HIV/SIV infection, we were also interested in whether other neurotoxic mechanisms were induced during acute disease, as these could provide targets for adjuvant therapies aimed at neuroprotection in HIV patients receiving cART. Excitoxic neuronal injury due to altered glutamate handling has been implicated in the pathogenesis of HAND, as well as many other neurodegenerative diseases, and while there has been much interest in targeting this system therapeutically, such approaches are complicated by the broad role of glutamate in the CNS [146,148]. Recently, glutamate has been shown to act as an important neuroglial signaling molecule in the PNS, and may impact pain signaling at the level of the sensory ganglia [164-166]. We therefore hypothesized that local immune activation in the DRG during acute SIV infection would be coincident with alterations to the peripheral glutamatergic system, which, compared to the CNS, may be more amenable to therapeutic manipulation. Nanostring analysis of DRG RNA from 7d SIV-infected macaques revealed significant downregulation of the gene encoding the glutaminase enzyme (GLS1), which catalyzes

the deamination of glutamine to form glutamate, and upregulation of gene encoding glutamine synthetase (GLUL), which converts glutamate to glutamine (Fig 3). Reduced glutaminase expression was contrary to what we expected based on previous work showing increased glutaminase mRNA in HIV-infected macrophages and microglia [167-169]. However, from a toxicity standpoint, this inverse regulation between glutaminase and glutamine synthetase may represent an adaptive host response to protect neurons from increased extracellular glutamate in the DRG. Although we were unable to measure glutamate levels in the DRG, other groups have shown that HIV-infected macrophages release glutamate, and that glutamate is a key mediator of neurotoxicity *in vitro* [170,171]. Whether glutamate is also released by SIV-infected macaque macrophages is a topic of current investigation in our lab.

Changes in glutaminase and glutamine synthetase gene expression in the DRG of 7d SIV-infected animals were not significantly reflected by Western blot analysis. However, it is plausible that this technique was simply not sensitive enough to detect subtle changes in total protein concentration in the DRG tissue, or that the assay was statistically underpowered due to small group size. It is also worth noting that the amount of total protein may not correlate with the level of enzymatic activity, which can be altered by post-translational changes. For instance, glutamine synthetase has been shown to be particularly vulnerable to oxidative and nitrative modifications, which decrease its catalytic activity [172,173]. In regards to glutaminase, expression of this enzyme in HIV-infected macrophages and microglia is quite complex, with differential regulation among isoforms and relocalization of the protein from the mitochondria to the cytosol [167-169], thus detailed characterization glutaminase dynamics in the DRG during SIV infection are

beyond the scope of the present study, but this remains an important topic for future investigations. By conducting immunostaining for glutaminase, we did find that this enzyme is highly expressed by the all neuron cell bodies in the DRG, and to a much lesser extent in scattered interstitial cells, presumably macrophages. Neither the extent nor cellular localization of glutaminase immunostaining was appreciably different in control and 7d SIV-infected DRG.

In contrast, we observed a clear increase in neuronal glutamine synthetase immunoreactivity in the DRG of 7d SIV-infected animals. Immunohistochemical studies of the DRG typically employ glutamine synthetase as a constitutively expressed, highly specific marker of satellite glial cells [174]. The situation is similar in the CNS, where glutamine synthetase is highly expressed by astrocytes and nearly undetectable in neurons under normal physiologic conditions [175]. While this altered expression pattern represents a novel finding in the PNS, there are a limited number of studies describing increased glutamine synthetase expression in neurons of the CNS. For example, glutamine synthetase expression has been observed in in pyramidal neurons of patients with advanced Alzheimer's disease, likely due to marked impairment of normal glutamate handling by nearby astrocytes [176,177], and in cultured rat neurons that have been deprived of extracellular glutamine and direct contact with astrocytes [178]. Taken together, these observations underscore the importance of glutamine as an essential metabolite for neuronal cells and suggest that, when the normal source of glutamine is diminished or absent, neurons can upregulate glutamine synthetase to meet their metabolic needs. Consequently, in the setting of the DRG, neuronal expression of glutamine synthetase may reflect depletion of the extracellular glutamine pool by non-neuronal cells

undergoing SIV-induced immune activation, and/or dysfunctional glutamate handling by the satellite glial cells. In either case, neuronal glutamine synthetase expression likely represents a profound shift in metabolic balance within the DRG, which could directly contribute to sensory nerve dysfunction and damage during acute SIV infection. Moreover, while endogenous glutamine synthetase expression appears to be neuroprotective under some conditions *in vitro*, including oxidative stress and DNA damage, it has also been shown to contribute to neuronal death in low-glutamine media [179].

Another unexpected finding was decreased expression of βIII tubulin in the DRG of acutely infected macaques, which was discovered by Western blot. This cytoskeletal protein is a microtubule element that is found almost exclusively in neurons and is typically used as a neuron-specific loading control for protein assays. At this time, we have been unable to find another study reporting decreased expression of βIII tubulin in tissues of the PNS during a disease state, natural or experimental. However, one can postulate that a decrease in protein levels without overt neuronal loss (which is not evident in the DRG until late stages of disease in our SIV model) or corresponding downregulation of the TUBB3 gene (also shown herein by Nanostring), could occur in one of three scenarios: 1) increased degradation of the protein, possibly to supply amino acids for enhanced metabolic demands, 2) redistribution within the cell, possibly related to accelerated transport of the protein from the neuron cell body into the axon, or 3) accrual of posttranslational modifications that alter binding properties of the primary antibody used for the Western blot. We plan to explore these scenarios in more detail in future studies.

Finally, we hypothesized that immune activation in the DRG would be accompanied by evidence of local oxidative stress. Similar to glutamate excitotoxicity, production of excess reactive oxygen species (ROS) in the brain is a potential source of neuronal damage in the context of HAND [145,147]. Elevated levels of oxidative modifications and mitochondrial ROS production have also been detected in the peripheral nerves of HIV patients with PN as well as SIV-infected pigtailed macaques with diminished ENFD [180]. Using Nanostring analysis, we measured the gene expression of two key antioxidant enzymes, SOD1, which localizes primarily to the cytoplasm, and SOD2, which is found in the mitochondrial matrix. While there was no difference between control and 7d SIV-infected DRG in regards to SOD1 gene expression, there were significantly higher levels of SOD2 RNA and protein in the DRG of acutely infected animals, suggestive of mitochondria-specific oxidative stress. We initially expected that enhanced SOD2 expression in the DRG would occur primarily within the sensory neurons, possibly as a result of mitochondrial injury. However, while there was a clear increase in the intensity of SOD2 staining in 7d SIV-infected animals compared to controls, it did not localize to neuron cell bodies, but rather the satellite glial cells and interstitial macrophages. One explanation for this finding would be that enhanced SOD2 expression is an adaptive response to increased mitochondrial ROS (mROS) production by cells undergoing immune activation. This phenomenon has been explored in macrophages and microglia, where production of mROS has been shown to augment immune signaling and cytokine production [181,182]. However, satellite glial cells, have not been studied in detail with resect to mROS.

This investigation represents the first comprehensive molecular and morphologic analysis of the DRG during acute SIV infection. Although limited by factors inherent to macaque studies, such as cross-sectional design, our findings provide valuable insights into the origins of sensory nerve dysfunction in HIV. The recognition of the DRG as a site of marked local immune activation and potentially neurotoxic metabolic alterations during acute infection, prior to the onset of significant neuropathology or neurophysiologic alterations, will greatly inform future studies on the pathogenesis of HIV-SN in the macaque model. Because managing HIV-SN is extremely challenging once neuropathic symptoms are established, effective approaches for preventing sensory nerve damage early during HIV infection are urgently needed. A more comprehensive understanding of neuropathologic mechanisms induced in the PNS during early HIV infection holds promise for elucidating neuroprotective strategies.

## Tables

| Primary Antibody | Host Species | Mono- or Polyclonal | Provider | Catalog # | Dilution Used | kDA of band |
|---|---|---|---|---|---|---|
| Glutaminase | Rabbit | Monoclonal | Abcam | ab166976 | 1:20,000 (WB) 1:2000 (IHC) | 73 kDa |
| Glutamine Synthetase | Rabbit | Polyclonal | Abcam | ab49873 | 1:20,000 (WB and IHC) | 42 kDa |
| SOD2 | Rabbit | Polyclonal | Abcam | ab13534 | 1:20,000 (WB) 1:2500 (IHC) | 25 kDa |
| βIII Tubulin | Mouse | Monoclonal | Promega | G712A | 1:20,000 | 55 kDa |
| β-actin | Mouse | Monoclonal | Sigma | A5441 | 1:20,000 | 42 kDa |

**Table 4-1**. Primary antibodies used for Western blotting (WB) and immunohistochemistry (IHC) assays.

| Secondary Antibody | Host Species | Provider | Catalog # | Dilution Used |
|---|---|---|---|---|
| HRP-conjugated Goat Anti-Rabbit IgG | Goat | Dako | P0448 | 1:20,000 |
| HRP-conjugated Goat Anti-Mouse IgG | Goat | Dako | P0447 | 1:20,000 |

**Table 4-2**. Secondary antibodies used for Western blotting.

## Figures

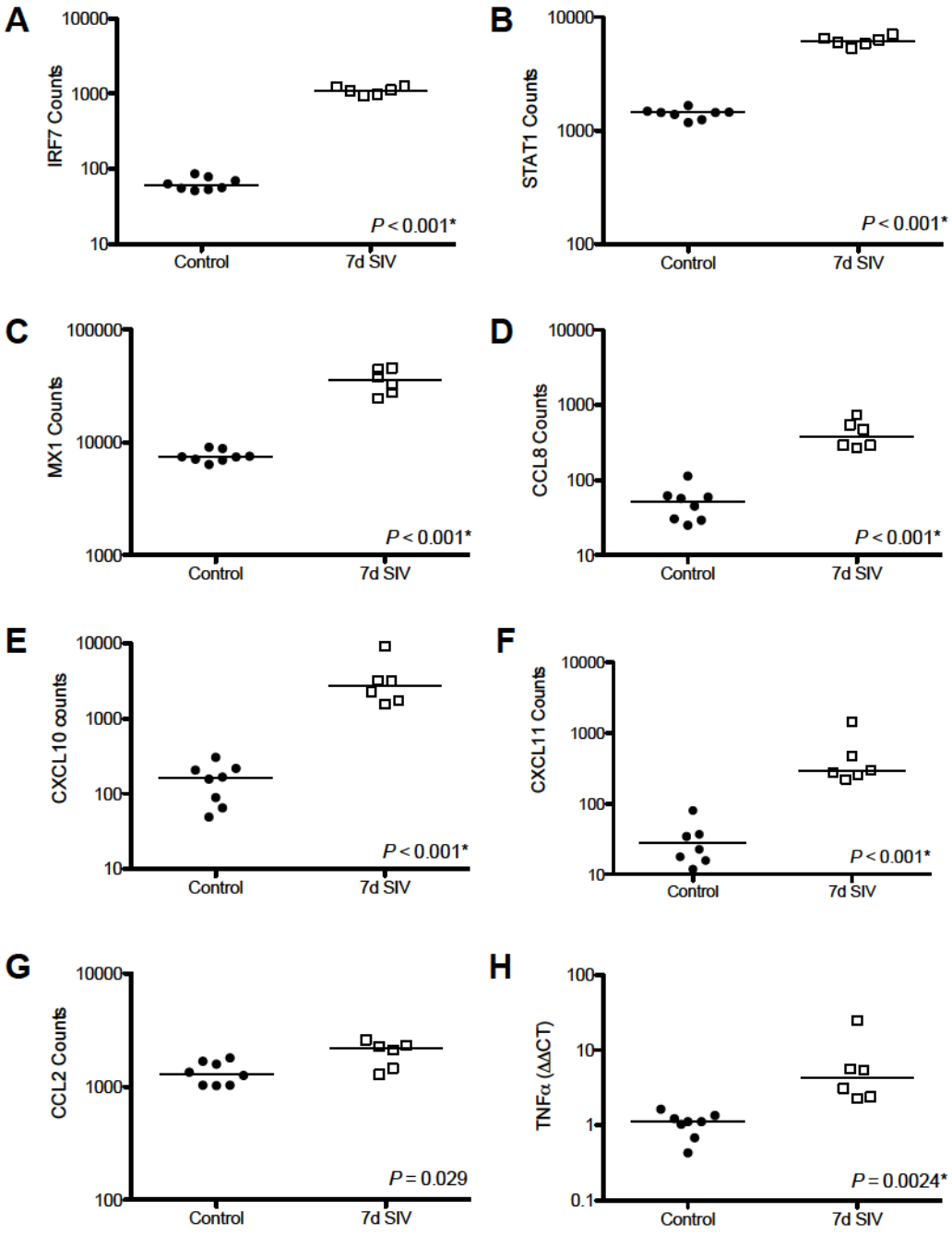
A
IRF7 Counts
10000
1000
100
10
P < 0.001*
Control
7d SIV
B
STAT1 Counts
10000
1000
100
P < 0.001*
Control
7d SIV
C
MX1 Counts
100000
10000
1000
P < 0.001*
Control
7d SIV
D
CCL8 Counts
10000
1000
100
10
P < 0.001*
Control
7d SIV
E
CXCL10 counts
10000
1000
100
10
P < 0.001*
Control
7d SIV
F
CXCL11 Counts
10000
1000
100
10
P < 0.001*
Control
7d SIV
G
CCL2 Counts
10000
1000
100
P = 0.029
Control
7d SIV
H
TNFα (ΔΔCT)
100
10
1
0.1
P = 0.0024*
Control
7d SIV

**Figure 4-1.** *Genes related to immune signaling and activation are upregulated in the DRG during acute SIV infection.* **A-F:** Nanostring nCounter gene expression analysis revealed marked upregulation of genes involved in immune signaling and the early antiviral response in the lumbar DRG 7d SIV-infected animals compared to controls. G: Although CCL2 gene expression was elevated in 7d SIV-infected animals, this did not reach statistical significance after correcting for multiple comparisons. H: 7d SIV-infected animals had significantly higher TNFa gene expression in the lumbar DRG, by qPCR analysis. Mann Whitney with Bonferroni correction for multiple comparisons (*$p < 0.0042$).

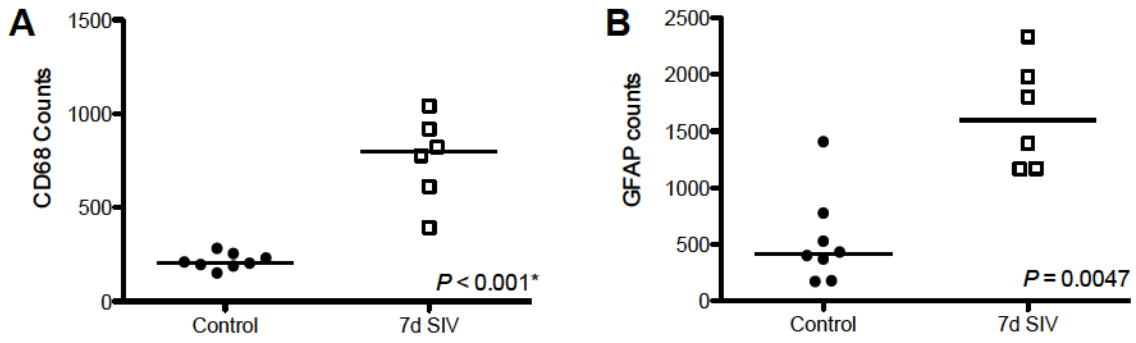


**Figure 4-2.** *Cellular immune activation in the DRG during acute SIV infection*. A: By Nanostring gene expression analysis Animals euthanized during acute SIV infection (7d SIV) had significantly higher levels of CD68 expression, an indicator of macrophage activation, compared to controls. B: Expression of the satellite glial cell activation marker GFAP, was also elevated in 7d SIV-infected animals; however this did not reach statistical significance after correcting for multiple comparisons. Mann Whitney with Bonferroni correction for multiple comparisons (*$p < 0.0042$).

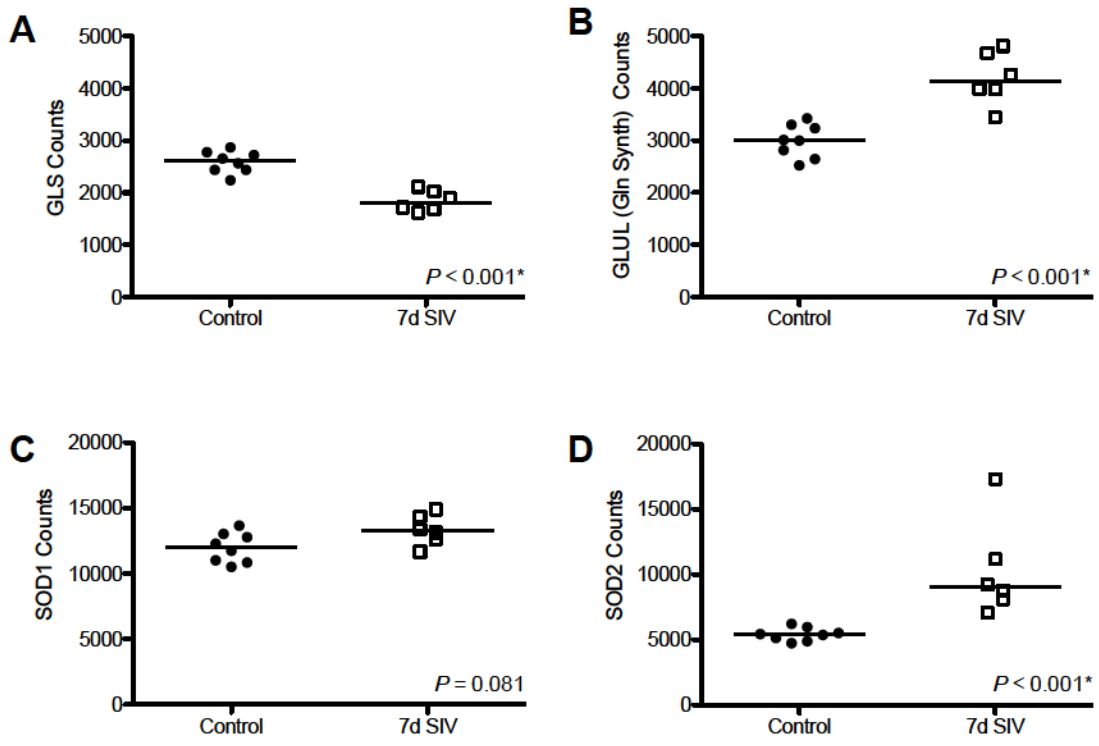


**Figure 4-3.** *Expression of genes related to glutamate metabolism and oxidative stress in the DRG during acute SIV infection*. A-B: By Nanostring gene expression analysis, we found significantly decreased glutaminase (GLS) expression and increased glutamine synthetase (GLUL) expression in the DRG of 7d SIV-infected macaques compared to controls. C-D: While there was no significant difference in DRG SOD1 expression between 7d SIV-infected animals and controls, SOD2 was significantly upregulated at 7d post SIV infection. Mann Whitney with Bonferroni correction for multiple comparisons (*$p < 0.0042$).

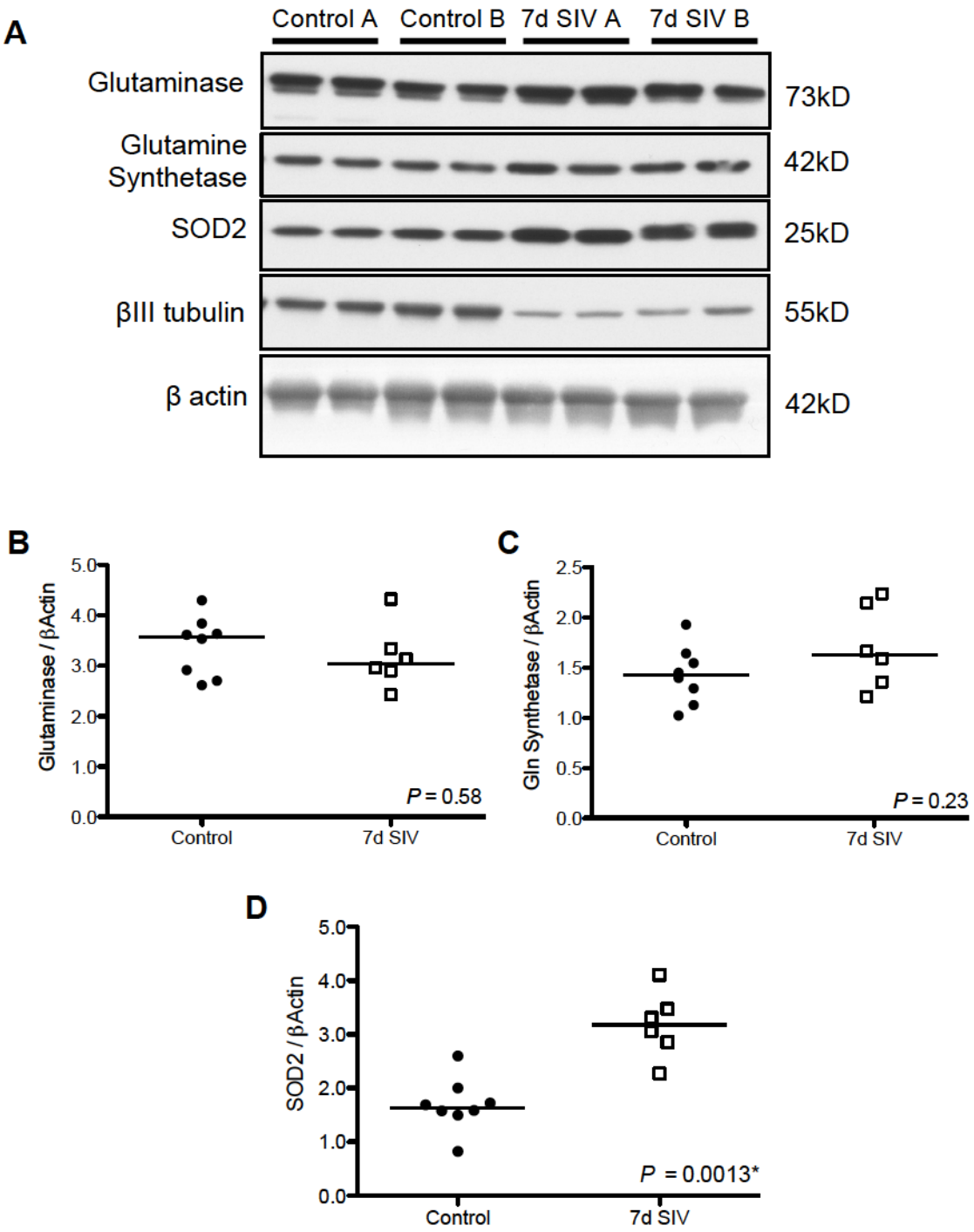
A
Control A
Control B
7d SIV A
7d SIV B
Glutaminase
73kD
Glutamine Synthetase
42kD
SOD2
25kD
βIII tubulin
55kD
β actin
42kD
B
Glutaminase / βActin
5.0
4.0
3.0
2.0
1.0
0.0
P = 0.58
Control
7d SIV
C
Gln Synthetase / βActin
2.5
2.0
1.5
1.0
0.5
0.0
P = 0.23
Control
7d SIV
D
SOD2 / βActin
5.0
4.0
3.0
2.0
1.0
0.0
P = 0.0013*
Control
7d SIV

**Figure 4-4.** *Quantification of DRG protein expression by Western blot*. **A:** A representative Western blot showing DRG homogenates from two control (Control A and B) and two 7d SIV-infected macaques (7d SIV A and B) run in duplicate. Protein expression levels were quantified by densitometry analysis and normalized to B actin for comparison between groups. Protein expression levels for glutaminase (**B**) and glutamine synthetase (**C**) were not significantly different between groups. **D:** SOD2 protein expression was significantly elevated in 7d SIV-infected animals compared to controls. Mann Whitney (*$p < 0.05$).

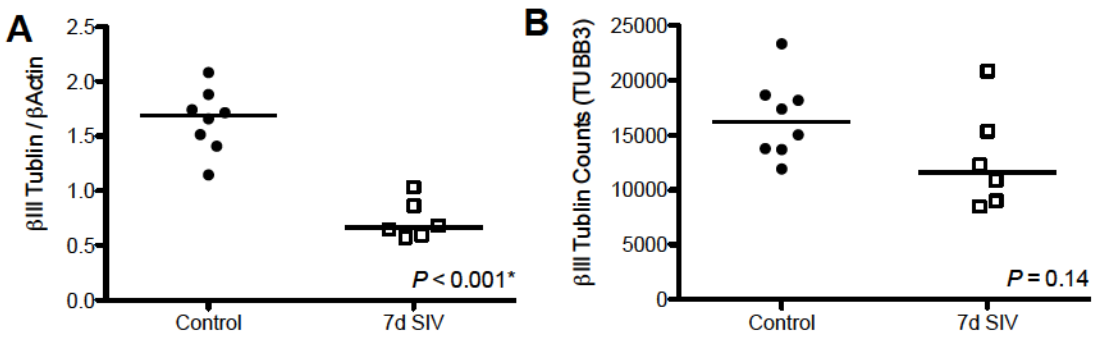


**Figure 4-5.** *βIII tubulin expression in the DRG during acute SIV infection*. **A:** 7d SIV infected animals had significantly lower DRG βIII tubulin expression compared to controls. **B:** There was no significant difference in the level of βIII tubulin RNA expression (TUBB3) between groups by Nanostring gene expression analysis. Mann Whitney (*$p < 0.5$)

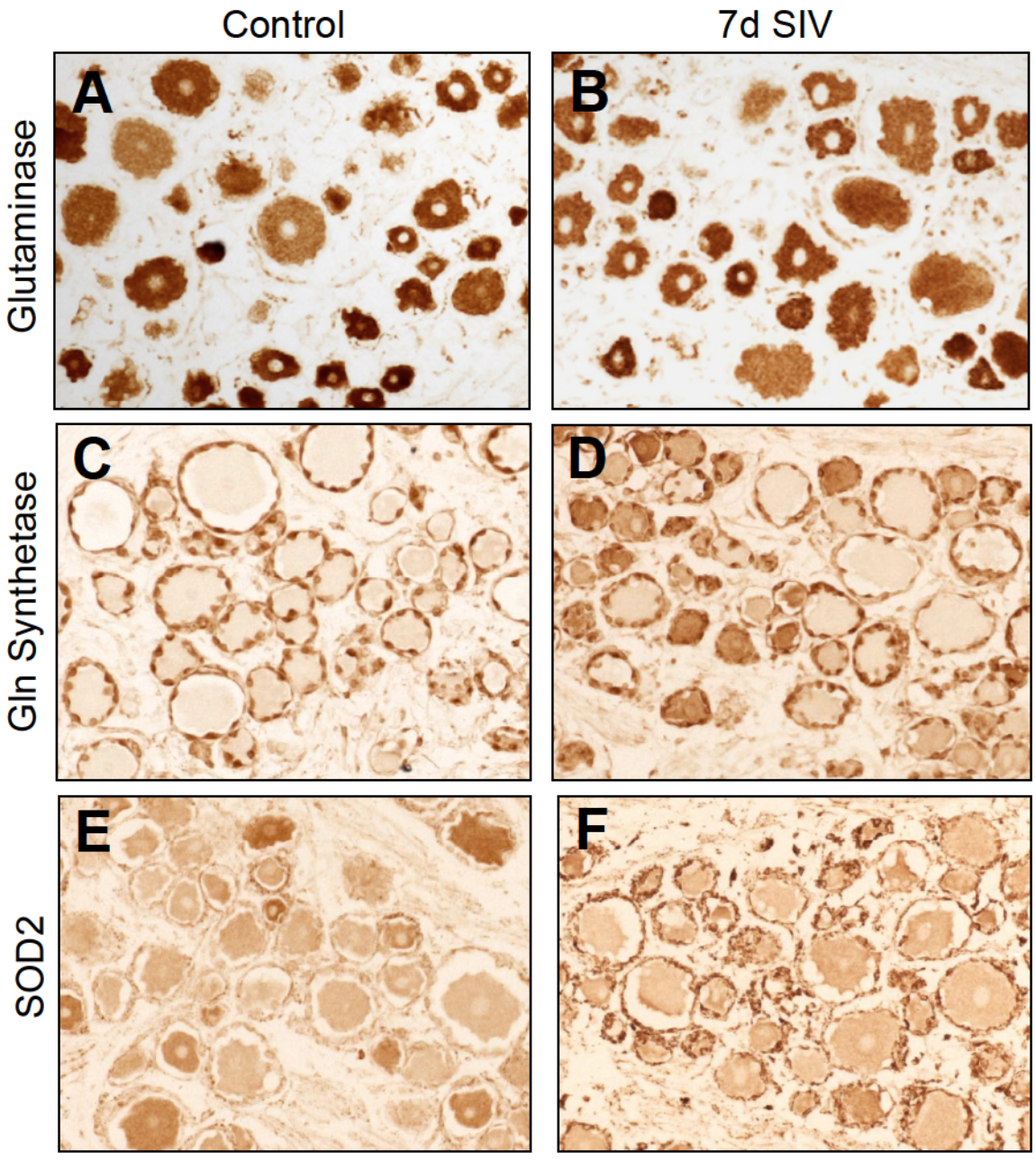
Control
7d SIV
Glutaminase
Gln Synthetase
SOD2
A
B
C
D
E
F

**Figure 4-6.** *DRG immunohistochemistry.* A-B: Glutaminase expression in both control and 7d SIV-infected animals was primarily restricted to the neurons, with diffuse, moderate to strong cytoplasmic staining of the neuronal cell bodies. Scattered interstitial cells, likely macrophages also showed light cytoplasmic reactivity for glutaminase. C-D: In uninfected animals, glutamine synthetase expression in the DRG was most apparent in the satellite glial cells, with little to no staining in the neuron cell bodies. In contrast, 7d SIV infected ganglia exhibited moderate glutamine synthetase expression in the cytoplasm of neuron cell bodies. E-F: SOD2 immunostaining demonstrated diffuse, light to medium cytoplasmic staining in all cell types in the DRG, with a finely stippled pattern consistent with mitochondrial localization. In 7d SIV-infected ganglia, there was increase in the intensity of SOD2 immunostaining, which localized primarily to the satellite glial cells and interstitial macrophages. DAB immunostaining without counterstain. Original magnification 200X.

# V: Summary and Future Directions

Despite widespread use of cART, HIV-SN remains a frequent neurologic complication of HIV infection. With prevalence rates as high as 60% in some cohorts, HIV-SN represents a vast and growing global health concern [1,23]. Because the pathogenesis of HIV-SN is complex and difficult to study in human patients, animal models of this condition are essential for elucidating the underlying neuropathologic mechanisms. Previous work by our laboratory has confirmed that the dual-inoculated SIV/macaque model closely recapitulates many of the morphologic and functional abnormalities seen in the PNS of HIV patients with neuropathy. The series of studies outlined in this dissertation build upon this groundwork by conducting in depth morphologic and molecular analyses of multiple components of the sensory pathway, namely the ENF, spinal cord, and DRG, and exploring neuropathologic mechanisms occurring during both acute and chronic SIV infection.

The translational value of any animal model is strengthened by the ability to employ outcome measures similar to those used in human subjects. In recent years, visualization and assessment of ENF in skin biopsies has become a standard clinical tool for the diagnosis and monitoring of PN in HIV patients [183]. As described in Chapter 2, we have adapted this technique for use in Asian macaques and now routinely obtain pre-infection and necropsy ENF skin biopsies from all SIV study animals, including those receiving various cART regimens. The resulting pool of longitudinal ENF data will be of immense value in tracking the impact of host and virus dynamics, as well as different antiretroviral drugs, on sensory nerve fiber integrity. In addition, we have also begun to use corneal confocal microscopy (CCM) to collect *in vivo* images of the sub-basal corneal nerve plexus from our study macaques, both rhesus and pigtailed. CCM is an

emerging, noninvasive clinical tool that is currently being used as a method to diagnose and longitudinally assess neuropathy in patients with diabetes [184,185] and has also been employed in rodent models of diabetic neuropathy [186]. Our hope is that by pioneering this technology in SIV-infected macaques, we will gain detailed longitudinal information on peripheral nerve health and be able to closely track the timing of nerve injury during the course of disease and cART, as well monitor the effects of putative neuroprotective and neuroregenerative agents.

Chapter 3 of this dissertation addresses the effects of SIV infection on the spinal cord, a site where sensory signals can undergo extensive modulation prior to transmission to the brain. While the spinal cord remains relatively underrepresented in the HIV literature, a series of recent reports based on autopsy tissues revealed evidence of enhanced glial activation and immune signaling in the spinal cords of HIV patients with histories of neuropathic pain [14-16]. Similarly, we found that untreated SIV-infected macaques exhibited significant elevations in CD68 immunostaining (a marker of macrophage/microglial activation) in the spinal cord, as well as enhanced expression of the proinflammatory mediators TNFα and CCL, and that these changes correlated with both the amount SIV RNA in the spinal cord and the degree of ENF loss. Also compelling was the finding that while SIV RNA was below the level of detection in the spinal cord tissue of cART-treated macaques, these animals exhibited marked spinal astrocyte activation, as measured by GFAP immunostaining. These significant and distinct differences in the spinal cords of cART-naïve and cART-treated animals suggest that the mechanisms leading to central sensitization may be differ between patients with uncontrolled HIV infection and those receiving effective cART. In future studies, we

intend to conduct more detailed analyses on spinal cord tissue of cART-treated macaques, including detection of low-copy viral RNA by means of digital droplet PCR, as well as detection of viral DNA, which, in the brain, was not significantly reduced by cART in a previous SIV study [38]. We also plan to collect more comprehensive gene expression data to identify which pro-nociceptive pathways may be persistently upregulated in the spinal cords of cART-treated SIV-infected macaques, as this could shed light on new therapeutic targets. This could be pursued either by Nanostring gene expression analysis, possibly with a redesigned panel of genes related to glial activation and pain signaling, or by pathway-focused qPCR assays.

Lastly, guided by emerging evidence of significant nervous system impairment in patients with early HIV, we chose to investigate alterations in the DRG of animals euthanized during acute SIV infection. By conducting Nanostring gene expression analysis on lumbar DRG from uninfected control macaques and animals euthanized at 7 days post infection (dpi), we found that acute SIV infection was associated with marked induction of local immune activation in the DRG, as well as alterations in genes encoding enzymes involved in glutamate metabolism and oxidative stress, all of which could plausibly contribute to early sensory nerve damage.

Perhaps the most intriguing observations in Chapter 4 were the unexpected, neuron-specific findings of increased glutamine synthetase expression in neuronal cell bodies in the DRG (by immunohistochemistry) and decreased βIII tubulin expression (by Western blot). While these are novel findings in the PNS, increased neuronal glutamine synthetase expression has been linked to deficient extracellular glutamine and metabolic stress *in vitro* [178,179], and impairment of astrocytic glutamate handling in the brains of

Alzheimer's patients [177]. Accordingly, we propose that glutamine synthetase expression by sensory neuron cell bodies is the result of a profound shift in the metabolic homeostasis within the DRG during acute SIV infection, possibly due to rapid, intense immune activation of the macrophages and satellite glial cells. This premise could also account for the decreased βIII tubulin expression in the DRG and early ENF decline, as metabolically-compromised neuronal perikarya may fail to regulate production or localization of structural proteins that are necessary to maintain axonal integrity.

Preliminary analyses of macaques euthanized at progressive time points throughout SIV infection (7, 35, 56, and 84 dpi) have shown that glutamine synthetase gene expression in the DRG strongly correlates with SIV RNA, GFAP, CD68, and SOD2 expression (Fig 1), supporting an association between increased glutamine synthetase gene expression and SIV-induced immune activation and oxidative stress in the DRG. There was also strong inverse correlation between βIII tubulin RNA and CD68 gene expression ($p < 0.001$, data not shown); however, in later stages of disease this may be attributable to decreased neuronal/axonal density in the DRG with increasing numbers of infiltrating activated macrophages. In future studies, I plan to extend these analyses to include cART-treated SIV-infected animal. We also hope to develop an *in vitro* primate DRG culture system, similar that employed by Zhu and colleagues [187] in their studies of feline immunodeficiency virus (FIV), which would facilitate molecular and electrophysiological investigation of cell specific biology and the effects of increased glutamine synthetase expression on sensory neuronal health and function.

## Figures

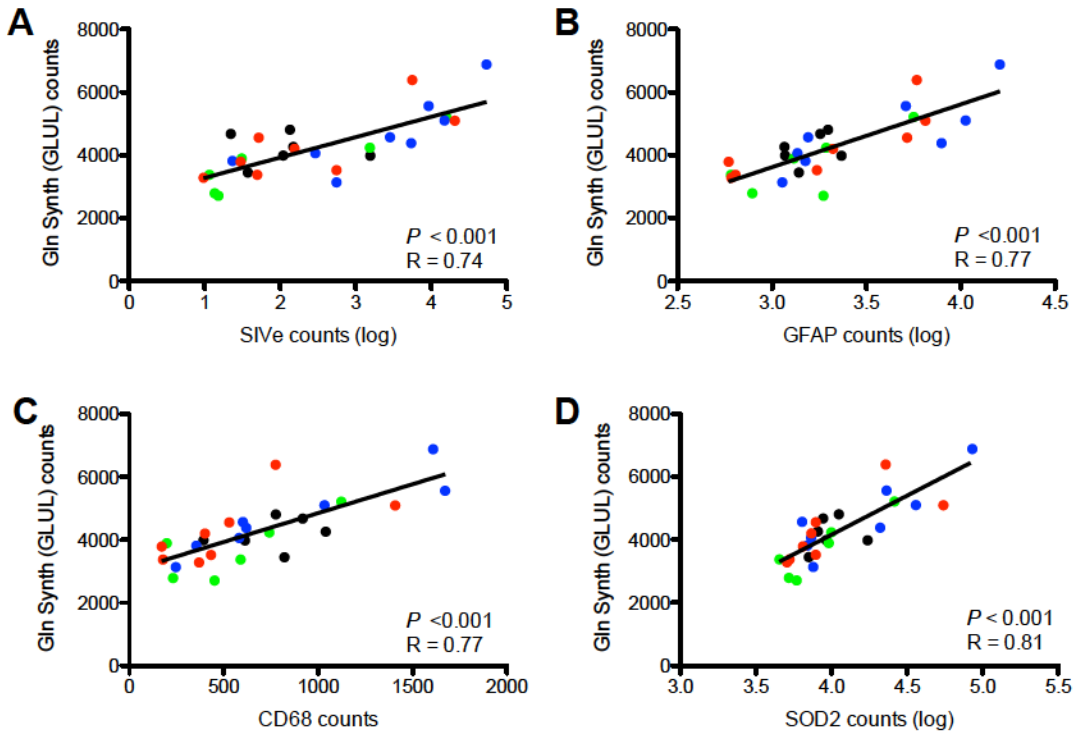


**Figure 5-1**. *Glutamine synthetase gene expression in the DRG correlates with markers of immune activation and oxidative stress.* Nanostring gene expression analysis demonstrates significant direct correlation between glutamine synthetase (GLUL) expression and levels of SIV(**A**), GFAP (**B**), CD68 (**C**), and SOD2 RNA (**D**) in animals euthanized at progressive time points throughout SIV infection. Spearman Rank correlation. (Black = 7 dpi, Green = 35 dpi, Blue = 56 dpi, Red = 84 dpi)

**References**


1 Ghosh, S., Chandran, A. & Jansen, J. Epidemiology of HIV-related neuropathy: a systematic literature review. *AIDS research and human retroviruses* **28**, 36-48 (2012).

2 Evans, S. R. *et al*. Peripheral neuropathy in HIV: prevalence and risk factors. *AIDS* **25**, 919-928 (2011).

3 Keswani, S. C., Pardo, C. A., Cherry, C. L., Hoke, A. & McArthur, J. C. HIV-associated sensory neuropathies. *AIDS* **16**, 2105-2117 (2002).

4 Cornblath, D. R. & McArthur, J. C. Predominantly sensory neuropathy in patients with AIDS and AIDS-related complex. *Neurology* **38** 794-796 (1988).

5 Gonzalez-Duarte, A., Robinson-Papp, J. & Simpson, D. M. Diagnosis and management of HIV-associated neuropathy. *Neurologic clinics* **26**, 821 (2008).

6 Ellis, R. *et al*. Continued high prevalence and adverse clinical impact of human immunodeficiency virus-associated sensory neuropathy in the era of combination antiretroviral therapy: the CHARTER Study. *Archives of neurology* **67**, 552-558 (2010).

7 Smith, H. S. Treatment considerations in painful HIV-related neuropathy. *Pain physician* **14**, 24 (2011).

8 Krashin, D. L., Merrill, J. O. & Trescot, A. M. Opioids in the management of HIV-related pain. *Pain physician* **15**, ES157-168 (2012).

9 Pardo, C. A., McArthur, J. C. & Griffin, J. W. HIV neuropathy: Insights in the pathology of HIV peripheral nerve disease. *Journal of the Peripheral Nervous System* **6**, 21-27 (2001).

10 Acharjee, S. *et al*. HIV-1 viral protein R causes peripheral nervous system injury associated with in vivo neuropathic pain. *FASEB journal* **24**, 4343-4353 (2010).

11 Bhangoo, S. K., Ripsch, M. S., Buchanan, D. J., Miller, R. J. & White, F. A. Increased chemokine signaling in a model of HIV1-associated peripheral neuropathy. *Molecular pain* **5**, 48 (2009).

12 Hahn, K. *et al*. Differential effects of HIV infected macrophages on dorsal root ganglia neurons and axons. *Experimental neurology* **210**, 30-40 (2008).

13 Kamerman, P. *et al*. Pathogenesis of HIV-associated sensory neuropathy: evidence from in vivo and in vitro experimental models. *Journal of the peripheral nervous system* **17**, 19-31 (2012).

14 Shi, Y., Gelman, B., Lisinicchia, J. & Tang, S.-J. Chronic-pain-associated astrocytic reaction in the spinal cord dorsal horn of human immunodeficiency virus-infected patients. *The Journal of neuroscience* **32**, 10833-10840, (2012).

15 Shi, Y., Shu, J., Gelman, B., Lisinicchia, J. & Tang, S.-J. Wnt signaling in the pathogenesis of human HIV-associated pain syndromes. *Journal of neuroimmune pharmacology* **8**, 956-964 (2013).

16 Yuan, S. *et al*. Gp120 in the pathogenesis of human HIV-associated pain. *Annals of neurology*, **75**, 837-850 (2014).

17 Zheng, W. *et al*. Glial TNFα in the spinal cord regulates neuropathic pain induced by HIV gp120 application in rats. *Molecular pain* **7**, 40 (2011).

18 Moyle, G. Clinical manifestations and management of antiretroviral nucleoside analog-related mitochondrial toxicity. *Clinical Therapeutics* **22** (2000).

19 Simpson, D. M. & Tagliati, M. Nucleoside analogue-associated peripheral neuropathy in human immunodeficiency virus infection. *Journal of acquired immune deficiency syndromes and human retrovirology : official publication of the International Retrovirology Association* **9**, 153-161 (1995).

20 Cherry, C. L., McArthur, J. C., Hoy, J. F. & Wesselingh, S. L. Nucleoside analogues and neuropathy in the era of HAART. *Journal of clinical virology : the official publication of the Pan American Society for Clinical Virology* **26**, 195-207 (2003).

21 Ellis, R. J. *et al*. Human immunodeficiency virus protease inhibitors and risk for peripheral neuropathy. *Annals of neurology* **64**, 566-572 (2008).

22 Pettersen, J. *et al*. Sensory neuropathy in human immunodeficiency virus/acquired immunodeficiency syndrome patients: protease inhibitor-mediated neurotoxicity. *Annals of neurology* **59**, 816-824 (2006).

23 Wiebe, L., Phillips, T., Li, J.-M., Allen, J. & Shetty, K. Pain in HIV: an evolving epidemic. *The journal of pain : official journal of the American Pain Society* **12**, 619-624 (2011).

24 Canter, J. A. *et al*. The mitochondrial pharmacogenomics of haplogroup T: MTND2*LHON4917G and antiretroviral therapy-associated peripheral neuropathy. *The pharmacogenomics journal* **8**, 71-77 (2008).

25 Kamerman, P. R., Wadley, A. L. & Cherry, C. L. HIV-associated sensory neuropathy: risk factors and genetics. *Current pain and headache reports* **16**, 226-236 (2012).

26 Lichtenstein, K. A. *et al*. Modification of the incidence of drug-associated symmetrical peripheral neuropathy by host and disease factors in the HIV outpatient study cohort. *Clinical infectious diseases : an official publication of the Infectious Diseases Society of America* **40** (2005).

27 Smyth, K. *et al*. Prevalence of and risk factors for HIV-associated neuropathy in Melbourne, Australia 1993-2006. *HIV medicine* **8**, 367-373 (2007).

28 Sina, S. T., Ren, W. & Cheng-Mayer, C. Coreceptor use in nonhuman primate models of HIV infection. *Journal of translational medicine* **9 Suppl 1** (2011).

29 Flaherty, M., Hauer, D., Mankowski, J.LK., Zink, M.C., & Clements, J.E. Molecular and biological characterization of a neurovirulent molecular clone of simian immunodeficiency virus. *Journal of Virology,* **71,** 5790-5798 (1997).

30 Mankowski, J., Clements, J. & Zink, M. Searching for clues: tracking the pathogenesis of human immunodeficiency virus central nervous system disease by use of an accelerated, consistent simian immunodeficiency virus macaque model. *The Journal of infectious diseases* **186 Suppl 2**, 208 (2002).

31 McArthur, J., Brew, B. & Nath, A. Neurological complications of HIV infection. *Lancet neurology* **4**, 543-555 (2005).

32 Zink, M. C., Amedee, A. M., Mankowski, J. L., Craig, L., Didier, P., Carter D.L., Muñoz, A., Murphey-Corb, M., Clements, J.E. Pathogenesis of SIV encephalitis. Selection and replication of neurovirulent SIV. *The American journal of pathology*, **151**, 793-803 (1997).

33 Clements, J. *et al*. The central nervous system as a reservoir for simian immunodeficiency virus (SIV): steady-state levels of SIV DNA in brain from

acute through asymptomatic infection. *The Journal of infectious diseases* **186**, 905-913 (2002).

34 Follstaedt, S. C., Barber, S. A. & Zink, M. C. Mechanisms of minocycline-induced suppression of simian immunodeficiency virus encephalitis: inhibition of apoptosis signal-regulating kinase 1. *Journal of neurovirology* **14**, 376-388 (2008).

35 Mankowski, J. L., Queen, S. E., Clements, J. E. & Zink, M. C. Cerebrospinal fluid markers that predict SIV CNS disease. *Journal of neuroimmunology* **157**, 66-70 (2004).

36 Mankowski, J. L. *et al*. Natural host genetic resistance to lentiviral CNS disease: a neuroprotective MHC class I allele in SIV-infected macaques. *PloS one* **3**, e3603 (2008).

37 Meulendyke, K. A. *et al*. Early minocycline treatment prevents a decrease in striatal dopamine in an SIV model of HIV-associated neurological disease. *J Neuroimmune Pharmacol* **7**, 454-464 (2012).

38 Zink, M. *et al*. Simian immunodeficiency virus-infected macaques treated with highly active antiretroviral therapy have reduced central nervous system viral replication and inflammation but persistence of viral DNA. *The Journal of infectious diseases* **202**, 161-170 (2010).

39 Höke, A. Animal models of peripheral neuropathies. *Neurotherapeutics : the journal of the American Society for Experimental NeuroTherapeutics* **9**, 262-269 (2012).

40 Keswani, S. C., Jack, C., Zhou, C. & Höke, A. Establishment of a rodent model of HIV-associated sensory neuropathy. *The Journal of neuroscience : the official journal of the Society for Neuroscience* **26**, 10299-10304 (2006).

41 Laast, V. *et al*. Pathogenesis of simian immunodeficiency virus-induced alterations in macaque trigeminal ganglia. *Journal of neuropathology and experimental neurology* **66**, 26-34 (2007).

42 Laast, V. *et al*. Macrophage-mediated dorsal root ganglion damage precedes altered nerve conduction in SIV-infected macaques. *The American journal of pathology* **179**, 2337-2345 (2011).

43 Burdo, T., Orzechowski, K., Knight, H., Miller, A. & Williams, K. Dorsal root ganglia damage in SIV-infected rhesus macaques: an animal model of HIV-induced sensory neuropathy. *The American journal of pathology* **180**, 1362-1369 (2012).

44 Clements, J. *et al*. The central nervous system is a viral reservoir in simian immunodeficiency virus--infected macaques on combined antiretroviral therapy: a model for human immunodeficiency virus patients on highly active antiretroviral therapy. *Journal of neurovirology* **11**, 180-189 (2005).

45 Esiri, M. M., Morris, C. S. & Millard, P. R. Sensory and sympathetic ganglia in HIV-1 infection: immunocytochemical demonstration of HIV-1 viral antigens, increased MHC class II antigen expression and mild reactive inflammation. *J Neurol Sci* **114**, 178-187 (1993).

46 Capuano, A. *et al*. Proinflammatory-activated trigeminal satellite cells promote neuronal sensitization: relevance for migraine pathology. *Molecular pain* **5**, 43 (2009).

47 Gosselin, R.-D. D., Suter, M. R., Ji, R.-R. R. & Decosterd, I. Glial cells and chronic pain. *The Neuroscientist : a review journal bringing neurobiology, neurology and psychiatry* **16**, 519-531 (2010).

48 Villa, G., Fumagalli, M., Verderio, C., Abbracchio, M. P. & Ceruti, S. Expression and contribution of satellite glial cells purinoceptors to pain transmission in sensory ganglia: an update. *Neuron glia biology* **6**, 31-42 (2010).

49 Gonzalez-Duarte, A., Cikurel, K. & Simpson, D. M. Managing HIV peripheral neuropathy. *Current HIV/AIDS Reports* **4**, 114-118 (2007).

50 Ebenezer, G. J., Hauer, P., Gibbons, C., McArthur, J. C. & Polydefkis, M. Assessment of epidermal nerve fibers: a new diagnostic and predictive tool for peripheral neuropathies. *Journal of neuropathology and experimental neurology* **66**, 1059-1073 (2007).

51 Lauria, G. & Lombardi, R. Skin biopsy in painful and immune-mediated neuropathies. *Journal of the peripheral nervous system : JPNS* **17 Suppl 3**, 38-45 (2012).

52 McArthur, J. C. Painful small fiber neuropathies. *Continuum (Minneapolis, Minn.)* **18**, 106-125 (2012).

53 Wendelschafer-Crabb, G., Kennedy, W. R. & Walk, D. Morphological features of nerves in skin biopsies. *Journal of the neurological sciences* **242**, 15-21 (2006).

54 Polydefkis, M. Skin biopsy findings predict development of symptomatic neuropathy in patients with HIV. *Nature clinical practice. Neurology* **2**, 650-651 (2006).

55 Rajan, B., Polydefkis, M., Hauer, P., Griffin, J. W. & McArthur, J. C. Epidermal reinnervation after intracutaneous axotomy in man. *The Journal of comparative neurology* **457**, 24-36 (2003).

56 Ebenezer, G. J. *et al*. Altered cutaneous nerve regeneration in a simian immunodeficiency virus / macaque intracutaneous axotomy model. *The Journal of comparative neurology* **514**, 272-283 (2009).

57 Albers, K. M. & Davis, B. M. The skin as a neurotrophic organ. *The Neuroscientist* **13**, 371-382 (2007).

58 Bentley, C. A. & Lee, K. F. p75 is important for axon growth and schwann cell migration during development. *Journal of Neuroscience* **20**, 7706-7715 (2000).

59 Song, X.-Y. Y., Zhou, F. H., Zhong, J.-H. H., Wu, L. L. & Zhou, X.-F. F. Knockout of p75(NTR) impairs re-myelination of injured sciatic nerve in mice. *Journal of neurochemistry* **96**, 833-842 (2006).

60 Thompson, D. M. & Buettner, H. M. Neurite Outgrowth is Directed by Schwann Cell Alignment in the Absence of Other Guidance Cues. *Annals of Biomedical Engineering* **34**, 669 (2006).

61 Ebenezer, G. J. *et al*. SIV-induced impairment of neurovascular repair: a potential role for VEGF. *Journal of neurovirology* **18**, 222-230 (2012).

62 Javed, S., Alam, U. & Malik, R. A. Burning through the pain: treatments for diabetic neuropathy. *Diabetes, obesity & metabolism*, **17**, 1115-1125 (2015).

63 Wang, S. X., Ho, E.L., Grill M., Lee, E., Peterson, J., Robertson, K., Fuchs, D., Sinclair, E., Price, R., & Spudich, S. Peripheral Neuropathy in Primary HIV Infection Associates with Systemic and CNS Immune Activation. *Journal of acquired immune deficiency syndromes*, **66**, 303-310 (2014).

64 Dorsey, J. L. *et al*. Persistent Peripheral Nervous System Damage in Simian Immunodeficiency Virus-Infected Macaques Receiving Antiretroviral Therapy. *Journal of neuropathology and experimental neurology* **74**, 1053-1060 (2015).

65 McGlone, F. & Reilly, D. The cutaneous sensory system. *Neuroscience and biobehavioral reviews* **34**, 148-159 (2010).

66 Hoeijmakers, J. G., Faber, C. G., Lauria, G., Merkies, I. S. & Waxman, S. G. Small-fibre neuropathies--advances in diagnosis, pathophysiology and management. *Nature reviews. Neurology* **8**, 369-379 (2012).

67 Gibbons, C. H. Small fiber neuropathies. *Continuum (Minneapolis, Minn.)* **20**, 1398-1412 (2014).

68 Russell, J. W. & Zilliox, L. A. Diabetic neuropathies. *Continuum (Minneapolis, Minn.)* **20**, 1226-1240 (2014).

69 Morkavuk, G. & Leventoglu, A. Small fiber neuropathy associated with hyperlipidemia: utility of cutaneous silent periods and autonomic tests. *ISRN neurology* **2014**, Article ID 579242 (2013).

70 Kaku, M. & Simpson, D. M. HIV neuropathy. *Current opinion in HIV and AIDS* **9**, 521-526 (2014).

71 Steiner, I. Herpes virus infection of the peripheral nervous system. *Handbook of clinical neurology* **115**, 543-558 (2012).

72 Brouwer, B. A. *et al*. Painful neuropathies: the emerging role of sodium channelopathies. *Journal of the peripheral nervous system* **19**, 53-65 (2014).

73 Oomatia, A., Fang, H., Petri, M. & Birnbaum, J. Peripheral neuropathies in systemic lupus erythematosus: clinical features, disease associations, and immunologic characteristics evaluated over a twenty-five-year study period. *Arthritis & rheumatology* **66**, 1000-1009 (2014).

74 Cavaletti, G. *et al*. Chemotherapy-Induced Peripheral Neurotoxicity assessment: a critical revision of the currently available tools. *European journal of cancer* **46**, 479-494 (2010).

75 Hong, J. S., Tian, J. & Wu, L. H. The influence of chemotherapy-induced neurotoxicity on psychological distress and sleep disturbance in cancer patients. *Current oncology* **21**, 174-180 (2014).

76 Authier, N. *et al*. Animal models of chemotherapy-evoked painful peripheral neuropathies. *Neurotherapeutics* **6**, 620-629 (2009).

77 Holland, N. R. *et al*. Intraepidermal nerve fiber density in patients with painful sensory neuropathy. *Neurology* **48**, 708-711 (1997).

78 Herrmann, D. N., Griffin, J. W., Hauer, P., Cornblath, D. R. & McArthur, J. C. Epidermal nerve fiber density and sural nerve morphometry in peripheral neuropathies. *Neurology* **53**, 1634-1640 (1999).

79 Lauria, G. *et al*. European Federation of Neurological Societies/Peripheral Nerve Society Guideline on the use of skin biopsy in the diagnosis of small fiber neuropathy. Report of a joint task force of the European Federation of

Neurological Societies and the Peripheral Nerve Society. *Journal of the peripheral nervous system* **15**, 79-92 (2010).

80 Hlubocky, A. *et al*. Skin biopsy for diagnosis of small fiber neuropathy: a critically appraised topic. *The neurologist* **16**, 61-63 (2009).

81 Lauria, G. *et al*. Intraepidermal nerve fiber density in rat foot pad: neuropathologic-neurophysiologic correlation. *Journal of the peripheral nervous system* **10** (2005).

82 David, N. H. Noninvasive and minimally invasive detection and monitoring of peripheral neuropathies. *Expert review of neurotherapeutics*, **8**, 1807-1816 (2008).

83 Zhou, L. *et al*. Correlates of epidermal nerve fiber densities in HIV-associated distal sensory polyneuropathy. *Neurology* **68**, 2113-2119 (2007).

84 Obermann, M. *et al*. Correlation of epidermal nerve fiber density with pain-related evoked potentials in HIV neuropathy. *Pain* **138**, 79-86 (2007).

85 Mangus, L. M. *et al*. Neuroinflammation and virus replication in the spinal cord of simian immunodeficiency virus-infected macaques. *Journal of neuropathology and experimental neurology* **74**, 38-47 (2014).

86 Clements, J., Gama, L., Graham, D., Mankowski, J. & Zink, M. A simian immunodeficiency virus macaque model of highly active antiretroviral treatment: viral latency in the periphery and the central nervous system. *Current opinion in HIV and AIDS* **6**, 37-42 (2011).

87 Beck, S. E. *et al*. Macaque species susceptibility to simian immunodeficiency virus: increased incidence of SIV central nervous system disease in pigtailed macaques versus rhesus macaques. *Journal of neurovirology* **21**, 148-158 (2015).

88 McCarthy, B. G. *et al*. Cutaneous innervation in sensory neuropathies: evaluation by skin biopsy. *Neurology* **45**, 1848-1855 (1995).

89 Smith, A. G. *et al*. The reliability of skin biopsy with measurement of intraepidermal nerve fiber density. *Journal of the neurological sciences*, **228**, 65-69 (2004).

90 Kennedy, W. R., Wendelschafer-Crabb, G., Polydefkis, M. McArthur, J.C. in *Peripheral Neuropathy* (ed P.J. Dyck, Thomas, P.K.) 869-896 (Saunders, 2005).

91 Mouton, P. R., Gokhale, A. M., Ward, N. L. & West, M. J. Stereological length estimation using spherical probes. *Journal of microscopy* **206**, 54-64 (2002).

92 Ebenezer, G. J. *et al*. Impaired neurovascular repair in subjects with diabetes following experimental intracutaneous axotomy. *Brain* **134**, 1853-1863 (2011).

93 Kelly, K. M. *et al*. Diastolic dysfunction is associated with myocardial viral load in simian immunodeficiency virus-infected macaques. *AIDS* **26**, 815-823 (2012).

94 Dorsey, J. L. *et al*. Loss of corneal sensory nerve fibers in SIV-infected macaques: an alternate approach to investigate HIV-induced PNS damage. *The American journal of pathology* **184**, 1652-1659 (2014).

95 Lakritz, J. R. *et al*. Monocyte Traffic, Dorsal Root Ganglion Histopathology, and Loss of Intraepidermal Nerve Fiber Density in SIV Peripheral Neuropathy. *The American journal of pathology*, **187**, 1912-1923 (2015).

96 Smith, S. B., Crager, S. E. & Mogil, J. S. Paclitaxel-induced neuropathic hypersensitivity in mice: responses in 10 inbred mouse strains. *Life sciences* **74**, 2593-2604 (2004).

97 Sullivan, K. A., Lentz, S. I., Roberts, J. L. & Feldman, E. L. Criteria for creating and assessing mouse models of diabetic neuropathy. *Current drug targets* **9**, 3-13 (2008).

98 Shikuma, C. M. *et al*. Ethnic differences in epidermal nerve fiber density. *Muscle & nerve* **48**, 462-464 (2013).

99 Shikuma, C. M. *et al*. Distal leg epidermal nerve fiber density as a surrogate marker of HIV-associated sensory neuropathy risk: risk factors and change following initial antiretroviral therapy. *Journal of neurovirology* **21**, 525-534 (2015).

100 Pardo, C.A, McArthyr, J.C., & Griffin, J.W. HIV neuropathy: Insights in the pathology of HIV peripheral nerve disease. *Journal of the Peripheral Nervous System* **6**, 21-27 (2001).

101 Desplats, P. *et al*. Molecular and pathologic insights from latent HIV-1 infection in the human brain. *Neurology* **80**, 1415-1423 (2013).

102 McArthur, J. C., Steiner, J., Sacktor, N. & Nath, A. Human immunodeficiency virus‐associated neurocognitive disorders: Mind the gap. *Annals of neurology*, **67**, 699-714 (2010).

103 Everall, I. P., Hansen, L. A. & Masliah, E. The shifting patterns of HIV encephalitis neuropathology. *Neurotoxicity research* **8**, 51-61 (2005).

104 Hénin, D., Smith, T., De Girolami, U., Sughayer, M. & Hauw, J. Neuropathology of the spinal cord in the acquired immunodeficiency syndrome. *Human pathology* **23**, 1106-1114 (1992).

105 Snider, W. *et al*. Neurological complications of acquired immune deficiency syndrome: analysis of 50 patients. *Annals of neurology* **14**, 403-418 (1983).

106 Maier, H., Budka, H., Lassmann, H. & Pohl, P. Vacuolar myelopathy with multinucleated giant cells in the acquired immune deficiency syndrome (AIDS). *Acta neuropathologica,* **78**, 497-503 (1989).

107 Dal Pan, G. J., Glass, J. D. & McArthur, J. C. Clinicopathologic correlations of HIV-1-associated vacuolar myelopathy: an autopsy-based case-control study. *Neurology* **44**, 2159-2164 (1994).

108 Petito, C. Review of central nervous system pathology in human immunodeficiency virus infection. *Annals of neurology* **23**, S54-S57 (1988).

109 Santosh, C. G., Bell, J. E. & Best, J. J. Spinal tract pathology in AIDS: postmortem MRI correlation with neuropathology. *Neuroradiology* **37**, 134-138 (1995).

110 Rappaport, J. Editorial: The Monocyte/Macrophage in the Pathogenesis of AIDS: The Next Frontier for Therapeutic Intervention in the CNS and Beyond: Part I. *Curr HIV Res* **12**, 75-76 (2014).

111 Churchill, M. & Nath, A. Where does HIV hide? A focus on the central nervous system. *Current opinion in HIV and AIDS* **8**, 165-169 (2013).

112 Mangus, L. M. *et al*. Unraveling the Pathogenesis of HIV Peripheral Neuropathy: Insights from a Simian Immunodeficiency Virus Macaque Model. *ILAR journal* **54**, 296-303 (2013).

113 Clements, J. E., Mankowski, J. L., Gama, L. & Zink, M. C. The accelerated simian immunodeficiency virus macaque model of human immunodeficiency virus-associated neurological disease: from mechanism to treatment. *Journal of neurovirology* **14**, 309-317 (2008).

114 Zink, M. C. *et al*. High viral load in the cerebrospinal fluid and brain correlates with severity of simian immunodeficiency virus encephalitis. *Journal of virology* **73**, 10480-10488 (1999).

115 Hazuda, D. J. *et al*. Integrase inhibitors and cellular immunity suppress retroviral replication in rhesus macaques. *Science* **305**, 528-532 (2004).

116 Schefe, J. H., Lehmann, K. E., Buschmann, I. R., Unger, T. & Funke-Kaiser, H. Quantitative real-time RT-PCR data analysis: current concepts and the novel "gene expression's CT difference" formula. *Journal of molecular medicine* **84**, 901-910 (2006).

117 Kennedy, J. M. *et al*. Peripheral neuropathy in lentivirus infection: evidence of inflammation and axonal injury. *AIDS* **18**, 1241-1250 (2004).

118 Soulas, C. *et al*. Recently infiltrating MAC387(+) monocytes/macrophages a third macrophage population involved in SIV and HIV encephalitic lesion formation. *The American journal of pathology* **178**, 2121-2135 (2011).

119 Zink, M. C. *et al*. Increased macrophage chemoattractant protein-1 in cerebrospinal fluid precedes and predicts simian immunodeficiency virus encephalitis. *The Journal of infectious diseases* **184**, 1015-1021 (2001).

120 Zheng, X. *et al*. TNFα is involved in neuropathic pain induced by nucleoside reverse transcriptase inhibitor in rats. *Brain, behavior, and immunity* **25**, 1668-1676 (2011).

121 Gao, Y.-J. J. *et al*. JNK-induced MCP-1 production in spinal cord astrocytes contributes to central sensitization and neuropathic pain. *The Journal of neuroscience* **29**, 4096-4108 (2009).

122 Ji, R.-R., Berta, T. & Nedergaard, M. Glia and pain: is chronic pain a gliopathy? *Pain* **154 Suppl 1**, 28 (2013).

123 White, F., Bhangoo, S. & Miller, R. Chemokines: integrators of pain and inflammation. *Nature reviews. Drug discovery* **4**, 834-844 (2005).

124 Ramesh, G., MacLean, A. G. & Philipp, M. T. Cytokines and chemokines at the crossroads of neuroinflammation, neurodegeneration, and neuropathic pain. *Mediators of inflammation* **2013**, Article ID 480739 (2012).

125 Edén, A. *et al*. Immune activation of the central nervous system is still present after >4 years of effective highly active antiretroviral therapy. *The Journal of infectious diseases* **196**, 1779-1783 (2007).

126 Yilmaz, A. *et al*. Persistent intrathecal immune activation in HIV-1-infected individuals on antiretroviral therapy. *Journal of acquired immune deficiency syndromes (1999)* **47**, 168-173 (2008).

127 Dubin A.E., & Patapoutian, A.P. Nociceptors: the sensors of the pain pathway. *Journal of Clinical Investigation*, **120**, 3760-3772 (2010).

128 Scholz, J. & Woolf, C. J. The neuropathic pain triad: neurons, immune cells and glia. *Nature neuroscience* **10**, 1361-1368 (2007).

129 Cao, H. & Zhang, Y.-Q. Q. Spinal glial activation contributes to pathological pain states. *Neuroscience and biobehavioral reviews* **32**, 972-983 (2008).

130 Grace, P. M., Hutchinson, M. R., Maier, S. F. & Watkins, L. R. Pathological pain and the neuroimmune interface. *Nature reviews. Immunology* **14**, 217-231 (2014).

131 Evans, S. *et al*. Peripheral neuropathy in HIV: prevalence and risk factors. *AIDS (London, England)* **25**, 919-928, doi:10.1097/QAD.0b013e328345889d (2011).

132 Nath, A. & Clements, J. Eradication of HIV from the brain: reasons for pause. *AIDS* **25**, 577-580 (2011).

133 Alexaki, A., Liu, Y. & Wigdahl, B. Cellular reservoirs of HIV-1 and their role in viral persistence. *Current HIV research* **6**, 388-400 (2008).

134 Simmons, S. B., Liggitt, D. & Goverman, J. M. Cytokine-Regulated Neutrophil Recruitment Is Required for Brain but Not Spinal Cord Inflammation during Experimental Autoimmune Encephalomyelitis. *Journal of immunology* ***193***, 555-563 (2014).

135 Olson, J. Immune response by microglia in the spinal cord. *Annals of the New York Academy of Sciences* **1198**, 271-278 (2010).

136 Baskar Jesudasan, S. J., Todd, K. G. & Winship, I. R. Reduced Inflammatory Phenotype in Microglia Derived from Neonatal Rat Spinal Cord versus Brain. *PloS one* **9**, e99443 (2013).

137 Campbell, S. J., Wilcockson, D. C., Butchart, A. G., Perry, V. H. & Anthony, D. C. Altered chemokine expression in the spinal cord and brain contributes to differential interleukin-1beta-induced neutrophil recruitment. *Journal of neurochemistry* **83**, 432-441 (2002).

138 Schnell, L., Fearn, S., Klassen, H., Schwab, M. E. & Perry, V. H. Acute inflammatory responses to mechanical lesions in the CNS: differences between brain and spinal cord. *The European journal of neuroscience* **11**, 3648-3658 (1999).

139 Stavros, K. & Simpson, D. M. Understanding the etiology and management of HIV-associated peripheral neuropathy. *Current HIV/AIDS Reports* **11**, 195-201 (2014).

140 Mann, R. *et al*. Burden of HIV-Related Neuropathic Pain in the United States. *Journal of the International Association of Providers of AIDS Care* (2015).

141 Yoshioka, M. *et al*. Expression of HIV-1 and interleukin-6 in lumbosacral dorsal root ganglia of patients with AIDS. *Neurology* **44**, 1120-1130 (1994).

142 Nagano, I. *et al*. Increased NADPH-diaphorase reactivity and cytokine expression in dorsal root ganglia in acquired immunodeficiency syndrome. *Journal of the neurological sciences* **136**, 117-128 (1996).

143 Hosseini, I., Gama, L. & Mac Gabhann, F. Multiplexed Component Analysis to Identify Genes Contributing to the Immune Response during Acute SIV Infection. *PloS one* **10**, e1026843 (2015).

144 Geiss, G. K. *et al*. Direct multiplexed measurement of gene expression with color-coded probe pairs. *Nature biotechnology* **26**, 317-325 (2008).

145 Turchan, J. *et al*. Oxidative stress in HIV demented patients and protection ex vivo with novel antioxidants. *Neurology* **60**, 307-314 (2003).

146 Potter, M. C., Figuera-Losada, M., Rojas, C. & Slusher, B. S. Targeting the glutamatergic system for the treatment of HIV-associated neurocognitive disorders. *Journal of neuroimmune pharmacology : the official journal of the Society on NeuroImmune Pharmacology* **8**, 594-607 (2013).

147 Akay, C. *et al*. Antiretroviral drugs induce oxidative stress and neuronal damage in the central nervous system. *Journal of neurovirology* **20**, 39-53, (2014).

148 Vázquez-Santiago, F. J., Noel, R. J., Porter, J. T. & Rivera-Amill, V. Glutamate metabolism and HIV-associated neurocognitive disorders. *Journal of neurovirology* **20**, 315-331 (2014).

149 Lipton, S. A. Neuronal injury associated with HIV-1: approaches to treatment. *Annual review of pharmacology and toxicology* **38**, 159-177 (1998).

150 Witwer, K. *et al*. Coordinated regulation of SIV replication and immune responses in the CNS. *PloS one* **4** (2009).

151 Stacey, A. R. *et al*. Induction of a Striking Systemic Cytokine Cascade prior to Peak Viremia in Acute Human Immunodeficiency Virus Type 1 Infection, in Contrast to More Modest and Delayed Responses in Acute Hepatitis B and C Virus Infections. *Journal of virology* **83**, 3719-3733 (2009).

152 Wada, N. I. *et al*. The effect of HAART-induced HIV suppression on circulating markers of inflammation and immune activation. *AIDS* **29**, 463-471 (2015).

153 Osborn, L., Kunkel, S. & Nabel, G. J. Tumor necrosis factor alpha and interleukin 1 stimulate the human immunodeficiency virus enhancer by activation of the nuclear factor kappa B. *PNAS* **86**, 2336-2340 (1989).

154 Gold, M. S. & Gebhart, G. F. Nociceptor sensitization in pain pathogenesis. *Nature medicine* **16**, 1248-1257 (2010).

155 Devor, M. Unexplained peculiarities of the dorsal root ganglion. *Pain* **Suppl 6**, 35 (1999).

156 Jimenez-Andrade, J. M., Herrera, M. B. & Ghilardi, J. R. Vascularization of the dorsal root ganglia and peripheral nerve of the mouse: implications for chemical-induced peripheral sensory neuropathies. *Molecular Pain* **4** (2008).

157 Ferrari, L. F. *et al*. Inflammatory sensitization of nociceptors depends on activation of NMDA receptors in DRG satellite cells. *PNAS* **111**, 18363-18368 (2014).

158 Co, J. G., Witwer, K. W., Gama, L., Zink, M. C. & Clements, J. E. Induction of innate immune responses by SIV in vivo and in vitro: differential expression and function of RIG-I and MDA5. *The Journal of infectious diseases* **204**, 1104-1114 (2011).

159 Sandler, N. G. *et al*. Type I interferon responses in rhesus macaques prevent SIV infection and slow disease progression. *Nature* **511**, 601-605 (2014).

160 Sivro, A., Su, R.-C. C., Plummer, F. A. & Ball, T. B. Interferon responses in HIV infection: from protection to disease. *AIDS reviews* **16**, 43-51 (2014).

161 Jones, G. *et al*. Peripheral nerve-derived HIV-1 is predominantly CCR5-dependent and causes neuronal degeneration and neuroinflammation. *Virology* **334**, 178-193 (2005).

162 White, F. A., Jung, H. & Miller, R. J. Chemokines and the pathophysiology of neuropathic pain. *PNAS* **104**, 20151-20158 (2007).

163 Kamerman, P. R. *et al*. Pathogenesis of HIV-associated sensory neuropathy: evidence from in vivo and in vitro experimental models. *Journal of the peripheral nervous system* **17**, 19-31 (2012).

164 Kung, L.-H. H. *et al*. Evidence for glutamate as a neuroglial transmitter within sensory ganglia. *PloS one* **8**, e68312 (2013).

165 Carozzi, V. A. *et al*. Expression, distribution and glutamate uptake activity of high affinity-excitatory aminoacid transporters in in vitro cultures of embryonic rat dorsal root ganglia. *Neuroscience* **192**, 275-284 (2011).

166 Laursen, J. C. *et al*. Glutamate dysregulation in the trigeminal ganglion: a novel mechanism for peripheral sensitization of the craniofacial region. *Neuroscience* **256**, 23-35 (2014).

167 Zhao, L. *et al*. Interferon-α regulates glutaminase 1 promoter through STAT1 phosphorylation: relevance to HIV-1 associated neurocognitive disorders. *PloS one* **7**, e32995 (2012).

168 Huang, Y. *et al*. Glutaminase dysregulation in HIV-1-infected human microglia mediates neurotoxicity: relevant to HIV-1-associated neurocognitive disorders. *The Journal of neuroscience : the official journal of the Society for Neuroscience* **31**, 15195-15204 (2011).

169 Erdmann, N. *et al*. In vitro glutaminase regulation and mechanisms of glutamate generation in HIV-1-infected macrophage. *Journal of neurochemistry* **109**, 551-561 (2009).

170 Jiang, Z. G. *et al*. Glutamate is a mediator of neurotoxicity in secretions of activated HIV-1-infected macrophages. *Journal of neuroimmunology* **117**, 97-107 (2001).

171 Gill, A. J. *et al*. Heme oxygenase-1 deficiency accompanies neuropathogenesis of HIV-associated neurocognitive disorders. *The Journal of clinical investigation* **124**, 4459-4472 (2014).

172 Swamy, M. & Sirajudeen, K. N. S. Nitric oxide (NO), citrulline-NO cycle enzymes, glutamine synthetase, and oxidative status in kainic acid-mediated excitotoxicity in rat brain. *Drug and chemical toxicology* **32**, 326-331 (2009).

173 Görg, B., Bidmon, H. J., Keitel, V. & Foster, N. Inflammatory cytokines induce protein tyrosine nitration in rat astrocytes. *Archives of biochemistry and biophysics* **449**, 104-114 (2006).

174 Hanani, M. Satellite glial cells in sensory ganglia: from form to function. *Brain research. Brain research reviews* **48**, 457-476 (2005).

175 Albrecht, J., Sonnewald, U., Waagepetersen, H. S. & Schousboe, A. Glutamine in the central nervous system: function and dysfunction. *Frontiers in bioscience* **12**, 332-343 (2007).

176 Robinson, S. R. Neuronal expression of glutamine synthetase in Alzheimer's disease indicates a profound impairment of metabolic interactions with astrocytes. *Neurochemistry international* **36**, 471-482 (2000).

177 Robinson, S. R. Changes in the cellular distribution of glutamine synthetase in Alzheimer's disease. *Journal of Neuroscience Research* **66**, 972-980 (2001).

178 Fernandes, S. P., Dringen, R., Lawen, A. & Robinson, S. R. Neurones express glutamine synthetase when deprived of glutamine or interaction with astrocytes. *Journal of neurochemistry* **114**, 1527-1536 (2010).

179 Chen, J. & Herrup, K. Glutamine acts as a neuroprotectant against DNA damage, beta-amyloid and H2O2-induced stress. *PloS one* **7**, e33177 (2012).

180 Lehmann, H. C., Chen, W., Borzan, J., Mankowski, J. L. & Höke, A. Mitochondrial dysfunction in distal axons contributes to human immunodeficiency virus sensory neuropathy. *Annals of neurology* **69**, 100-110 (2011).

181 West, A. P., Shadel, G. S. & Ghosh, S. Mitochondria in innate immune responses. *Nature reviews. Immunology* **11**, 389-402 (2011).

182 Ishihara, Y., Takemoto, T., Itoh, K., Ishida, A. & Yamazaki, T. Dual role of superoxide dismutase 2 induced in activated microglia: oxidative stress tolerance and convergence of inflammatory responses. *The Journal of biological chemistry* **290**, 22805-22817 (2015).

183 Ebenezer, G., Hauer, P., Gibbons, C., McArthur, J. & Polydefkis, M. Assessment of epidermal nerve fibers: a new diagnostic and predictive tool for peripheral neuropathies. *Journal of neuropathology and experimental neurology* **66**, 1059-1073 (2007).

184 Tavakoli, M. *et al*. Corneal confocal microscopy: a novel means to detect nerve fibre damage in idiopathic small fibre neuropathy. *Experimental neurology*, **223**, 245-250 (2010).

185 Petropoulos, I. N. *et al*. Rapid Automated Diagnosis of Diabetic Peripheral Neuropathy With In Vivo Corneal Confocal Microscopy. *Investigative Ophthalmology & Visual Science*, **55**, 2071-2078 (2014).

186 Chen, D. K. *et al*. Repeated monitoring of corneal nerves by confocal microscopy as an index of peripheral neuropathy in type-1 diabetic rodents and the effects of topical insulin. *Journal of the peripheral nervous system* **18**, 306-315 (2013).

187 Zhu, Y. *et al*. Lentivirus infection causes neuroinflammation and neuronal injury in dorsal root ganglia: pathogenic effects of STAT-1 and inducible nitric oxide synthase. *Journal of immunology* **175**, 1118-1126 (2005).

**Lisa M. Mangus**
lmangus1@gmail.com | 304.639.7628
March 2016

## EDUCATION

**Ph.D. in Cellular and Molecular Medicine.** Johns Hopkins University, School of Medicine, 2016
Dissertation Title: *Investigating the pathogenesis of HIV-associated sensory neuropathy in the SIV/macaque model*
**DACVP (Anatomic),** Johns Hopkins University, School of Medicine, 2014
**DVM,** *magna cum laude*, The Ohio State University, College of Veterinary Medicine, 2009
**BS in Biologic Sciences**, *summa cum laude*, Duquesne University, Bayer School of Natural and Environmental Sciences, 2004

## RESEARCH AND PROFESSIONAL EXPERIENCE

**Thesis Research in Cellular and Molecular Medicine**, 2012-present
Advisor: Dr. Joseph Mankowski

- Conducted research that required cohesive knowledge of immunology, virology, neuroanatomy, and histopathology
- Became adept at numerous laboratory techniques including nucleic acid and protein isolation from tissues, qRT-PCR, immunohistochemistry, western blot, cell culture, fluorescent and confocal microscopy, and software-aided image analysis
- Pioneered and optimized a method for isolating and culturing primary dorsal root ganglia neurons from adult macaques
- Gained familiarity with electrophysiological techniques, such as conduction velocity testing in teased nerve fibers and whole-cell patch clamping
- Performed necropsies and peripheral nervous system dissections of SIV-infected macaques while adhering to BSL-3 practices

**Comparative Pathology Fellow**, 2010-2014
Department of Molecular and Comparative Pathobiology, JHU SOM

- Performed gross and histologic postmortem examinations on wide variety of laboratory animals, including non-human primates, as well as companion animals and zoo/exotic species
- Gained unique experience in comparative pathology by completing a 6-week rotation on human autopsy and surgical biopsy service
- Instituted monthly 'Comparative Neuropath Rounds' in conjunction with faculty specializing in human neuropathology
- Served as liaison between JHU, the National Aquarium in Baltimore, and the Maryland Zoo in Baltimore to facilitate and enhance collaborative diagnostic and research efforts

**Associate Veterinarian**, 2009-2010
VCA Veterinary Referral Associates

- Completed a one-year internship in small animal medicine and surgery
- Strengthened diagnostic and therapeutic skills
- Maintained high standards of patient care while working in a fast-paced clinical setting

ADDITIONAL EXPERIENCE AND TRAINING

- **Practical Training Course in Confocal Microscopy and Stereology**, Sponsored by NeuroRenew, Inc. and Micro Bright Field (MBF), August 2013
- **Microbiology Laboratory Technician**, The Ohio State University, Veterinary Teaching Hospital, 2006-2007

TEACHING EXPERIENCE

- **Training Program in Comparative Pathology**, Johns Hopkins University, September 2014-present
  - Since obtaining ACVP board-certification, I have been actively involved in the ongoing training of residents and fellows by signing-out necropsy and surgical biopsy cases, reviewing histology reports, and assisting with boards preparation activities
- **Principles of Toxicology**, guest lecturer, "Toxicological Pathology of the Eye", Johns Hopkins University School of Medicine, Spring 2015
- **Mouse Pathobiology and Phenotyping Course**, necropsy lab assistant/instructor, Dept. of Molecular & Comparative Pathobiology, Johns Hopkins University School of Medicine, Summer 2012-2015
- **Basic Mechanisms of Disease**, histology lab instructor, Pathobiology graduate program, Johns Hopkins University School of Medicine, Fall 2012 and 2013
- **Principles of Immunology**, tutor, CMM graduate program, Johns Hopkins University School of Medicine, Fall 2012

AWARDS AND SCHOLARSHIPS

- C.L. Davis Foundation for the Advancement of Veterinary and Comparative Pathology, Student Scholarship Award, 2015
- Conference on Retroviruses and Opportunistic Infections (CROI), Young Investigators Award, 2013
- Practical Workshop in Confocal Microscopy & Stereology, Graduate Student Scholarship, 2013
- American College of Veterinary Pathology, Graduate Student/Resident Travel Award, 2012
- Western Veterinary Conference Scholar, 2008

- Salsbury Scholarship for Veterinary Medicine, 2008
- Phi Zeta Honor Society of Veterinary Medicine, 2008

PEER-REVIEWED PUBLICATIONS

- **Mangus LM**, Dorsey JL, Laast VA, Hauer P, Queen SE, Adams RJ, McArthur JC, Mankowski JL. 2015. Neuroinflammmation and virus replication in the spinal cord of SIV-infected macaques. *Journal of Neuropathology and Experimental Neurology*. 74(1): 38-47.
- **Mangus LM**, Dorsey JL, Laast VA, Ringkamp M, Ebenezer GJ, Hauer P, Mankowski JL. 2014. Unraveling the pathogenesis of HIV peripheral neuropathy: insights from an SIV/macaque model. *ILAR Journal*. 54(3): 296-303.
- Dorsey JL, **Mangus LM**, Hauer P, Ebenezer GJ, Queen SE, Laast VA, Adams RJ, Mankowski JL. 2015. Persistent peripheral nervous system damage in a simian immunodeficiency virus-infected macaques receiving antiretroviral therapy. *Journal of Neuropathology and Experimental Neurology*. 74(11): 1053-60.
- Beck SE, Queen SE, Witwer KW, Metcalf Pate KA, **Mangus LM**, Gama L, Adams RJ, Clements JE, Zink MC, Mankowski JL. 2015. Paving the path to HIV neurotherapy: predicting SIV CNS disease. *European J Pharmacology*. 15;759:303-12.
- Dorsey JL, **Mangus LM**, Oakley JD, Beck SE, Kelly KM, Queen SE, Metcalf Pate KA, Adams RJ, Marfurt CF, Mankowsky JL. 2014. Loss of corneal sensory nerve fibers in SIV-infected macaques: an alternate approach to investigate HIV-induced PNS damage. *American Journal of Pathology*. 184(6):1652-1659.
- Hadfield CA, Clayton LA, Clancy MM, Beck SE, **Mangus LM**, Montali RJ. 2012. Proliferative thyroid lesions in three diplodactylid geckos: Nephrurus amyae, Nephrurus levis, and Oedura marmorata. *Journal of Zoo and Wildlife Medicine*. 43(1): 131-140.
- Carroll EE, Fossey SL, **Mangus LM**, Carsillo ME, Rush LJ, McLeod CG, Johnson, TO. 2010. Malignant pilomatricoma in three dogs. *Veterinary Pathology*. 47(5): 937-943.

ORAL PRESENTATIONS

- **Mangus LM** (2015) Does SIV infection alter glutamate signaling in the peripheral nervous system? Dept. of Molecular and Comparative Pathobiology Seminar Series, Johns Hopkins University, School of Medicine.
- **Mangus LM** (2015) Beyond the brain: neuroinflammation and virus replication in the spinal cord of SIV-infected macaques. NeuroAIDS Lecture Series, Johns Hopkins University, School of Medicine.
- Mankowski JL, **Mangus LM**, Beck SE, Gama L (2015) Case presentation. Primate Pathology Pre-Conference Workshop at the Annual Meeting of the American College of Veterinary Pathologists, Minneapolis, MN.

- **Mangus LM** (2014) Investigating the pathogenesis of HIV-peripheral neuropathy using an SIV/macaque model. Dept. of Molecular and Comparative Pathobiology Seminar Series, Johns Hopkins University, School of Medicine
- **Mangus LM**, Lin WH, Hauer D, Griffin D (2011) Detection and cellular localization of Measles virus RNA in rhesus macaque tissue by *in situ* hybridization. CMM graduate program, student rotation presentation, Johns Hopkins University, School of Medicine.

POSTER PRESENTATIONS

- **Mangus LM**, Dorsey JL, Mankowski JL (2013) A window to the peripheral nervous system: corneal sensory nerve fiber loss in SIV-infected macaques. Annual meeting of the American College of Veterinary Pathologists, Montreal, ON.
- **Mangus LM**, Dorsey JL, Mankowski JL (2013) Morphologic and molecular pathology in the spinal cord of SIV infected macaques. Conference for Retroviral and Opportunistic Infections (CROI), Atlanta, GA.
- **Mangus LM**, Dorsey JL, Mankowski JL (2012) Morphologic and molecular pathology in the spinal cord of SIV infected macaques. Annual meeting of the American College of Veterinary Pathologists, Seattle, WA.
- **Mangus LM**, Beck SE, Montali R, Hadfield C, Clayton LA, Clancy M (2011) Pathologic findings in the thyroid glands of three captive diplotactylid geckos. Annual meeting of the American College of Veterinary Pathologists, Nashville, TN.

EXTRAMURAL FUNDING

R25MH08066108 (L. Mangus)
07/01/2014 – 06/30/2015
**Pilot Grant for Translational Research in Neuro-AIDS and Mental Health**
Project title: Beyond the brain: SIV replication, reservoirs, and inflammation in the CNS spinal cord compartment
Co-investigator: Joseph Mankowski
Role: Principal Investigator

2T32RR007002-35 (C. Zink)
07/01/2011 - 06/30/2015
**Training Veterinarians for Careers in Biomedical Research**
PI: Christine Zink
Research mentor: Joseph Mankowski, DVM, PhD, DACVP
Role: PhD Candidate / Graduate Student
The primary objective of this T32 training grant is to train veterinarians for careers in biomedical research.